2002

The effects of rock and fluids characteristics on reservoir wettability

Chandra S. Vijapurapu
Louisiana State University and Agricultural and Mechanical College

THE EFFECTS OF ROCK AND FLUIDS CHARACTERISTICS ON RESERVOIR WETTABILITY

A Thesis

Submitted to the Graduate Faculty of the
Louisiana State University and
Agricultural and Mechanical College
in partial fulfillment of the
requirements for the degree of
Master of Science in Petroleum Engineering

In

The Department of Petroleum Engineering

By
Chandra S. Vijapurapu
B.S (Chem. Engg), Andhra University, 2000
December 2002

DEDICATION

This work is dedicated to my parents and my family…

ACKNOWLEDGEMENTS

I am grateful to my esteemed Professor Dr. Dandina N.Rao under whose able guidance was this work performed. I am also thankful to Dr. Zaki Bassiouni and Dr. Jeremy K. Edwards who served as the members on the examination committee.

The financial support from the Louisiana Board of Regents support fund (LEQSF 2000-03-RD-B-06) and Marathon Oil Company is gratefully acknowledged. Sincere thanks are due to British Petroleum for donating the computerized Wilhelmy apparatus to Louisiana State University.

I am also grateful to Rick Young, Geology Department (LSU) for his help in preparing the solid samples, Margaret Cindy Henk, Biological Sciences (LSU) in coating the samples and with the use of the SEM, Dr. Kun Lian, Asst. Professor at Center for Advanced Microstructures and Devices (CAMD) for his help in using the Optical and Stylus Profilometers for characterizing the roughness of the rock samples. I would also like to thank Dan Lawrence, Department of Petroleum Engineering (LSU), Victor G Ramirez, CAMD for their valuable technical help, Varshni Singh and Pankaj Gupta, Mechanical Engineering (LSU) for their help in using the Optical Profilometer, Paul Rodriguez, Jr., Chemical Engineering (LSU) for help in sandblasting the samples.

I would like to thank all the faculty members and my colleagues in the Department of Petroleum Engineering at Louisiana State University who assisted me in every possible way. My heartfelt thanks to my family and all my friends who have been of constant support all through the way until I finished what I started a couple of years ago.

TABLE OF CONTENTS

LIST OF TABLES

LIST OF FIGURES

NOMENCLATURE

N_c = Capillary Number

ν = Velocity

μ = Viscosity

σ = Interfacial tension

θ = Contact angle

σ_{os} = Interfacial energy between oil and solid

σ_{ws} = Interfacial energy between water and solid

σ_{ow} = Interfacial energy between oil and water

θ = Contact angle at the oil/water/solid boundary

δ_w = wettability index to water

V_{osp} = oil volume displaced by spontaneous water imbibition

V_{ot} = the total oil volume displaced by imbibition and centrifugal (forced) displacement

δ_o = wettability index to oil

V_{wsp} = water volume displaced by spontaneous oil imbibition alone

V_{wt} = total displaced by oil imbibition and centrifugal (forced) displacement

N_W = wettability number

A_1 = areas under the capillary versus saturation curves obtained during oil drive

A_2 = areas under the capillary versus saturation curves brine drives

θ_a = apparent contact angle

θ_E = true contact angle

r = the roughness factor

γ =Interfacial tension,

R_1, R_2 = principal radii of curvature

ΔP = pressure difference across the interface or the capillary pressure

ABSTRACT

Wettability is the ability of a fluid to spread or adhere on a rock surface in the presence of other immiscible fluids. Knowledge of wettability is important to decide what production strategy needs to be employed for optimum oil recovery. Wettability is affected by several factors including rock mineralogy, rock surface roughness, and brine compositions.

Most of the previous studies have largely dealt with solid-liquid-vapor systems and those involving wettability characterization in solid-liquid-liquid systems have used contact angle techniques that have known to have poor reproducibility problems. In this study, a new technique called the Dual-Drop-Dual-Crystal (DDDC) Technique has been used to characterize wettability in terms of dynamic contact angles. The Wilhelmy Plate technique has also been used in this study to measure dynamic contact angles for a comparative evaluation of the DDDC results. In studying the effects of factors such as surface roughness, brine dilution and surfactant addition in crude oil-brine-rock systems, the Wilhelmy technique was found to be insensitive, while the DDDC technique showed significant effects of mineralogy, roughness, brine dilution and surfactant addition on dynamic contact angles.

Interfacial tension is another important fluid-fluid interaction parameter that affects trapping of oil in reservoirs through capillary pressure. Flow of fluids in a reservoir is generally governed by rock-fluid and fluid-fluid interactions of the system. In this study, interfacial tension has been measured using the image-capture and applying

the Drop Shape Analysis (DSA) technique and the results have been compared with those obtained using the du Nuoy ring Tensiometer.

Brine dilution and its effect on reservoir wettability are important as they can influence water flood recoveries. Study of the effects of brine dilution on dynamic contact angles was conducted using Yates brine and its diluted mixtures with deionized water in different proportions. Wettability effects are studied by measuring the dynamic contact angles and interfacial tension of the mixture. A parabolic trend in interfacial tension was observed, with an initial decrease in interfacial tension with increasing brine percentage in the mixture and then an increase after attaining a certain minimum. An unexpected effect was observed in this study that appears not to have been reported in the literature so far. For certain brine dilutions, the oil drop began spreading on the rock surface yielding large receding contact angles. This spreading phenomenon was correlated to the receding angle and interfacial tension as discussed by Zisman [36] in solid-liquid-vapor systems and by Rao [24] in solid-liquid-liquid systems. A similar effect of oil spreading was also observed when using synthetic brine in place of reservoir brine.

Chemical flooding as a means of enhanced oil recovery through reduction in oil-water interfacial tension has lost its flavor in the oil industry; however the use of surfactants to enhance production by altering wettability of the system is being considered. This study has investigated the effect of a nonionic surfactant on wettability. The effect of addition of ethoxy alcohol surfactant to Yates fluids pair on dolomite has been studied using the DDDC tests. Initial oil-wet nature of the Yates system was rendered intermediate-wet at certain concentrations of the surfactant. At higher concentrations of the surfactant, although very little change in interfacial tension was

noticed, the advancing angle continued to decrease from an intermediate-wet angle to a strongly water-wet angle, indicating the ability of the surfactant to alter the wettability of the crude oil-brine-rock system by the surfactant.

In addition to the unexpected observation of oil spreading due to brine dilution, this experimental study confirms the ability of a surfactant to alter the wettability of a crude oil-brine-rock system from its initial strongly oil-wet state to one of strongly water-wet.

CHAPTER 1

INTRODUCTION

Most of today's energy needs are met by crude oil, which is recovered from the ground. The processes currently being practiced have been successful in recovering only approximately one third of the original oil in place leaving behind nearly two-thirds untapped. This points out the need to study and implement new and innovative methods to recover the remaining oil. This in turn requires an in-depth study of reservoir characteristics such as properties of the crude oil, brine, the mineralogy of the rock surface and their effects on the interactions that take place between crude oil, brine and the rock surface.

In order to study and understand these interactions, the parameter that has been considered for this present study is wettability. Wettability is the ability of one fluid to spread or adhere on a rock surface in the presence of other immiscible fluids. The fluids are crude oil and brine and the solid surface is the rock surface. Wettability is affected by various factors such as aging time between the fluids and the rock surface, surface heterogeneity, roughness and mineralogy of the rock surfaces and also on the composition of the brines and crude oils. The wetting nature of a particular fluid on the rock surface in preference to the other is measured in terms of contact angle. Contact angle is the angle between a tangent drawn on the drop's surface at the resting or contact point and a tangent to the supporting surface.

Surface and capillary forces account for most of the oil being left behind in the reservoirs after secondary production. Capillary forces are generally quantified by the capillary number, $N_{c,}$ which is the ratio of viscous to capillary forces and is given by

$$N_c = \frac{v\mu}{\sigma \cos\theta} \quad \text{.....(1)}$$

where v is the velocity, μ is the viscosity,σ, is the interfacial tension and θ is the contact angle.

The greater the capillary number, the lower the residual oil saturation and hence greater the recoveries. All the recovery of residual oil is thus linked to capillary number, which in turn depends on viscosity of the fluid, interfacial tension between the fluids, and the contact angle. So far, in the development of Enhanced Oil Recovery (EOR) processes, our attention has been to reduce the oil-water interfacial tension to a minimum so that capillary number would increase thereby yielding higher oil recovery.

Neglecting contact angle, by assuming it to be zero, has been an erroroneus assumption made in the past. As can be noticed from Equation (1), we can increase the capillary number to infinity without even altering the interfacial tension term just by increasing the contact angle to 90^o ($\text{Cos}\theta=0$ when $\theta=90^o$). A contact angle of 90^o means the system is intermediate-wet. Thus the focus of this study has been to find ways to make the contact angle 90^o or impart intermediate-wettability to the rock-fluid system.

Wettability characterization by contact angle is treated with skepticism in the oil industry due to the poor reproducibility of results. So, a new method of measuring contact angle called the Dual-Drop-Dual-Crystal (DDDC) method [4] was used in this study. This method has been proven to be sensitive and reliable, consistently yielding reproducible results [4].

The variables examined in this study are the aging time, mineralogy of solid surfaces, surface roughness solid samples, brine dilution and surfactant concentration, for their effects on wettability as characterized by dynamic contact angles measured using

the Dual-Drop-Dual-Crystal Technique as well as the Wilhelmy plate apparatus. The review of literature concerning these variables is presented in Chapter 2, the experimental procedures are included in Chapter 3 and the results of this experimental study are presented and discussed in Chapter 4. The salient conclusions and recommendations for future work are the subject matter for Chapter 5.

CHAPTER 2

LITERATURE REVIEW

2.1 Contact Angle

2.1.1 What Are Contact Angles?

Contact angles are easy to visualize and they measure manifestation of surface energy, which in turn is a characteristic of chemical bonding. Contact angles, *per se,* describe the shape of a liquid drop on a solid surface.

The contact angle is the angle between a tangent drawn on the drop's surface at the resting or contact point and a tangent to the supporting surface. The shape of the drop reveals information about the chemical bonding nature of the surface. This bonding determines its wettability and adhesion. The relationship of drop shape to bonding is contact angle's utility.

Chemical bonds are the attractive forces between the atoms in a molecule and between adjacent molecules in a substance. These are the forces that hold things together. When molecules exit in close proximity in a liquid or solid, the atoms arrange themselves to optimally satisfy the bonding forces with nearby neighbors.

Consider the idealized solid as shown in Figure 1[(1)]. An atom in the interior has satisfied bonds in all directions: four in this 2-D drawing and six in the real 3-D world. But the atoms in the top row do not have one bond satisfied, because there is no neighbor above. These unsatisfied bonds constitute surface energy; a potential energy in the sense that another object brought up close might satisfy some of these "dangling" bonds. These bonds are the source of wetting and adhesion. We use the contact angles to estimate the nature and strength of these bonds.

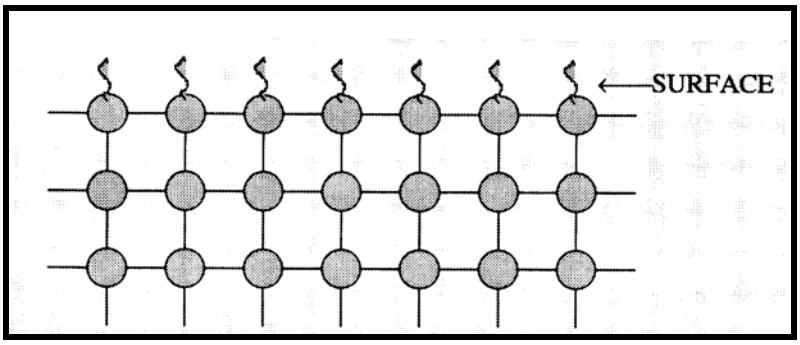

Figure 1: Schematic of an Idealized solid surface[1]

2.1.2 Contact Angle and Young's Equation

The contact angle is the best wettability measurement method when pure fluids and artificial cores are used because there is no possibility of surfactants or other compounds altering the wettability. This method can also be used for determining whether a crude oil can alter the wettability and to examine the effects of temperature, pressure and brine chemistry on wettability [3].

Contact angle is a measure of the intrinsic wettability of a reservoir rock. When a drop of oil is placed on mineral surface immersed in water, a contact angle is formed which can range from 0^0 to 180^0. The contact angle formed at the three-phase boundary defines the wetting or non-wetting behavior of a liquid on a solid surface and is a measure of the equilibrium between adhesive and cohesive forces that exist between the molecules at the liquid-solid interface.

Interfacial tension and contact angle are related by Young's equation, which is a force balance along the surface, as shown in Figure 2,

$$\sigma_{os} = \sigma_{ws} + \sigma_{ow} \cos\theta \quad \text{.....(2)}$$

where

σ_{os} = Interfacial energy between oil and solid

σ_{ws} = Interfacial energy between water and solid

σ_{ow} = Interfacial energy between oil and water

θ = Contact angle at the oil/water/solid boundary.

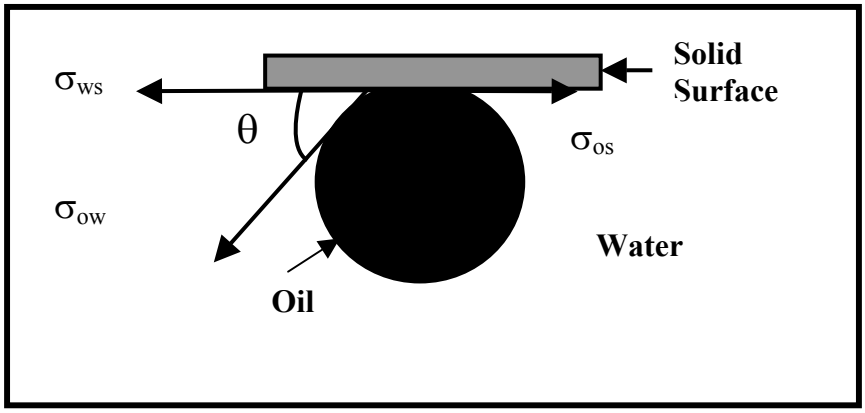

Figure 2: Contact Angle in an Oil/Water/Solid System (after Rao[2])

Figure 3 depicts different states of wettability in terms of the contact angle. When the contact angle is less than 70^0, the surface is referred to as being water-wet; when it is greater than 115^0, the surface is considered to be oil-wet; and the intermediate range from 70^o to 115^o is considered as intermediate-wet[(3)].

2.1.3 Cleanliness while Measuring Contact Angles

Contact angle measurements can determine the surface energy, γ, of a solid. To accurately measure the surface energy, we must use a set of fluids and the Lewis acid/base theory with the contact angles, θ, for each fluid. However, a simple contact angle measurement with water will give an approximate answer. This is useful because almost all "contaminants" on a surface affect the measured surface energy. This connection is what we exploit when using contact angles.

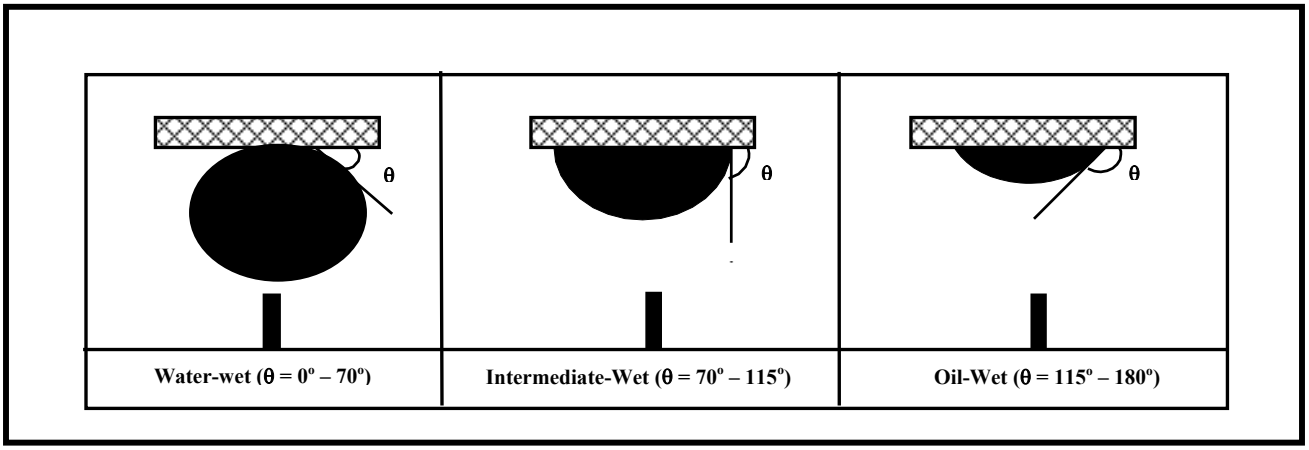

Figure 3. The Conventional Sessile Drop Contact Angle Technique (after Rao[2])

2.2 Wettability In Solid-Liquid-Liquid Systems

2.2.1 What Is Wettability?

Wettability is defined as the ability of one fluid to spread or adhere on a rock surface in the presence of other immiscible fluids. It is the means of characterizing the nature of rock-fluid interactions in reservoirs. Wettability affects relative permeability, electrical properties, and saturation profiles in the reservoir. The wetting state impacts waterflooding and aquifer encroachment into a reservoir. Wettability play an important role in the production of oil and gas as it not only determines initial fluid distributions, but also is a main factor in the flow processes in the reservoir rock. Wettability affects primary recovery, oil recovery by water flooding, and also the shape of the relative permeability curves.

2.2.2 Methods of Measuring Wettability

Many different methods have been proposed for measuring the wettability of a system. They include quantitative methods- contact angles, imbibition and forced displacement (Amott), and USBM Wettability method; and qualitative methods like imbibition rates, microscope examination, flotation, glass slide method, relative permeability curves, permeability/saturation relationships, capillerimetric method.

Although no single accepted method exists, three quantitative methods for determining wettability are generally accepted and used:

(1) Contact Angle Measurement Techniques

(a) Sessile Drop Technique

The concept of wettability is generally illustrated using the sessile drop technique. A drop of crude oil is placed on the solid surface immersed in water or brine. As the oil drop is placed on the surface, the drop makes an angle with the solid surface. The angle between the surface and the tangent at the drop boundary is then measured. The angle is usually referred to as the contact angle the liquid makes with the solid surface. Wettability is generally referred by the water-advancing contact angle [4], but here in this technique water recedes to make way for the oil, thus actually depicting the water receding angle.

(b) Modified Sessile Drop Technique

The modified sessile drop technique is one wherein a drop of crude oil is placed between two solid surfaces immersed in water. In this technique, the drop on the upper crystal behaves as a sessile drop and on the lower crystal behaves as a pendant drop. This difference in exposure was the reason for the inconsistent results from this technique [4].

(c) DDDC Technique

This technique, which is used in this experimental study, will be discussed in more detail in Section 3.1.

(d) Wilhelmy Plate Technique

This technique will be discussed further in Section 3.2

(2) The Amott Method

The Amott method combines natural imbibition and forced displacement to measure the average wettability of the core. This method is based on the fact that the wetting fluid will generally imbibe spontaneously into the core, displacing the non-wetting one.

The wettability index to water, δ_w, is given by

$$\delta_w = \frac{V_{osp}}{V_{ot}} \quad \text{.....(3)}$$

V_{osp} = oil volume displaced by spontaneous water imbibition

V_{ot} = the total oil volume displaced by imbibition and centrifugal (forced) displacement

$$\delta_o = \frac{V_{wsp}}{V_{wt}} \quad \text{.....(4)}$$

V_{wsp} = water volume displaced by spontaneous oil imbibition alone

V_{wt} = total displaced by oil imbibition and centrifugal (forced) displacement.

The difference $\delta_w - \delta_o$ is often used to characterize wettability by a number δ_{AH} called the Amott-Harvey index. The main shortfall of this method and its modification is that they are insensitive near neutral wettability, and another weakness is its failure to distinguish between important degrees of water-wetness, all of which will give a δ_w very close to unity [3].

(3) The USBM Method

This test, like the Amott test, measures the average wettability of the core. In the USBM method, drainage and imbibition capillary pressures are measured using a centrifuge. The wettability number is defined by

$$N_W = \log\left(\frac{A_1}{A_t}\right) \quad \text{.....(5)}$$

where A_1, A_2 are the areas under the capillary versus saturation curves obtained during oil and brine drives, respectively.

A major advantage, which the USBM method has over the Amott test, is its sensitivity near neutral wettability, and the disadvantage is that USBM wettability index can only be measured on plug sized samples because the samples must be spun in a centrifuge.

2.2.3 Dynamic Contact Angles and Wettability

In rock-oil-brine systems, the water advancing contact angle correlates with wettability and is defined as the angle subtended by the oil-water interface with the solid surface when water advances over a previously oil-occupied surface. This dynamic mode corresponds to the situation in the reservoir, where during oil production the resident brine or the injected water advances over the rock surface that was previously exposed to crude oil [(2)]. Similarly when oil advances over a previously water-occupied surface, the angle measured is the water-receding contact angle. The difference between the advancing and receding angles is called hysteresis, which is discussed further in the next section. Based on the extensive literature review, there appears to be very little work done in measuring dynamic contact angles in solid-liquid-liquid systems. Much of the current knowledge is based on studies involving solid-liquid-vapor systems. The same is the case for hysteresis.

2.3 Hysteresis

The difference between the maximum (advancing) and minimum (receding) contact angle values is called the contact angle hysteresis. Understanding contact angle

hysteresis is essential for mastering and controlling many wetting processes, such as coating, spraying, adhesion, and printing. These processes may either rely on contact angle hysteresis or be hindered by it, depending on the specific underlying mechanism. Also successful characterization of wettability depends on a correct interpretation of contact angle hysteresis.

There are three major causes for contact angle hysterisis [5,6]:

a. Surface Heterogeneity.

b. Surface Roughness.

c. Surface Immobility on macromolecular scale.

Much of research has been done in analyzing the significance of hysteresis. It has been used [7] to help characterize surface heterogeneity, roughness, and mobility. Briefly, for surfaces, which are not homogeneous, there will exist domains on the surface that present barriers to the motion of the contact line. For the case of chemical heterogeneity, these domains represent areas with different contact angles than the surrounding surface. For example, when wetting with water, hydrophobic domains will pin the motion of the contact line as the liquid advances thus increasing the contact angles. When the water recedes, the hydrophilic domains will hold back the draining motion of the contact line thus decreasing the contact angle. From this analysis it can be seen that, when testing with water, advancing angles will be sensitive to the hydrophobic domains and receding angles will characterize the hydrophilic domains on the surface. The larger the hysteresis, the greater the impediment to flow.

Hysteresis is usually attributed to surface heterogeneity, roughness, adsorption/desorption, and/or surface deformation [7]. With the exception of roughness and surface deformation, the other causes are physiochemical and have been implicitly

assumed to be contact liquid specific. It is quite relevant for this study to note that surface roughness will generally diminish the apparent contact angle for water-wet surface and increase it for oil-wet surface. Hysteresis resulting from surface heterogeneity can be caused either by heterogeneity in the rock surface composition or differential adsorption of wettability altering compounds. Surface immobility can cause hysteresis by preventing fluid motion necessary for the contact angle to reach its equilibrium value [3].

For situations in which surface roughness generates hysteresis, the actual microscopic variations of slope in the surface create the barriers, which pin the motion of the contact line and alter the macroscopic contact angles. The contact angle can also be considered in terms of the thermodynamics of the materials involved. This analysis involves the interfacial free energies between the three phases and for a solid-liquid-liquid system is given by:

$$\sigma_{lv} \cos \theta = \sigma_{sv} - \sigma_{sl} \quad \text{.....(6)}$$

where σ_{lv}, σ_{sv} and σ_{sl} refer to the interfacial energies of the liquid/vapor, solid/vapor and solid/liquid interfaces, θ, is the contact angle.

Extrand et al. [7], in their experimental study of contact angle hysteresis in a solid-liquid-vapor system, used a wide range of contact liquids with varying molecular weights, viscosities, polarities and surface tensions along with a wide range of substrates such as five varieties of polymers and silicon wafers. Surface roughness was measured using an Atomic Force Microscope (AFM). Advancing and receding contact angles were measured at room temperature using an inclined plane. All surfaces were relatively smooth with Polytetraflouroethylene (PTFE) being the roughest and silicon being the smoothest. Hysteresis was calculated using four different techniques and it was found that $\Delta\theta$, $\Delta\text{Cos}\theta$ and $\gamma_l \Delta\text{Cos}\theta$, increased with γ_l and decreased with γ_s. If $\theta_r = 0$, H=1,

otherwise H had a unique value for each surface, independent of the contact liquid used. They also reported that surface roughness was supposed to be the least cause of hysteresis. They concluded that surface roughness played a minor role and hysteresis was dominated by chemical interactions or heterogeneities.

Murmur [8], in his review on contact angle hysteresis in solid-liquid-vapor systems on heterogeneous smooth surfaces observed the dependence of drop volume and asymmetry on contact angle hysteresis. He used a simple two-dimensional drop on a heterogeneous, but smooth surface. Energy barriers between successive equilibrium states play an important role in contact angle hysteresis. This free energy depends on the drop volume. Such dependence would lead to hysteresis, since the barriers would change when the drop volume is increased or decreased during experimental measurement of contact angle hysteresis. As the drop volume increases, the metastable equilibrium points and the barriers associated with them increase and hence the contact angle hysteresis. He also showed that asymmetry in placing the drop relative to the pattern of heterogeneity of the surface may have a major effect on the behavior of the drop.

2.4 Effect of Surface Roughness on Wettability

2.4.1 Solid-Liquid-Vapor Systems

Wenzel [9] studied the effect of roughness on contact angle and proposed a theory which is used to derive the relationship between the angle observed on a smooth surface, θ_E, and the advancing angle on a rough surface θ_A:

$$\text{Cos } \theta_A = r \text{ Cos } \theta_E. \qquad (7)$$

where r is the roughness factor, defined as the ratio of the surface area of the rough surface to that given if the solid were microscopically smooth.

If the surface is rough enough with a large number of asperities in it, the angle measured with the horizontal will actually be the apparent contact angle because the asperity on the surface might not be horizontal as illustrated by Adamson [5]. The true contact angle can be much larger than what we measure with the horizontal.

Cassie and Baxter [10] in their study on waterproofing fabrics used the example of bird feathers to show the difference between true and apparent contact angles. They reported an apparent contact angle of 150^{o} as opposed to a true contact angle of 100^{o}.

Oliver et al. [11] and Mason[12] in their theoretical study of the influence of surface roughness on spreading and wettability showed by calculation of the equilibrium shape of the liquid drop resting on a rough surface the relation between the true equilibrium contact angle at the three phase contact line and the apparent contact angle observed microscopically at the geometrical contour plane of the solid. In their attempt to clarify the Wenzel's relation between the apparent and true contact angles they considered surfaces having random roughness to derive a statistical relation between these angles. They concluded that in addition to surface roughness, surface texture is one of the primary causes of hysteresis.

Mason [12] examined the equilibrium spreading in solid-liquid-vapor systems by using polymer melts and low vapor pressure liquids at two extremes of surface roughness. On examining spiral grooves he observed a stick-jump in contact line movement, which agreed well with the theory of concentric grooves. On radial grooves the contact line movement was reversible and advancing contact angle agreed well with Wenzel's equation. On other forms, the contact line jump movement was less evident as channeling increased, with the result that spreading varied between limiting cases. On further study using scanning electron microscope, Mason suggested that hysteresis might

be due to other roughness factors such as sharp edges, which inhibit contact line advance and recess.

Morrow [13] showed the importance of surface roughness on the apparent contact angle and contact angle hysteresis in solid-liquid-vapor systems. He studied the effect of roughness on contact angle through capillary rise in PTFE tubes. He reported an increase in contact angle hysteresis between smooth tubes and rough ones. Furthermore, he reported that severe roughness did not change the value of previously obtained contact angles on rough surfaces.

Anderson [14] in his wettability review noted the following regarding surface roughness on wettability. Contact angle on a smooth surface remains fixed, whereas on rough surfaces, as in reservoir rocks, where there are sharp edges, the angle depends on the geometry of the rock surface. Surface roughness diminishes the apparent contact angle when the contact angle measured on a flat plate is less than 90^{o}, and increases the apparent contact angle when the true contact angle is greater than 90^{o}.

Robin et al. [15] describe an experimental study of how chemical heterogeneity and surface roughness can affect wetting phenomenon. They used various heterogeneous substrates such as horizontal stripes, vertical stripes, checkerboard patterns, and low surface energy PTFE solids. Contact angles were measured using the Wilhelmy Plate technique. Their study led to the conclusion that uniform distribution of heterogeneities yield larger advancing and receding angles than random distribution. They developed a model for the effects of both heterogeneity and roughness, and the results from their modeling were found to be consistent with experimental measurements of Cassie [10]. They concluded that heterogeneity and roughness have significant effects on contact

angle hysteresis, and that in reservoir rocks the contact angle within pore space will exhibit more hysteresis than that observed on a smooth surface.

2.4.2 Solid-Liquid-Liquid Systems

Yang et al. [16] studied various mechanisms for contact angle hysteresis and advancing contact angles. They used the atomic force microscope to characterize the mica surfaces that have been equilibrated in brine and then aged in crude oil at an elevated temperature of 80^{o}C. They used two crude oils, brine and mica surfaces. They recorded a linear correlation between the advancing contact angle and the surface mean roughness. The advancing angle increased from 20^{o} for an average roughness of 0.08 nm to 144^{o} for roughness of 28 nm, thereby showing that surface roughness has significant effect on the advancing contact angle measured by the sessile drop technique. They concluded that in addition to surface topology, there are other properties like chemical properties of the oil, which are important in determining the advancing contact angle.

2.4.3 Summary

Most of the above reported studies, except that by Yang et al. [16], have considered solid-liquid-air systems. In spite of these limited number of studies there is very little known about the impact of surface roughness on contact angles involving two immiscible liquids such as in reservoirs containing brine and crude oil.

2.4.4 Apparent versus True Contact Angle

Contact angle θ, (as shown in Figure 4) which is a representation of solid-liquid-fluid system in equilibrium. Knowledge of contact angle is important as it is a means of characterizing wettability.

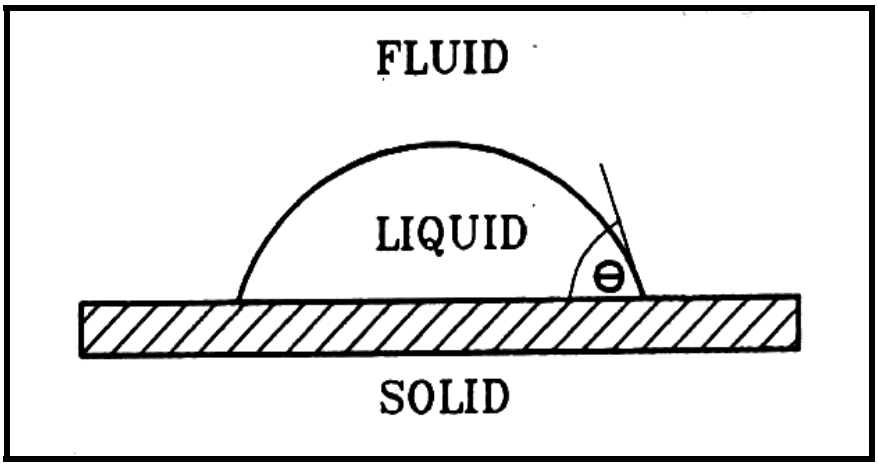

Figure 4: Schematic diagram of a drop on a solid surface (after Marmur[8])

Physical structure and mineralogical composition of a particular rock surface has a varied impact on contact angle and is a major problem associated in measuring contact angle. The physical structure of a particular rock sample refers to the surface texture of the sample as to how smooth or rough the surface is. The contact angle measured or obtained by using the Young's equation is based on an ideal surface, which is smooth in texture and chemically homogenous [(8)].

The reservoir rock samples are generally far from "ideal" as they are rough and can be chemically heterogeneous. The measurement of contact angle when using such rough surfaces requires a distinction between the true contact angle θ, and the observed or apparent contact angle θ_a. The difference between the apparent and true contact angle is shown in Figure 5. The measurement of true contact angle requires that measurements be made on an ideally smooth surface and angle measured microscopically. Since all the surfaces we come across are rarely "ideal," the angle observed is the apparent contact angle and not the true contact angle, θ [(8)].

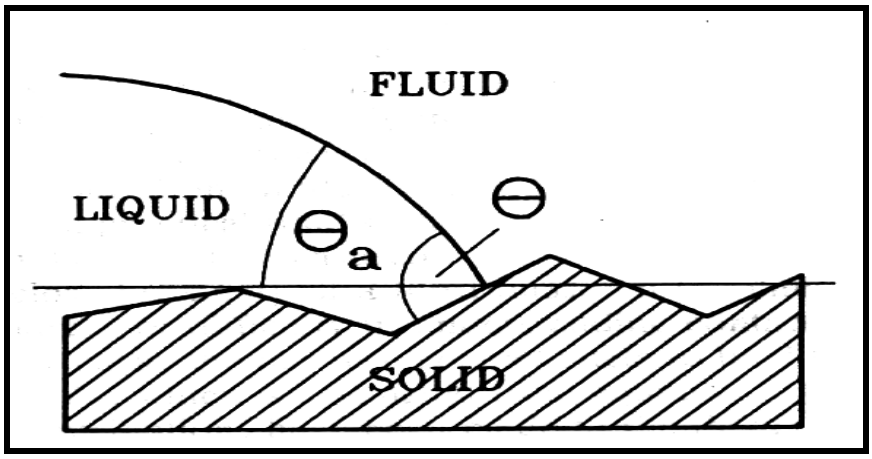

Figure 5: Intrinsic Contact angle, θ, and the apparent contact angle, θ_a, on a model rough surface (after Marmur[8])

2.5 Effect of Brine Composition on Wettability

Several previous studies have been reported in the literature that describes the effect of brine composition on oil recovery by waterflooding. Jones [17] reported the capabilities of small proportions of divalent cations, such as calcium and magnesium, for controlling clay blocking. The behavior evidently depended upon the Cation exchange properties of the clays, which favor adsorption of calcium and magnesium over sodium. Clays having sufficient adsorbed calcium and magnesium resisted dispersion by water and consequent blocking of permeability.

Mungan [18] investigated the role of pH and salinity changes on core damage. He concluded that the primary cause of permeability reduction was blocking of the pore passages by dispersed particles. Cores that were essentially free of clays were damaged by flow of acidic or alkaline solutions. Permeability reduction due to salinity changes occurred regardless of the type of clay. Clay particles are negatively charged (anions) and adsorb positively charged species (cations). Cations can have one or more positive charges, for example: monovalent (K^+, Na^+), divalent (Ca^{2+}, Mg^{2+}, Ba^{2+}), etc. Clay

particles are also naturally dispersed on the pore surface of the reservoir rock. A change in the salt concentration (salinity) or pH of the reservoir fluid can liberate these clay particles. A change in salinity can also cause the clay particle to swell and clog the pores thus resulting in lower permeability.

Kwan et al. [19] investigated the permeability damage due to fines migration in extracted core material from the Clearwater formation of Cold Lake, Alberta. They observed that the absolute permeability of the preserved core, typically between one and three darcies was not significantly affected when brine (NaCl or $CaCl_2$) alternating with distilled water was injected. They concluded permeability and oil recovery were nearly independent of brine composition.

Souto et al. [20] dealt with the effects physico-chemical changes induced by brine replacement on the permeability behavior of consolidated argillaceous sandstones. They observed formation damage due to clay migration when the injected brine replaces connate water during operations such as waterflooding, chemical flooding including alkaline, surfactant, and polymer processes. Core flow experiments were conducted with clayey sandstones with brines prepared from sodium and potassium salts. They developed a model, which can demonstrate the batch effects of brine composition based on the pH and salinity changes. They studied the effects of clay content using these different brines and found out that permeability damage occurs less with potassium salts than with sodium salts

Yildiz and Morrow [21] investigated the effect of brine composition on oil recovery by waterflooding. Two brine compositions were tested, namely 4 % NaCl + 0.5 % $CaCl_2$ and 2 % $CaCl_2$. Tests in which the same brine was used throughout were referred to as standard waterfloods and standard imbibition tests and those in which the brine

composition was changed one or more times during the test were referred to as mixed-brine tests. In standard waterfloods, 2 % $CaCl_2$ gave 5.5 % higher waterflood recovery than 4 % NaCl + 0.5 % $CaCl_2$. For mixed waterfloods, Berea sandstone gave waterflood recoveries of Moutray crude oil ranging from 59 –72 % of original oil-in-place (OOIP), according to the choice of initial and injected brine compositions and initial water saturation. Changes in brine composition can be favorable to recovery as compared to standard waterfloods. They observed that waterflood recoveries were improved significantly if the core was initially equilibrated with 2 % $CaCl_2$ and subsequently flooded first with 4 % NaCl + 0.5 % $CaCl_2$ and then with 2 % $CaCl_2$, they attributed this to the presence of divalent Ca^{2+}.

Tang and Morrow [22] investigated the effect of aging and displacement temperatures, brine and oil composition on wettability and the recovery of crude oil by spontaneous imbibition and waterflooding. Brine concentration was varied by changing the concentration of total dissolved solids of the synthetic brine in proportion to give brine of twice, one tenth, and one hundredth of the reservoir brine concentration. Tests on the effect of brine concentration showed that salinity of the connate and invading brines could have a major influence on wettability and oil recovery at reservoir temperature. Oil recovery increased over that for the reservoir brine with dilution of both the initial (connate) and invading brine or dilution of either, for all crude oils, water-wetness (measured by using core floods) and oil recovery increased with increase in displacement temperature.

Yildiz et al. [23] investigated the effect of brine composition on waterflood recoveries of a Prudhuoe Bay crude oil. They used 4 wt % NaCl + 0.5 wt % $CaCl_2$ and 2 wt % $CaCl_2$ brine compositions and obtained 16 % higher recovery with 4 wt % NaCl +

0.5 wt % $CaCl_2$ composition. They demonstrated that brine composition could have a large effect on oil recovery and that displacement efficiency was not necessarily dominated by the composition of the initial brine.

Muhammad [34] in his study on the effect of brine composition in solid-liquid-liquid systems reported an increase in water-advancing angle as the concentration of monovalent salts in the aqueous phase increased. He further reported that as the concentration of salts increased, the water film on the rock surface between the drop phase (crude oil) and the rock substrate weakened.

2.6 Effect of Surfactants on Wettability

A surfactant is a polar compound, consisting of an amphiphilic molecule, with a hydrophilic part (anionic, cationic, amphoteric or nonionic) and a hydrophobic part. As a result, the addition of surfactant to oil –water mixture would lead to a reduction in the interfacial tension.

Depending upon the nature of the hydrophilic group, the surfactants are classified as:

1. Anionic - the surface-active portion of the molecule bears a negative charge, for example, $RC_6H_4SO_3^-Na^+$ (alkyl benzene sulphonates).
2. Cationic – the surface active portion bears a positive charge, for example $RNH_3^+Cl^-$ (salt of a long- chain amine)
3. Amphoteric (or) Zwitterionic – both positive and negative charges may be present in the surface active portion, for example $RN^+H_2CH_2^-COO^-$ (long chain amino acid)
4. Nonionic - the surface active portion bears no apparent ionic charge, for example, $RCOOCH_2CHOHCH_2OH$ (monoglyceride of long chain fatty acid)

When a surfactant is injected, it disperses into oil and water and thus creates a low interfacial tension zone, in which the capillary number increases greatly. As a result, more of the otherwise immobile oil becomes mobile. At the same time, an oil-in-water emulsion would form, the drops of which would tend to block the larger pores. This often leads to an improvement in the effective mobility ratio. The injected surfactant continues to mobilize oil and bank it up until the surfactant is diluted and otherwise lost to such an extent that it is no longer able to lower the interfacial tension sufficiently to mobilize oil. At that point, the process degenerates into a water flood. The use of surfactants to enhance the oil recovery has the limitations of cost as well as reservoir flow. Cost of suitable surfactants can vary greatly from $0.50 to 2.00 per lb, but the cost has been coming down over the years, although it is linked with the oil prices.

From the viewpoint of reservoir flow, loss of surfactant as a result of adsorption and reaction with minerals are of great concern. Such losses increase as the clay content increases. Gravity segregation of surfactant is also a significant factor given the slow injection rates and large areas involved in the field. Mixing of surfactant with water especially where the process is initiated after a water flood can dilute it to a point where the surfactant is not effective.

Opawale et al. [25] used the Wilhelmy plate apparatus to report on the lipophilic surfactants and to study the interfacial behavior of these surfactants in emulsion formation at the mineral oil-water interface. The value of interfacial tension as a function of the log concentration of the nonionic surfactants has been reported, platinum plate was the solid substrate used.

Sophany et al. [26] in their study on the effect of polyoxyethylene nonyl phenol surfactant on Berea sandstone cores saturated with 1% NaCl found that the ratio of

adsorption and desorption of surfactant on the core increased with the number of ethylene groups by measuring the breakthrough of the surfactant. They also stated that hydrogen bonding was the mechanism that explained the adsorption and desorption of the surfactant on Berea cores. The equilibrium isotherms for the nonionic surfactants became asymptotic at the critical micelle concentration. A similar study was done by Lawson [27] on Berea cores using polyoxyethoxylated octyl phenols and that the isotherms obtained were very similar to those obtained by Sophany et al.

Bock et al. [28] used the Wilhelmy plate apparatus to study the influence of hydrocarbon chain branching on solid-liquid interface. They measured the advancing and receding angles at the Teflon-water interface using linear and branched chain surfactants and found that higher branched surfactants increased the water-wetness of the Teflon surface.

Muhammad [34] in his study on the effect of surfactant concentration on wettability of Yates rock-fluid system using the Wilhelmy apparatus reported that as the concentration of surfactant increased the interfacial tension reduced to a certain values beyond which it did not change even for a higher concentration of the surfactant. The measured advancing and receding angles were 90^{o} for all the concentrations of the surfactant indicating intermediate wettability of dolomite.

2.7 Summary of Literature Review

The previous sections have reported the effects of brine composition, rock mineralogy and surfactants on reservoir wettability. Most of the work reported on surface roughness has been concerned with solid-liquid-vapor systems using smooth surfaces. These are not representative of the reservoir rock-fluid systems. Furthermore, there is very little work that has been reported on solid-liquid-liquid systems, which is of interest

to the petroleum industry. The effect of surface roughness on wettability and hysteresis in solid-liquid-vapor systems has conflicting conclusions. Some stated that roughness does not affect hysteresis and wettability, while others reported that roughness along with other parameters such as heterogeneity and topography of the rock surface affected hysteresis and yielded larger advancing contact angles.

The use of surfactants to alter reservoir wettability as a means to enhance oil recovery is gaining attention in the industry. This study thus aims at examining the effects of rock characteristics (surface roughness and rock mineralogy), addition of a nonionic surfactant and brine composition on reservoir wettability as characterized by dynamic contact angles.

CHAPTER 3

EXPERIMENTAL APPARATUS AND PROCEDURES

3.1 Dual-Drop-Dual-Crystal Apparatus

The Dual Drop Dual Crystal (DDDC) cell and the associated apparatus for carrying out the contact angle tests at ambient conditions are shown in Figures 6 and 7. The apparatus is set up in such a way that the upper crystal moves in the vertical direction and the lower one moves in the horizontal direction. The lower crystal can be rotated around its horizontal axis so that both of its surfaces could be used for experimentation. There is a provision for letting the crude oil into the cell through a syringe, which is connected to 1/16" diameter tubing, which can be inserted in the cell, and its height adjusted as required by the particular experiment.

3.1.1 Preparation and Cleaning of the Apparatus

The cell is first cleaned with deionized water and is then filled with brine. After an experiment is completed, the inlet valve is opened to let some brine in so that it drains the oil floating at the top. This is done to avoid the floating oil from entering the cell and contacting the Teflon interior.

All glassware were cleaned by soaking overnight in hot sulphuric acid to which ammonium persulphate crystals were added followed by boiling in deionized water for two hours to dissolve any traces of acid that remain. Soaking them in benzene first to dissolve all the crude oil and then in acetone to dissolve all the benzene cleaned the glassware that was used with crude oil.

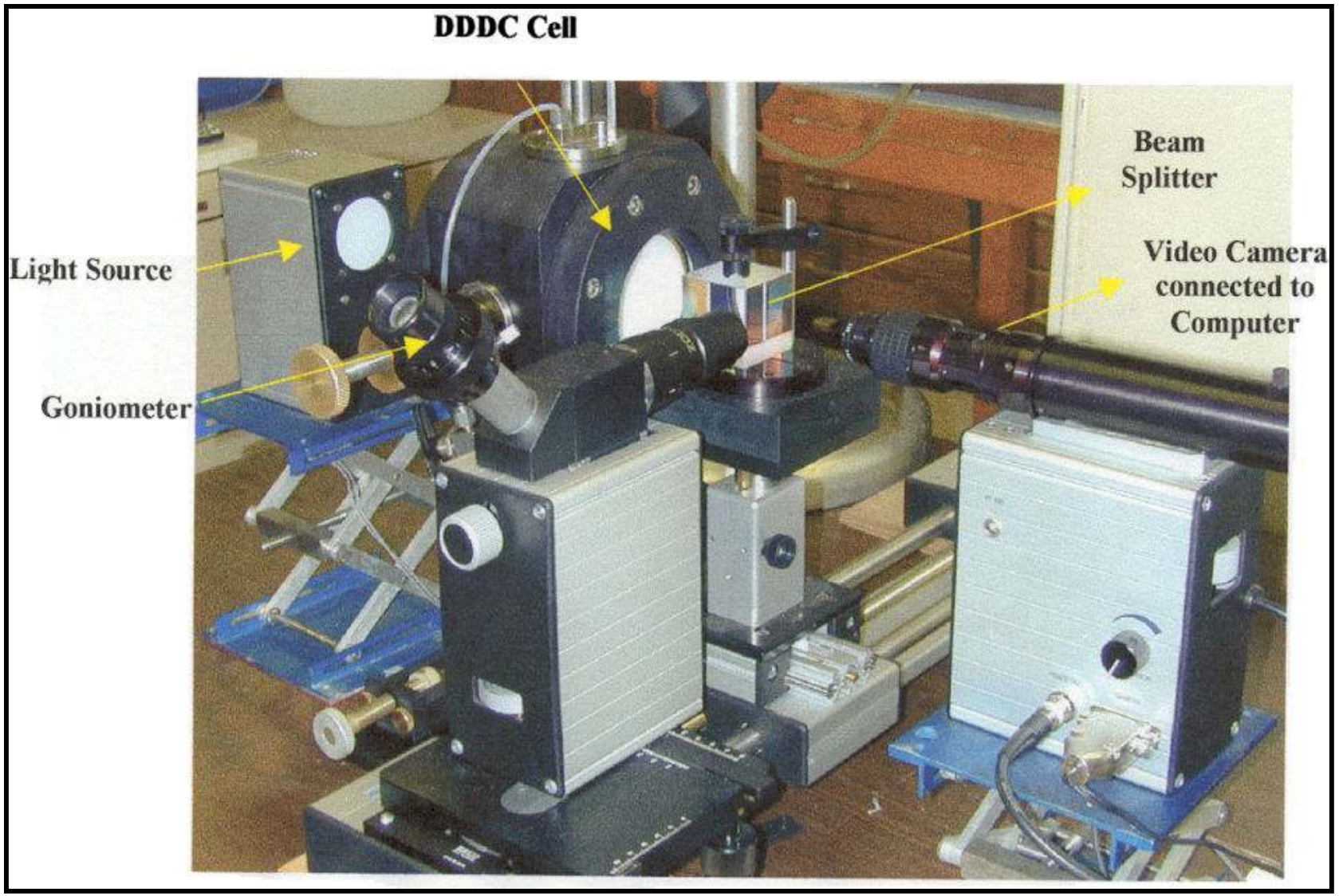

Figure 6: Assembled Dual-Drop-Dual-Crystal Ambient Cell with Goniometer, Digital Video Camera and Beam Splitter

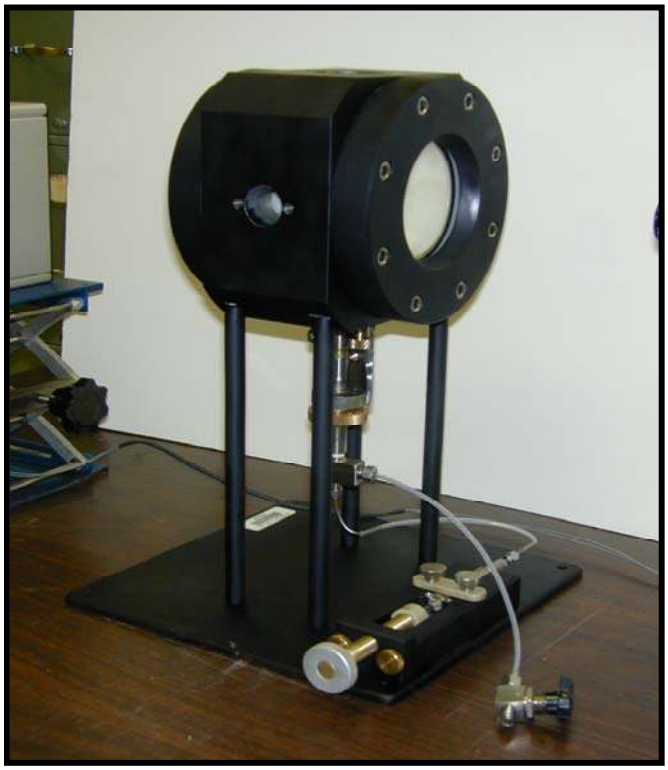

Figure 7(a): Close-up View of the Ambient DDDC Cell

Figure 7(b): Close-up View of the Upper and Lower Crystal Holders

3.1.2 Experimental Procedure

Previously cleaned rock substrates are placed in both the upper and lower holders, which are then assembled carefully into the thoroughly cleaned cell. The reservoir brine is taken in a large container kept at a sufficient height above the cell to allow flow by gravity. The cell is gradually filled up and some fluid is allowed to drain from the top to ensure that there are no air bubbles trapped in the cell.

The crude oil is now let into the cell drop by drop using the needle inserted at the bottom of the cell. After releasing a few oil drops to float on water at the top of the cell, to allow for oil-brine equilibrium, then two separate oil drops are placed on the bottom surfaces of the two crystals. This is done by first sliding the lower crystal sideways (out of the way), raising the oil-dropper tip and placing the drop on the upper crystal, lowering the tip, sliding

the lower crystal back, and placing a drop on the lower crystal. The sizes of the drops are chosen so as to cover as much of the crystal width as possible without losing the drops. The cell is then set aside with all the valves closed to age for a predetermined time for the oil-brine-crystal interactions to reach equilibrium.

The lower crystal holder is then rotated slowly so that the lower surface and the oil drop on it are now facing upwards. When the lower crystal is rotated there are three possible ways the drop could behave: (1) the drop stays attached to the surface due to adhesion, or (2) part of the oil drop floats to the top of the cell due to buoyancy while leaving behind some of the oil on the surface, or (3) all of the oil drop detaches cleanly form the lower crystal without leaving any oil on the surface as shown in Figure 8. In the first two cases the upper crystal is brought down so that the two oil drops merge, and in the third instance the oil drop on the upper surface is made to contact the same area as was previously occupied by the lost oil drop.

Once the two drops are merged, or the upper drop is brought in contact with the lower crystal, the angles and the distances of the drop corners from the edge of the lower solid surface are measured to provide the initial values at zero time. Then the lower crystal is shifted sideways in small steps thus enabling water to advance over a previously oil occupied surface. This lateral shift in the lower crystal position creates a water receding angle on the other side of the oil drop as the oil advances; the angles are measured until they show negligible change. Then a second shift of the lower crystal is made measuring the angles until they become stable. This procedure is repeated until at least two consecutive shifts yield similar water-advancing contact angles.

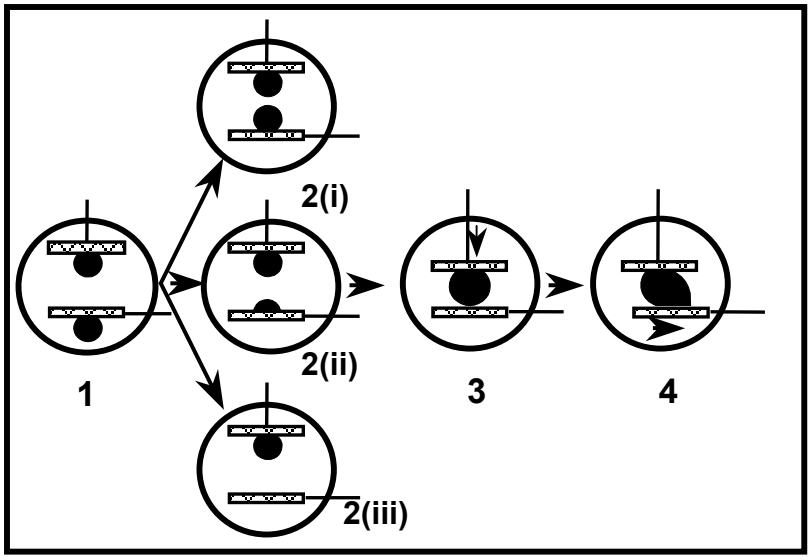

Figure 8: Schematic Depiction of the New Dual-Drop-Dual-Crystal (DDDC) Contact Angle Technique (Reference # 4)

3.1.3 Why Was DDDC Technique Used?

The DDDC Technique is very different from the conventional modified sessile drop technique, wherein a drop of crude oil is placed between two crystals to initiate the experiment. In such a case, the drop behaves as a sessile drop on the upper crystal and as a pendant drop on the lower crystal surface. In other words, the two crystal surfaces possess different histories of exposure to crude oil.

In the new DDDC technique, both oil drops on the two crystal surfaces are aged as sessile drops with buoyancy forces acting upwards. This initial uniformity in the exposure of both surfaces to crude oil is a key factor in obtaining consistent and meaningful contact angle results. It also helps in monitoring, without ambiguity, of the solid-oil-water three phase contact line (TPCL) movements within the areas previously exposed to crude oil [(4)].

In order to get reliable results from the DDDC technique, it was important to monitor the TPCL movement. In almost all the experiments, the TPCL on the lower surface was observed to move because of the fact that both the buoyancy force and the lateral force due to crystal displacement acted in such a manner as to pull the oil drop away from the lower

surface. This was not the case at the upper surface, since buoyancy acted upon to push the oil drop against it. Therefore, the contact angle measured at the upper surface did not meet the definition of either water-advancing or water-receding contact angle due to the absence of the TPCL movement on it. Hence the contact angles were measured on the lower surface.

It was important to ascertain that the movement of the TPCL occurred within the area of the lower surface that was initially occupied by the oil. If the TPCL was made to move beyond the oil exposed area, erroneous results will be obtained. The method of monitoring the movement of TPCL within and beyond the initial-oil occupied area is shown in Figure 9 below.

Monitoring TPCL is done by initially measuring R_i and L_i. these are the distances of the right and the left edges of the drop from the left edge of the lower crystal. As the TPCL moves when the lower crystal is shifted, new R and L distances are obtained. As long as the R/Li remains greater than or equal to 1, the contact angle satisfies the definition of water-advancing contact angle since it lies within the previously oil-exposed area. As we move the crystal further the R/Li ratio falls below unity thereby showing that the drop has moved out of the oil exposed area, thus signifying the end of the experiment.

3.2 Wilhelmy Plate Apparatus

Figure 10 shows the setup for the Wilhelmy apparatus. The instrument utilizes a Cahn 2000 microbalance having a sensitivity of 1 μg, and a control unit, which are interfaced to a computer. A stepper motor (Seiberco Inc.) with a platform is connected to the computer and can raise or lower the platform with controlled movements from the computer. The microbalance consists of a balance beam with three fine metal loops attached to it from where the samples and counterweights are suspended.

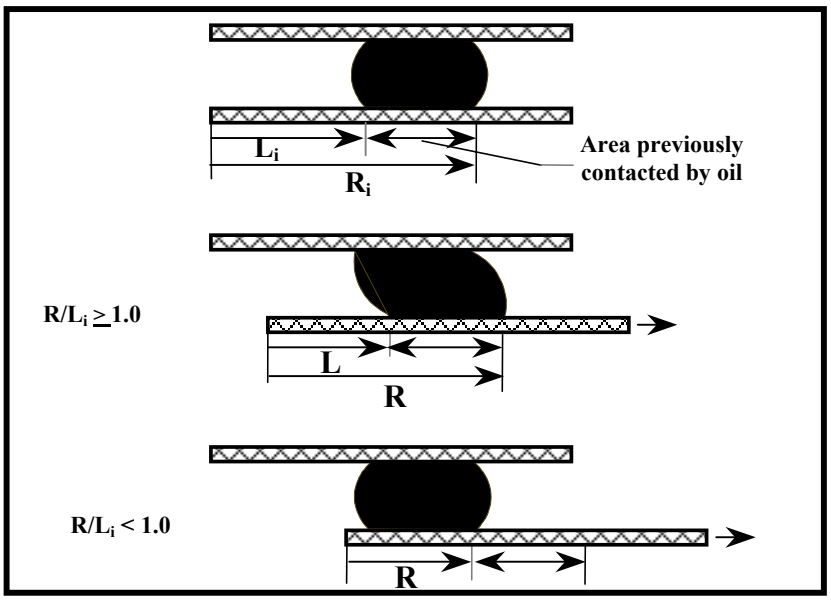

Figure 9: Monitoring of Contact Line Movement, L/R_i
(Reference # 4)

Raising the platform until the oil-air interface touches the glass slide, which is suspended from the microbalance, simulates the movements of the fluids in the reservoir. The change in weight as the slide touches the oil surface is detected by the microbalance and sent to the computer, which reads this as adhesion tension. The shaft, which raises or lowers the platform, was adjusted to move at a speed of 255 revolutions per minute. The platform travels a total distance of approximately one inch in the advancing mode and moves down the same distance in the receding mode. The entire assembly is housed inside a cabinet especially designed for this setup to prevent air currents from affecting the sensitive measurements. All measurements were carried out at 24°C.

3.2.1 Dynamic Wilhelmy Plate Technique and Interpretation of Wilhelmy Results

The Wilhelmy Plate apparatus was calibrated by conducting tests with the same fluids and solid substrate pairs as reported in the published literature [29]. Once the calibrations were apparatus completed, experiments were run with different combinations of fluid pairs on the

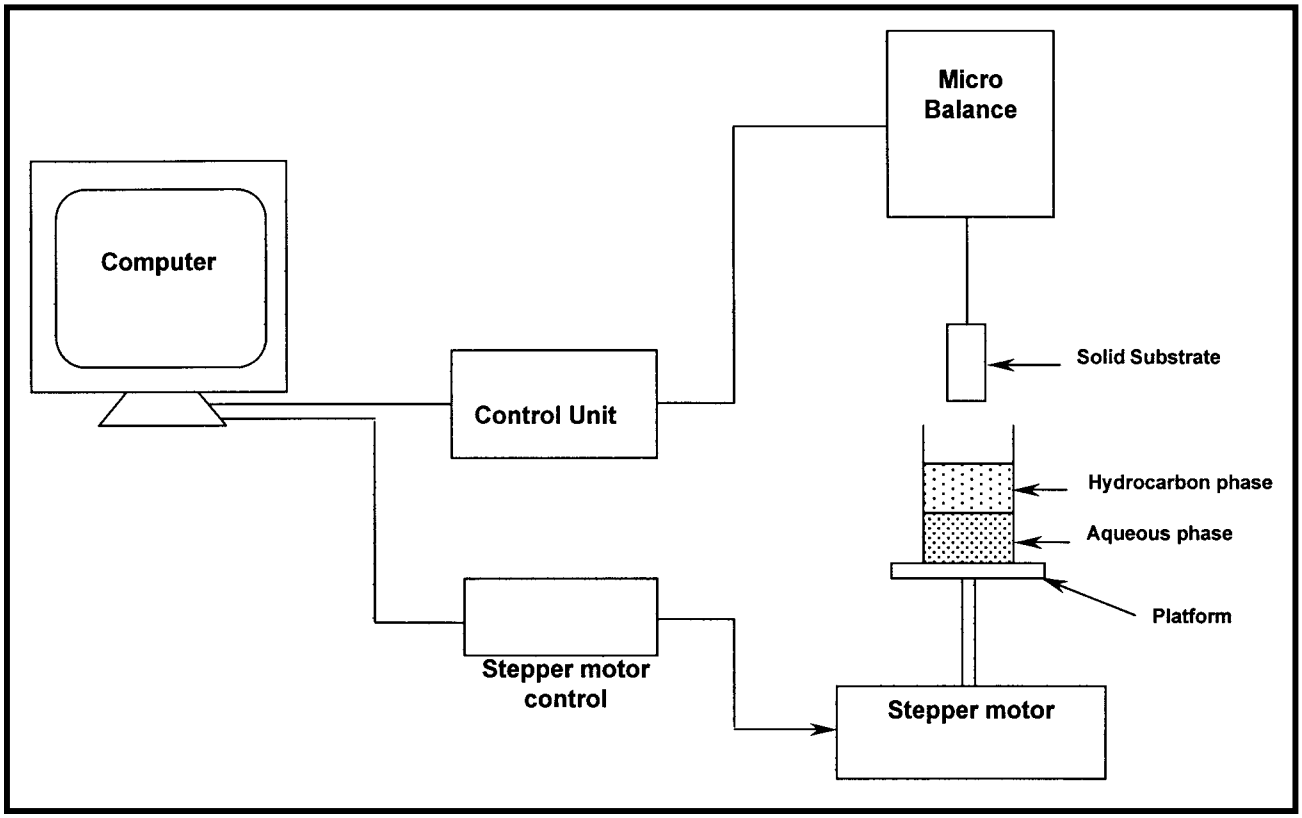

Figure 10: Wilhelmy Plate Apparatus

Wilhelmy using solid substrates and aging the solid substrates in the liquid phases. The aging was done by immersing the slide in the aqueous phase followed by immersing the same slide in the hydrocarbon phase for an equal length of time of around 24 hrs.

The procedure used for the measurement of advancing and receding adhesion tension and calculating advancing and receding contact angles are shown in Figures 11a and 11b, which show the Wilhelmy test data for water-wet and oil-wet cases, respectively. Hexadecane-water fluid pair shows a water-wet behavior on a glass slide (Figure 11a) and an oil-wet behavior on a Teflon slide. The Wilhelmy plots obtained here are similar to those reported in the literature [30]. The weight of the thin surface of the solid is tared before the run is made so the microbalance scale only senses the force as the solid touches the liquid surface. The slide is acted upon by gravitational force as it hangs from the balance. The forces of buoyancy and

interfacial tension come into play as the slide traverses through the fluids and the fluid-fluid interface.

The dark solid lines in Figures 11a and 11b show the advancing mode as the platform is raised and the vessel containing the oil and water phases is brought closer to the glass slide that is suspended from the microbalance. As the slide touches the oil phase, a sudden vertical rise is seen on the profile, which is due to the surface tension of oil. The downward slope is due to the movement of the slide in the oil phase and represents buoyancy force as the slide moves within the oil phase.

A second rise in the profile is seen at the oil/water interface, which is the adhesion tension in the water-advancing mode. Adhesion tension is the product of interfacial tension and Cos θ. The downward slope corresponds to the movement of slide within the aqueous phase. As the advancing mode is completed, the platform starts traveling downward and the substrate is gradually pulled out from the aqueous phase first, and then from the oil phase. This receding mode is shown in Figure 11a and 11b as dotted lines. Due to adhesive forces that exist at the interface of solids and liquids, the liquid surface is pulled up a small distance in the receding mode before the slide can detach itself and this causes the receding cycle to take slightly different path than the advancing cycle.

The upward jump in force shown in Figure 11a at the three-phase line of contact demonstrates water-wet behavior since the solid surface is preferentially wetted by the denser phase in advancing mode. A downward adhesion tension at the oil/water as in Figure 11b indicates oil-wet behavior. The adhesion tension for the oil-wet case is calculated by extrapolation of the receding line to the oil-water interface and measuring the vertical distance as shown in Figure 11b. The solid surface prefers to be wetted by the lighter phase and the

force on the slide is decreased. It can be understood in terms of the two forces acting in opposite directions.

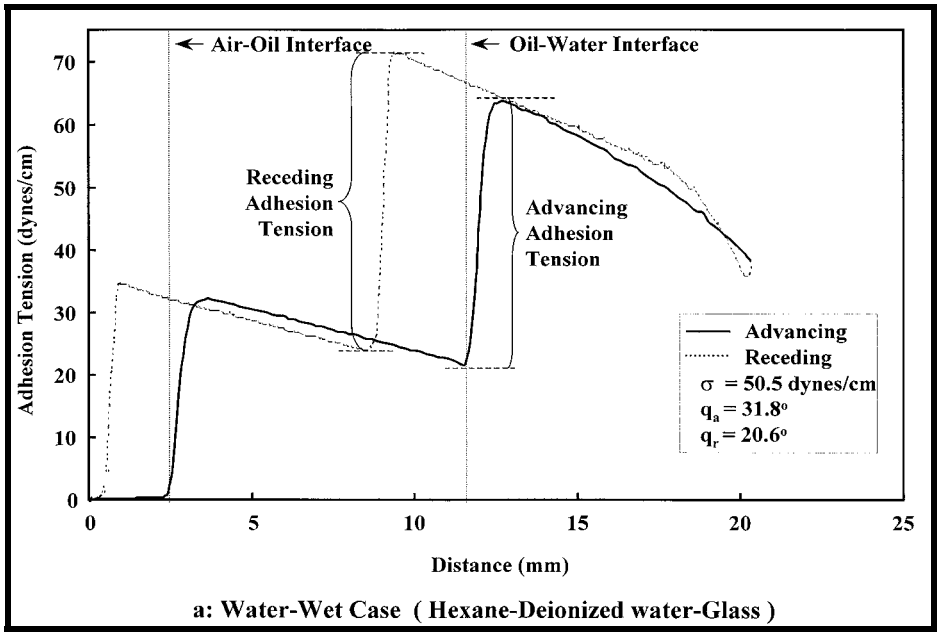

Figure 11 a: Wilhelmy Plots for Water-Wet Cycle (Reference # 34)

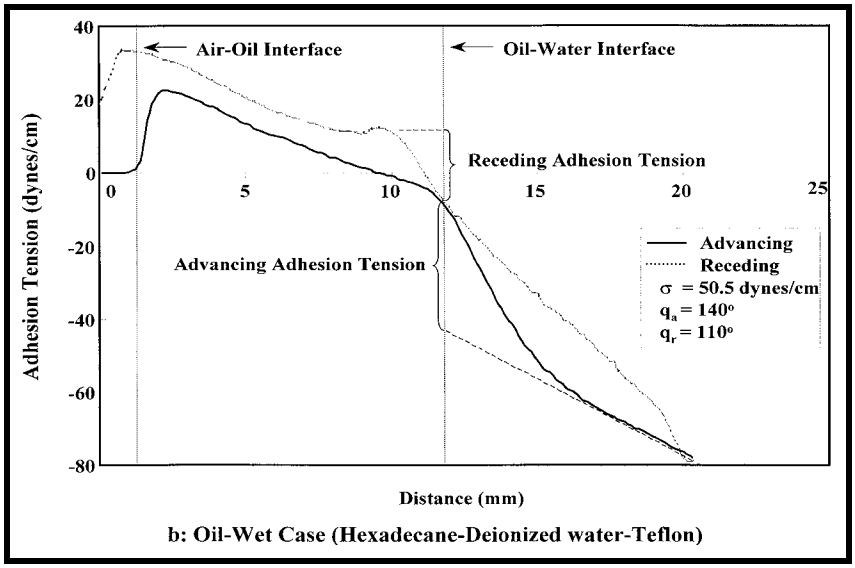

Figure 11 b: Wilhelmy Plots for Oil-Wet Cycles (Reference # 34)

The aqueous phase is trying to pull the slide down whereas the hydrocarbon phase is trying to pull the slide up. What is seen on the plot is the resultant of the two forces acting on the slide. This wetting behavior is quantified by the contact angles that are calculated from measured adhesion tension and interfacial tension**.**

3.3 Interfacial Tension

3.3.1 What Is Interfacial Tension and Why Is It Important?

The surface free energy that exists between two immiscible liquid phases, such as oil and water is known as the interfacial tension. The reservoir fluid mechanics involving the flow of oil, gas and water in the porous medium is governed by both the fluid-fluid and rock-fluid interactions. The fluid-fluid interactions include the phase behavior and miscibility aspects – both of which are influenced by the interfacial tension at the operating thermodynamic conditions of composition, pressure and temperature. Wettability and adhesion are interconnected through the oil-water interfacial tension [(24)].

Capillary pressure and relative permeabilities are dependent on rock wettability as well as the location and nature of distribution of oil, water, and gas phases, which are governed by the spreading coefficient. This spreading coefficient depends on the interfacial tension of the oil/water/gas interfaces. Therefore, it can be seen that the tension at the three interfaces between oil/water/gas phases influences almost all the parameters that govern their flow behavior and trapping mechanisms. Hence there is a need for the knowledge of the behavior of oil-water-gas interfacial tensions at reservoir conditions.

3.3.2 Computerized Axisymmetric Drop Shape Analysis

Drop shape analysis is a convenient way to measure surface tension. Rotenberg et al.[(31)] traced the developments and limitations of various methods used with the pedant and sessile

drops for liquid-liquid interfacial tension measurements. They presented a procedure for obtaining the values of surface and interfacial tension and contact angle from the shape of the axisymmetric fluid interfaces. This method is known as the axisymmetric drop shape analysis (ADSA) technique. The ADSA technique relies on numerical integration of the Laplace equation of capillarity:

$$\Delta P = \gamma \left(\frac{1}{R_1} + \frac{1}{R_2} \right) \quad \text{.....(8)}$$

Where γ is the interfacial tension, R_1 and R_2 are the principal radii of curvature and ΔP is the pressure difference across the interface or the capillary pressure.

The principal practical advantage of the technique is that calibration is straightforward in that only optical magnification is needed. This can be measured with high accuracy and is easy to trace to national standards. (density must be known for this and all methods).

The advent of digital imaging analysis has made possible the use of several data points in defining the profile of an image, be it a pendant or a sessile drop, in order to determine the interfacial tension by fitting to the Young-Laplace equation to the drop profile images.

The analysis of the shape of the drop is the basis for an accurate method of measuring the surface or interfacial tension. This type of analysis has the added advantage of requiring very few samples and it has the ability to measure the dynamic interfacial tensions. It can be applied to liquids under both ambient and as well as high pressures. It can also be applied to measure the interfacial tension between two liquids and one liquid in air.

Rapid analysis of the surface tension by a computer has been applied to track changing surface tension in non-equilibrium systems. First, the geometry of the drop is determined and there are four combinations to choose from [35]:

- Pendant drop hanging down: The drop is the heavier of the two media and hangs down from a dispensing tip.
- Pendant drop floating up: The dispensing tip is below the bubble and the bubble or drop is the lighter of the two phases.
- Sessile drop: This is a sitting drop, as in a drop of water resting on a glass slide. The drop is the heavier phase.
- Sessile drop: The bubble (drop) is floating up against the solid surface and is the lighter phase.

The pendant drop mode is always more accurate than the sessile drop because the assumption of the axisymmetry is easier to satisfy [35]. Sessile drop measurements are used when it is not convenient to form a pendant drop. The choice of drop-down or bubble-up is a matter of convenience in liquid-liquid interfacial work if both fluids transmit light. Otherwise the outside media must be transparent. In liquid-vapor work, the drop-down mode is always used [35].

For a given drop size and shape, interfacial tension is directly proportional to the density difference between the two immiscible fluids. For a given drop shape, interfacial tension is directly proportional to drop size. For a given drop size, a "round" drop will have a high interfacial tension and a stretched "long" drop will have a low interfacial tension.

The major source of error associated with the pendant drop measurements using the axisymmetric drop shape imaging analysis is vibration. The method of eliminating this error is by placing the apparatus in a place free of vibrations so as to minimize this error.

Interfacial tensions are strongly influenced by the solubility of each fluid in the other. In the case of liquid/vapor measurements, the solubilities are intrinsically low. However this is

often not true with liquid /liquid measurements. The presumption is that each is saturated in the other. With liquids, this may take exposures of 24 hours or more to obtain.

Procedure:

The computer analysis of surface tension by pendant or sessile drop first involves the identification of the edge of the drop from the digital image, and the drop profile is identified by a set of points around the image. After identification of the drop profile, the Young- Laplace equation (Equation 8) for an axisymmetric interface is solved for an initial estimate of the parameters on which it depends. The parameters governing the theoretical drop profile are adjusted and Equation (8) is then solved repeatedly until a best fit to the drop profile in the experiment is observed.

3.3.3 du Nuoy Ring Tensiometer for High Interfacial Tension Measurements

Figure 12 shows the Fisher Surface Tensiomat, Model 21, which is used to determine the surface tension and interfacial tension of liquids. In the du Nuoy method [(32)], a platinum-iridium ring of precisely known dimensions is suspended from a counter-balanced lever-arm. The arm is held horizontal by torsion applied to a taut stainless steel wire, to which it is clamped. Increasing the torsion in the wire raises the arm and the ring, which carries with it a film of the liquid in which it is immersed. The force necessary to pull the test ring free from the surface film is measured. The surface or interfacial tension is read from the calibrated dial.

Cleaning of the Apparatus:

All glassware used for this experiment should be cleaned prior to being used for the experimentation. They should be cleaned of any residual oil with benzene followed by cleaning with acetone and water; the glassware is then immersed in a hot boiling solution of sulphuric acid overnight and then boiled in deionized water for couple of hours. The platinum-iridium

ring is cleaned by first dipping it in benzene (to remove hydrocarbons), then squirting it with acetone (to dissolve and benzene) and allowing the acetone to evaporate. The ring is then heated in a Bunsen burner flame to remove any residual hydrocarbons.

Procedure:

Figure 13 shows the figurative description as to how the interfacial tension is measured using the du Nuoy ring Tensiometer. The denser liquid is first poured into the beaker and placed on the sample table beneath the ring. The sample table is raised until the ring is immersed about 1/8" and wetted by the heavier liquid. The knob on the right side is adjusted until the index and its reference are exactly in line with the reference mark on the mirror. Then the lighter liquid is poured onto the surface of the heavier liquid to a depth of about ¼ to ½ inch. The layer of lighter liquid should be deep enough so that the ring will not break through the upper surface of the lighter liquid before the interface film ruptures

The sample table is then lowered till the until the ring is in the interface between the two liquids, while at the same time adjusting the knob on the right side of the case to keep the index lined up with the reference mark on the mirror. The interface between the two liquids will become distended, but the index must be kept on the reference. The two simultaneous adjustments are continued until the distended film at the interface ruptures. The scale reading at the breaking point of the interfacial film is the interfacial tension.

3.3.4 Spinning Drop Interfacial Tensiometer for Low Interfacial Tension Measurements

Spinning drop interfacial Tensiometer shown in Figure 14, is used for the measurements of very low interfacial tensions. This method involves rotating an oil drop in an aqueous phase at high speed in a precision Pyrex bore tube. Muhammad [34] has discussed this method at length in his work on compositional dependence of reservoir wettability.

Figure 12: du Nuoy Ring Tensiometer for High Interfacial Tension Measurements

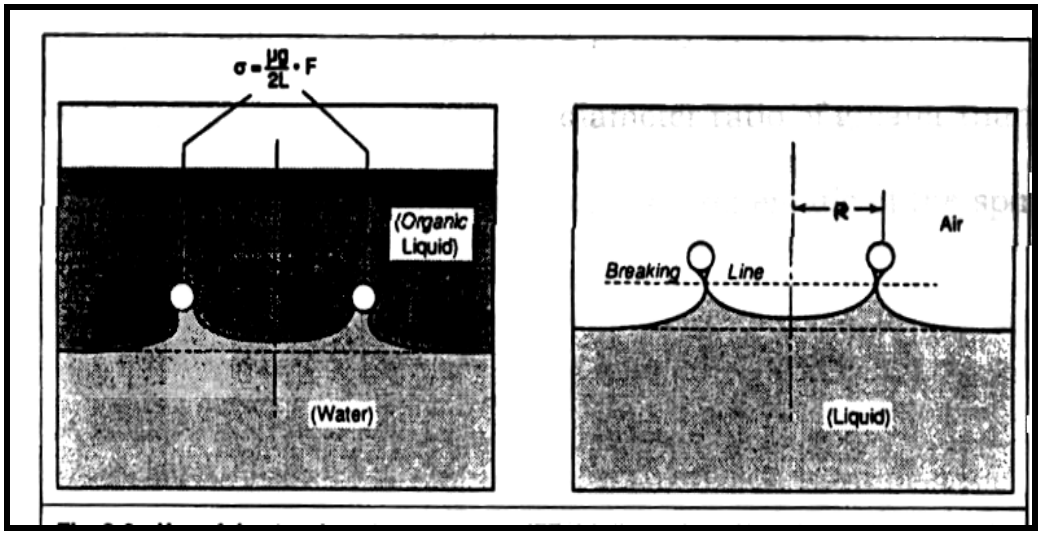

Figure 13: Principle of du Nuoy Ring Interfacial Tensiometer (after Green and Willhite[33])

Figure 14: Spinning Drop Interfacial Tensiometer for Low Interfacial Tension Measurements

3.4 Roughness Measurement And Characterization

3.4.1 Preparation of the Rock Substrates

The selected rock substrates were carefully cut using a circular cutting blade and are then thinned by polishing on a graded wheel plate using 240 grit according to the required specifications. Roughening of the samples was done individually and using various chemicals and methods for different substrates. Different levels of roughness for quartz were obtained by soaking the substrates in hydrofluoric acid for a few minutes. To generate much rougher surface, sandblasting was used. Soaking the dolomite samples in hydrochloric acid for a couple of minutes increased roughness and emery paper was used to get the desired amount of roughness in the calcite samples. These cut and prepared rock samples were then cleaned by soaking them in a mixture of methanol (87%) and chloroform (13%) for two hours and boiling them in deionized water for 30 minutes.

3.4.2 S 150 Sputter Coater

In order to characterize the roughness of the samples/rock surfaces that have been used in the study, they needed to be coated with a reflecting agent before being used on the Optical Profilometer. The samples were thoroughly cleaned following the procedure outlined previously and they were placed one at a time in the sputter coater (shown in Figure 15) chamber. The chamber was then connected to a vacuum to remove all the air. After attaining a certain pressure in the chamber, a high voltage current was passed into the chamber for about two minutes, after which a thin layer of gold and palladium mixture was deposited on the exposed parts of the rock surface. After a few minutes, the chamber is opened and the crystal surface is reversed and the whole process is repeated again until both the surfaces are coated uniformly. It should be noted here that the coated samples were used for roughness characterization and not used in any of the contact angle tests which required clean samples

3.4.3 Optical Profilometer

Characterizing the roughness of the rock substrates was done using the Optical Profilometer shown in the Figure 16 below. This optical profilometer works on the principle of analyzing the amount of reflected light from the sample. Since the rock surfaces used in the experiments would not reflect light on their own, they were coated with a gold and palladium mixture using the S-150 sputter coater. The Optical Profilometer gives the value of roughness at a particular point on the rock surface, so a number of readings have been taken on both sides of each of the surfaces and an average value of the roughness has been used in the plots.

3.4.4 Stylus Probe Type Profilometer

The Stylus Probe Profilometer measures the roughness by scanning a mechanical stylus across the sample. The Profilometer can be used to measure etch

Figure 15: S-150 Sputter Coater for coating the rock surfaces with gold and palladium

Figure 16: Optical Profilometer connected to the computer used for roughness characterization

depths, deposited film thickness and surface roughness. This profilometer is used for samples which are not very rough and brittle. In this profilometer a probe/stylus moves over the surface measuring the surface profile by plotting a graph, as shown in Figure 17, which shows the depth of the valleys on the surface of the substrate. An average depth in terms of roughness

from several scans is calculated from the computer thus giving an average value of the roughness of the sample.

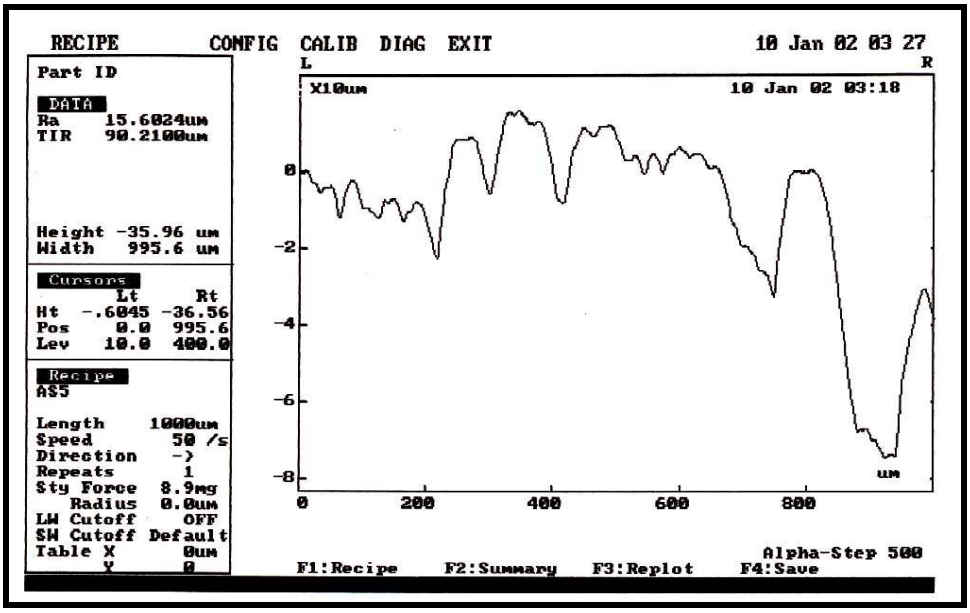

Figure 17: Measurement of Roughness of a sample using the Stylus Type Profilometer

3.4.5 Surface Topography

The surface topography of the samples used in this study have been measured using a Scanning Electron Micrograph (SEM) shown in the Figure 18 below, at magnifications of viz. 250X, 500X, 1000X and 1500X. The SEM scans the surface of the rock substrate and pictures the surface topography of the sample. This is used to compare the surface topography of different samples at the same magnification. It can also be used to study the rock/grain structure of a single sample at various magnifications.

3.5 Materials

All the reagents used in the experiments were of analytical grade. Hexane, benzene, acetone, xylene, chloroform and methanol were from Fisher Scientific having a purity of 99.9%. Sulphuric acid was from Fisher Scientific, A.C.S. certified.

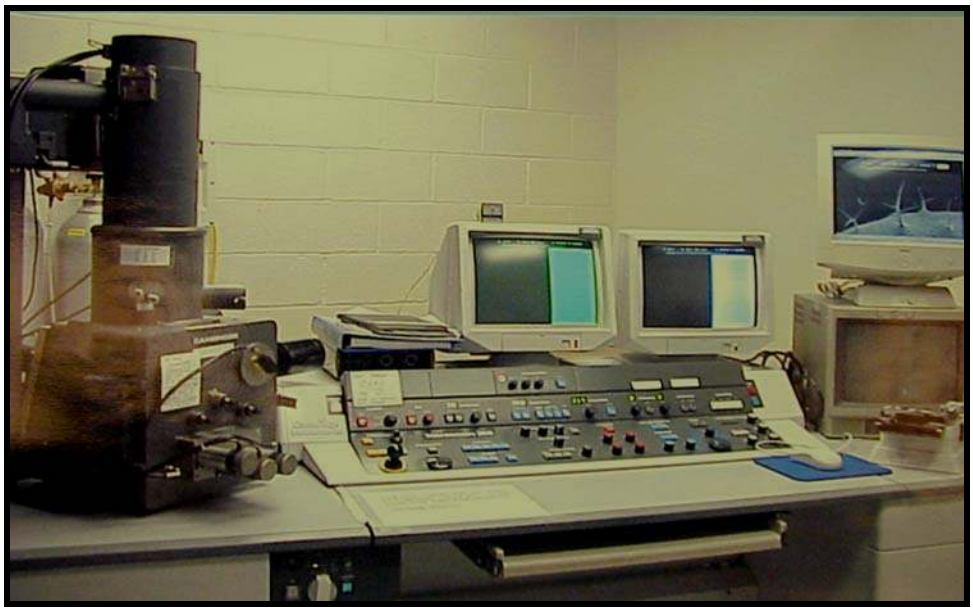

Figure 18: Scanning Electron Microscope for analyzing Surface Topography

Deionized water was acquired from the Water Quality laboratory at Louisiana State University. All the rock substrates were obtained from Ward Scientific and were processed at the Geology Department at Louisiana State University. Yates reservoir crude oil, Yates reservoir brine and ethoxy alcohol surfactant samples were supplied by Marathon Oil Company. The crude oil was kept under a nitrogen blanket to prevent oxidation. Filtration of brine was done using Whatman No.1 and also through 0.2 micron filter paper under vacuum. ESML Laboratories, NJ, did analysis of reservoir brine.

CHAPTER 4

RESULTS AND DISCUSSION

Knowledge of formation wettability is important in determining what production strategy is needed in the field. The wettability is influenced by various factors such as oil composition, brine composition, mineralogy and roughness of rock surfaces. Rock mineralogy and surface roughness are the two main parameters we have attempted to examine in this study for their effects on reservoir wettability. Three different mineralogical surfaces were chosen, namely silica, dolomite and calcite. For each of the three mineralogies, surfaces with different roughness were obtained as mentioned earlier by etching with hydrofluoric or hydrochloric, by polishing, or by sandblasting.

Brine composition variations in the reservoir occur commonly due to injection water differing in composition from that of reservoir brine. Hence the effect of brine dilution on wettability formed the second objective of this study.

The use of surfactants has long been established in the industry to enhance oil recovery by reducing the interfacial tension to facilitate the mobility of oil through the pores of the rock. This study focuses on the use of a nonionic surfactant altering wettability and thereby enhancing oil recovery. The results obtained from the various experiments are presented and discussed in this chapter.

4.1 Interfacial Tension Measurements

4.1.1 Drop Shape Analysis Technique versus du Nuoy Ring Tensiometer for Interfacial Tension Measurement

All the instruments were calibrated before being used for experimental work.

The du Nuoy Ring Tensiometer for measuring the interfacial tension was calibrated by making measurements using a standard fluid pair of benzene and deionized water and comparing it with the standard results as shown in Table 1. These results and several other comparisons presented later in Section 4.2 indicate the reliability of du Nuoy ring method for high interfacial tension measurements.

Table 1: Calibration of du Nuoy Ring Apparatus

Interfacial Tension value of standard [37] benzene-water mixture, dynes/cm	**Measured Interfacial Tension, dynes/cm**
35.0	36.1,36.25,36.2,36.0 (Average=36.14)

After making sure that the du Nuoy Ring Tensiometer was functioning properly, the drop shape analysis software was calibrated by conducting tests with the same fluids as with the du Nuoy ring. The capability of the dual-crystal optical cell to make interfacial tension measurements using the image capture and Drop Shape Analysis (DSA) techniques was evaluated for various liquid-liquid pairs and the results are shown in Table 2 and 3 along with comparative measurements made using the du Nuoy ring method. For almost all of the fluid-pairs in Table 3, a reasonably good agreement can be seen between the two techniques. However, the DSA technique, based on fitting the entire profile of the drop image through iterative solution of Laplace capillary equation, is considered more accurate and reliable. For the liquids pair of Yates crude oil and Yates brine, the interfacial tension was measured to be 28 dynes/cm by the du Nuoy ring method and 29 dynes/cm by the DSA technique**.**

4.2 Contact Angle Measurements From DDDC And Wilhelmy Techniques

The initial tests were aimed at comparing the advancing and receding contact angles measured by the DDDC technique against those calculated from the force measurements using the Wilhelmy apparatus.

Table 2: Comparison of DSA Technique and du Nuoy Ring Technique for (a) n-Hexane-Deionized water (b) Benzene-Deionized water

(a)

n-Hexane - Deionized Water		
Run Number	**IFT from du Nuoy Ring (dynes/cm)**	**IFT from DSA (dynes/cm)**
1	49.0	55.9
2	49.1	54.9
3	49.0	55.6
Avg.	49.03	55.5

(b)

Benzene – Deionized Water		
Run Number	**IFT from du Nuoy Ring (dynes/cm)**	**IFT from DSA (dynes/cm)**
1	36.1	34.6
2	36.4	36.0
3	36.2	33.6
Avg.	36.2	34.7

Table 3: Summary of Interfacial Tension Measurements using du Nuoy Ring Technique and the Drop Shape Analysis Technique

Interfacial Tension (dynes/cm)		
Fluid Pair	**du Nuoy Ring Method**	**DSA**
n-Hexane – deionized water	49.0	55.5
Benzene – deionized water	36.1	34.7
Yates Crude oil – Yates brine	28.0	29.0

It should be noted that the Wilhelmy apparatus enables the calculation of 'average' dynamic angles over the surface of the solid substrate used, while the DDDC test yields a direct measurement of the 'point-value' of the dynamic angles at a given position of the three-phase contact line on the surface of the substrate. Therefore comparing the two techniques is important to infer the value of DDDC results, especially of the advancing angle that

characterizes wettability and its correlation with the surface-average advancing angle calculated from Wilhelmy plate technique.

For an n-hexane-deionized water-glass system and a benzene-deionized water-glass system the results of initial experiments are given in Tables 4 and 5, respectively. It can be seen that the advancing angles by the two techniques agree quite well - within about eight degrees (Table 4A) using different interfacial tensions, and within about four degrees (Table 4B) when the interfacial tensions measured by the drop shape analysis (DSA) technique is used in both cases. Similar results are indicated in Table 5 for the benzene-deionized water-glass system. Such a close agreement of the DDDC advancing angle with that from Wilhelmy plate technique is encouraging from the viewpoint of verifying the DDDC technique. In addition, it is interesting to note that the point values of advancing angle from the DDDC technique correspond well with the surface-average values calculated from force measurements by the Wilhelmy plate apparatus.

There is a fairly good match of the advancing angles measured by both techniques. However, the mismatch in the receding angles measured using the DDDC technique is attributed to the fact that the drop might have moved over to that part of the crystal surface where oil was not previously occupying it. Three tests were made for each case in order to check for reproducibility of the DDDC results, which can be noticed from the tables below to be within two degrees in all cases.

4.3 Determination of Optimum Aging Time

Aging is always a crucial factor in determining the wettability of substances with regard to a particular pair of fluids. The aging of the solid substrate was done by

immersing the rock surface in the aqueous phase followed by aging in crude oil.

Andersen et al. [30] stated that pure hydrocarbons did not exhibit any change in wettability

Table 4: Comparison of Dynamic Contact Angles from DDDC Technique and Wilhelmy Plate Technique for n-Hexane - Deionized Water – Glass System at Ambient Conditions

A: Using Different Interfacial Tensions by du Nuoy Ring and DSA Methods

Wilhelmy Test				DDDC		
Run Number	**IFT from du Nuoy Ring (dynes/cm)**	**Advancing Angle (Degrees)**	**Receding Angle (Degrees)**	**IFT from DSA (dynes/cm)**	**Advancing Angle (Degrees)**	**Receding Angle (Degrees)**
1	49.0	52	32.79	55.9	59	11
2	49.1	49.55	32	54.87	58	12
3	49.0	51	33	55.62	59	11

B: Using Interfacial Tensions by the DSA Technique

Wilhelmy Test				DDDC		
Run Number	**IFT from DSA (dynes/cm)**	**Advancing Angle (Degrees)**	**Receding Angle (Degrees)**	**IFT from DSA (dynes/cm)**	**Advancing Angle (Degrees)**	**Receding Angle (Degrees)**
1	55.9	57.34	42.53	55.9	59	11
2	54.87	54.5	40.63	54.87	58	12
3	55.62	56.33	42.36	55.62	59	11

Table 5: Comparison of Dynamic Contact Angles from DDDC Technique with Wilhelmy Plate Technique for Benzene – Deionized Water – Glass System at Ambient Conditions

A: Using Different Interfacial Tensions by du Nuoy Ring and DSA Methods

Wilhelmy Test				DDDC		
Run Number	**IFT from du Nuoy Ring (dynes/cm)**	**Advancing Angle (Degrees)**	**Receding Angle (Degrees)**	**IFT from DSA (dynes/cm)**	**Advancing Angle (Degrees)**	**Receding Angle (Degrees)**
1	36.1	34.3	0*	34.55	42	13
2	36.35	35.3	0*	36.02	41	14
3	36.2	34.8	0*	33.62	42	13

0* since Cos $\theta > 1$

(Table 5 Cont'd)

B: Using Interfacial Tensions by the DSA Method

Wilhelmy Test				DDDC		
Run Number	**IFT from DSA (dynes/cm)**	**Advancing Angle (Degrees)**	**Receding Angle (Degrees)**	**IFT from DSA (dynes/cm)**	**Advancing Angle (Degrees)**	**Receding Angle (Degrees)**
1	34.55	36.33	0*	34.55	42	13
2	36.02	38.42	0*	36.02	41	14
3	33.62	37.56	0*	33.62	42	13

0* since Cos $\theta > 1$

even when exposed to air for several days; however, crude oil-brine system on glass substrate was slightly sensitive to aging as the advancing contact angle changed from 143^{o} for an aging time of 22 hours to 148^{o} for an aging time of 3 days.

Muhammad [34] during his investigation on the compositional dependence of reservoir wettability studied the effect of aging time using Yates crude oil and Yates brine using glass and dolomite as the rock surfaces. Table 6 and Figure 19 show the effect of aging time reported by Muhammad [34]. He found out that an aging time of one hour was sufficient for the system to develop equilibrium.

Several DDDC tests were conducted to determine the optimum aging time for the Yates stock-tank oil and Yates brine with dolomite as the solid substrate (Yates reservoir is in a dolomite formation). Tables 7, 8 and Figures 20, 21 show the effect of aging time on contact angle. From all the tables and graphs shown below, very little change in the advancing angle was observed between an aging times of four hours and one week of aging. The system seems to have attained equilibrium after 4 hours, as there was no appreciable change in the advancing angle. However, it was decided that an aging time of 24 hours would be allowed in all the experiments to ensure equilibrium. Henceforth all the DDDC and Wilhelmy experiments were conducted with a minimum aging time of 24 hours.

Table 6: Comparison of various aging times using the Wilhelmy pate technique (Reference # 34)

Fluid-Pair	**Solid Substrate**	**σ,** dynes/cm	$\sigma Cos\theta_a$, dynes/cm	$\sigma Cos\theta_r$, dynes/cm	θ_a*	θ_r*
Yates crude oil-Yates brine	Glass 1 hour	12.3	17.21	19.56	Zero*	Zero*
Yates crude oil-Yates brine	Glass 24 hours	12.3	-2.42	2.93	101	76.2
Yates crude oil-Yates brine	Dolomite 1 hour	12.3	0.02	3.54	89.9	79.2
Yates crude oil-Yates brine	Dolomite 24 hours	12.3	2.12	2.31	80.1	79.2

Table 7: Dynamic Contact Angles using DDDC Technique for Yates Crude Oil - Yates Reservoir Brine - Dolomite at Ambient Conditions for various Aging Times in Test # 1

Aging Time (Hours)	**Advancing Angle (Degrees)**	**Receding Angle (Degrees)**
0	72	nv*
1	88	nv
2	158	6
4	156	6
24	157	5
48	156	7

Table 8: Dynamic Contact Angles using DDDC Technique for Yates Crude Oil - Yates Reservoir Brine - Dolomite at Ambient Conditions for various Aging Times in Test # 2

Aging Time (Hours)	**Advancing Angle (Degrees)**	**Receding Angle (Degrees)**
2	146	10
4	146	10
24	163	9
168	166	9

nv*: not visible clearly to enable measurement

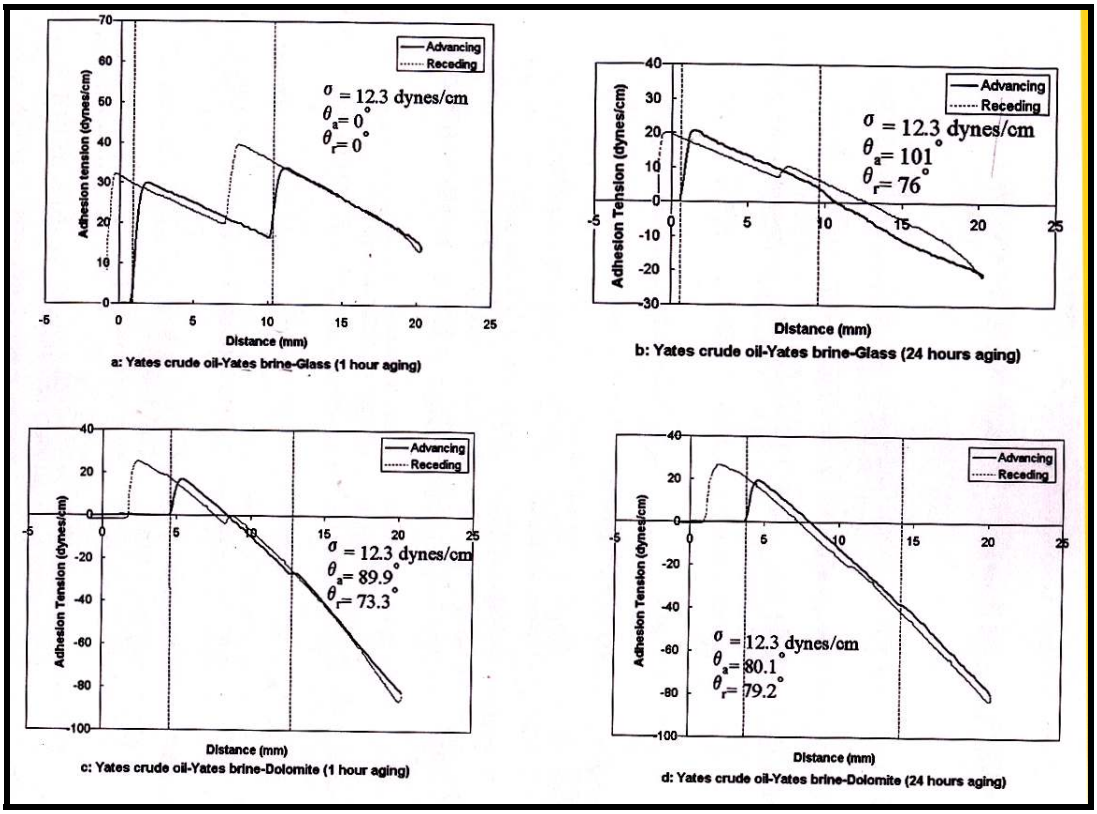

Figure 19: Effect of aging on adhesion tension and dynamic contact angle (reference # 34)

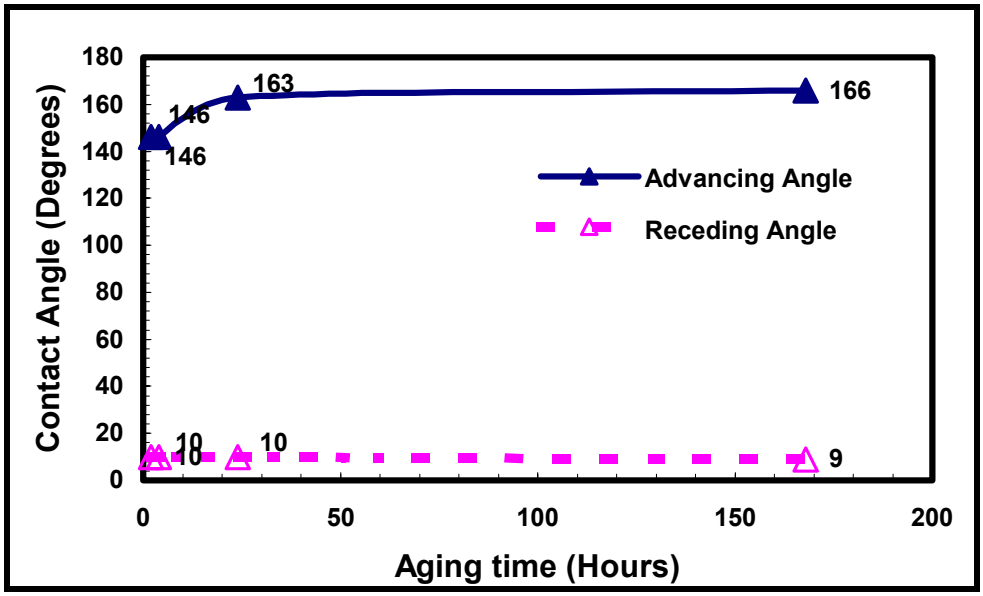

Figure 20: Dynamic Contact Angles using DDDC Technique for Yates Crude oil-Yates Reservoir Brine-Dolomite system for different aging times in Test #1

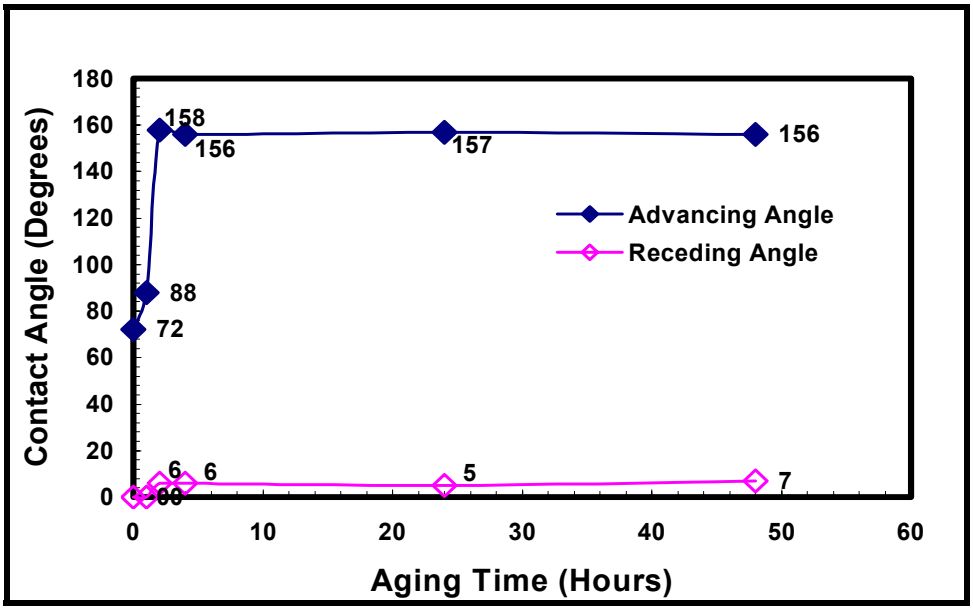

Figure 21: Dynamic Contact Angles using DDDC Technique for Yates Crude oil-Yates Reservoir Brine-Dolomite system for different aging times in Test # 2

4.4 Effect of Rock Surface Roughness on Wettability

One of the common criticisms of contact angle measurements is that they use smooth crystal surfaces in place of reservoir rocks, which are not only rough but also are mineralogically heterogeneous. The main purpose of studying the effects of surface roughness on contact angles has been to investigate the possibility of relating contact angles measured on smooth surfaces to those likely to be operative on rough surfaces within porous media. Although the importance of surface roughness to wetting behavior is recognized, difficulties have been reported in obtaining a definitive account of roughness effects. This study is an attempt to address these concerns.

Experiments were conducted using stock-tank reservoir fluids obtained from Yates field (brine and crude oil), and the rock samples were obtained from Ward Scientific. The solid surfaces that were used consisted of glass, quartz, Berea sandstone, dolomite and calcite. Quartz, dolomite and calcite were cut and treated using hydrofluoric

acid, hydrochloric acid, graded wheel plate, and sandblasted respectively, to have two levels of roughness. Glass and Berea were taken as the two extreme cases of roughness for the silica-based surfaces.

The solid substrates were prepared and cleaned as described in section 3.4.1. For characterization of roughness these treated samples were coated with gold and palladium mixture as described in section 3.4.2 to enable them to reflect light when used on the Optical Profilometer for measuring their roughness. However, the coated samples were not used in any of the contact angle tests.

Characterizing the surface roughness of these samples was done using a sputter coater and an optical profilometer. Surface roughness was calculated by averaging several point values measured using the optical profilometer. The surface topography of the samples used in this study has been measured using a Scanning Electron Micrograph (SEM). The SEM can be used to study the grain structure and grain packaging of a particular sample at various magnifications. Based on these observations, we can analyze how the grains are packed and thus how permeable the rock is. Figure 22 shows the grain structure of a dolomite sample at magnifications of 250X, 500X, 1000X and 1500X.

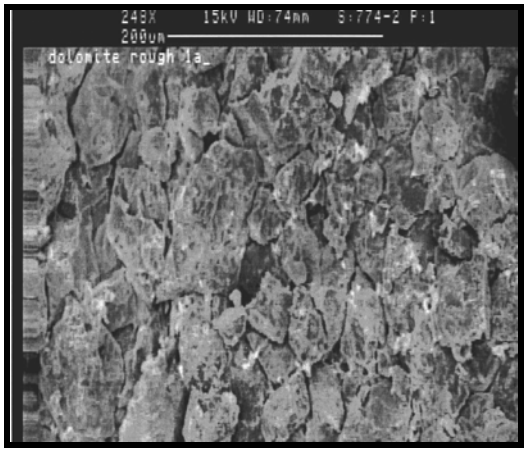

a

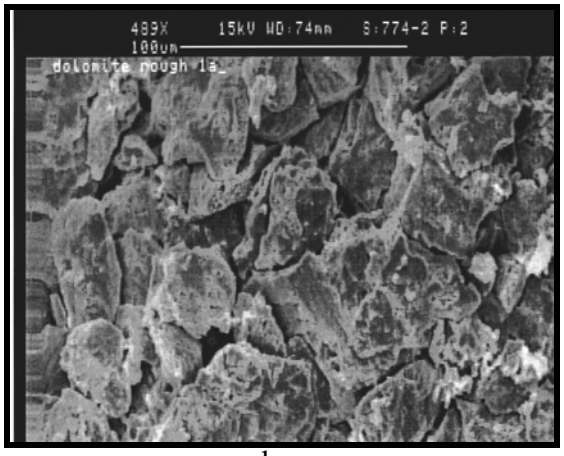

b

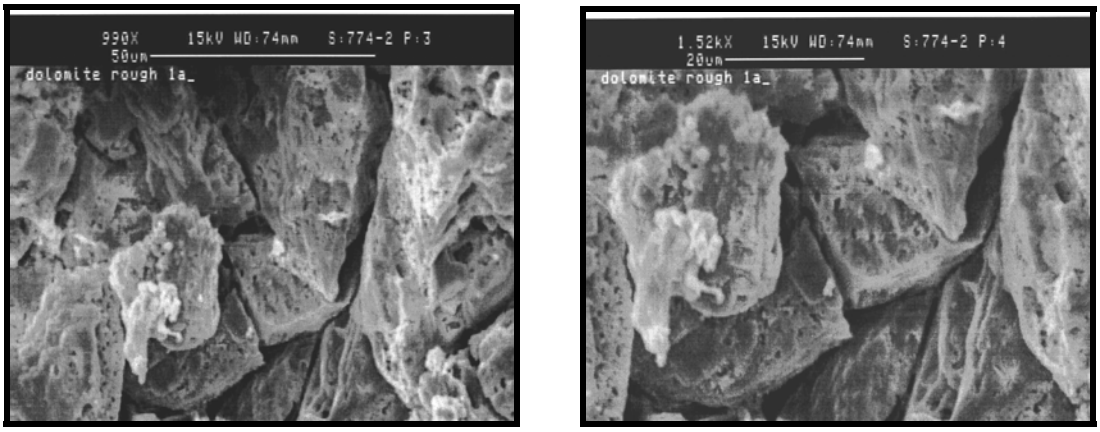

c d

Figure 22: Scanning Electron Micrograph images of dolomite sample at various magnifications (a) 250X (b) 500X (c) 1000X (d) 1500X

Figure 23a shows the SEM image of a glass plate at a magnification of 250x, and Figure 23b shows the image of the same glass slide as observed from the optical profilometer. The optical profilometer gives the average as well as the root-mean-square value of the roughness over the area of the particular sample. For this particular case the value of the roughness of the sample is 0.17 μm. At similar magnification, Quartz A surface can be seen in Figure 24 with a roughness of 1.81 μm. Figure 25 is Quartz B whose roughness is 6.81 μm. From 24a and 25a we can compare the how the grains are packed and what the surface texture is for these surfaces at the same magnification. Similar comparisons can be made with Quartz C (shown in Figure 26).

Figure 27 shows the SEM image of a Berea sample, which is the roughest surface used in this study with a roughness of 30.23 μm. Figure 28 shows the SEM image of a smooth dolomite sample along with the profilometer image showing an average roughness of 1.95 μm. Surface topography and roughness of a dolomite sample roughened using HCl can be obtained from Figure 29. Similar comparison can be made for calcite, which is shown in Figures 30 and 31.

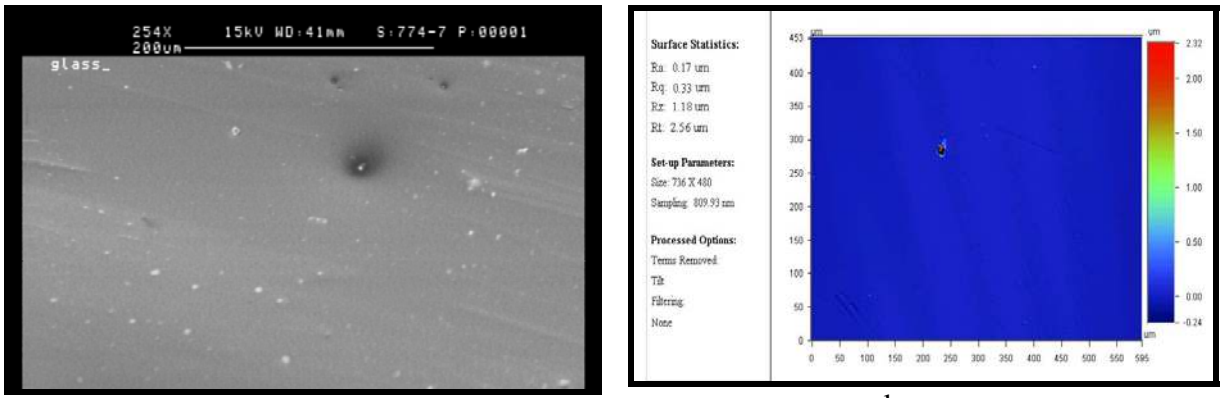

a b

Figure 23: Surface Characterization image for Glass (R_a = 0.17 μm) using
(a) Scanning Electron Micrograph, (b) Optical Profilometer

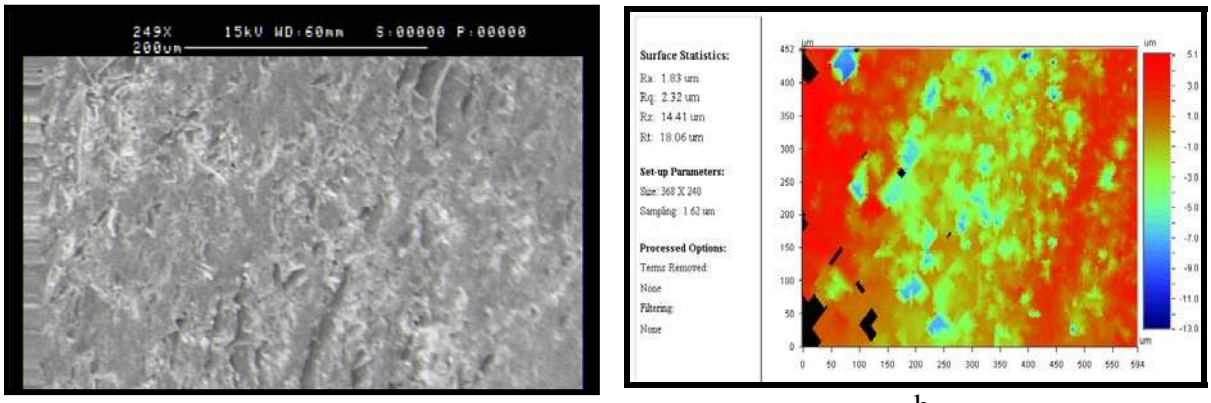

a b

Figure 24: Surface Characterization image for Quartz A (R_a = 1.81 μm) using
(a) Scanning Electron Micrograph, (b) Optical Profilometer

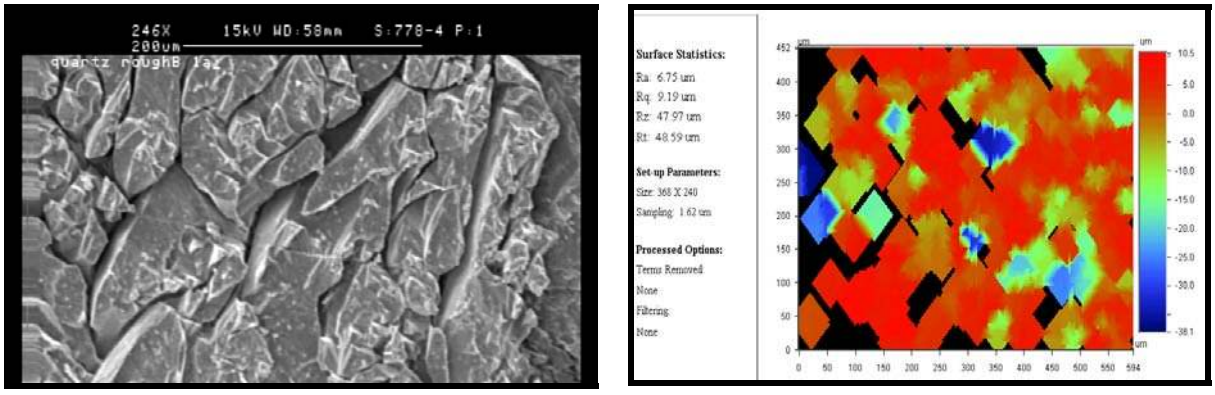

a b

Figure 25: Surface Characterization image for Quartz B (R_a = 6.81 μm) using
(a) Scanning Electron Micrograph, (b) Optical Profilometer

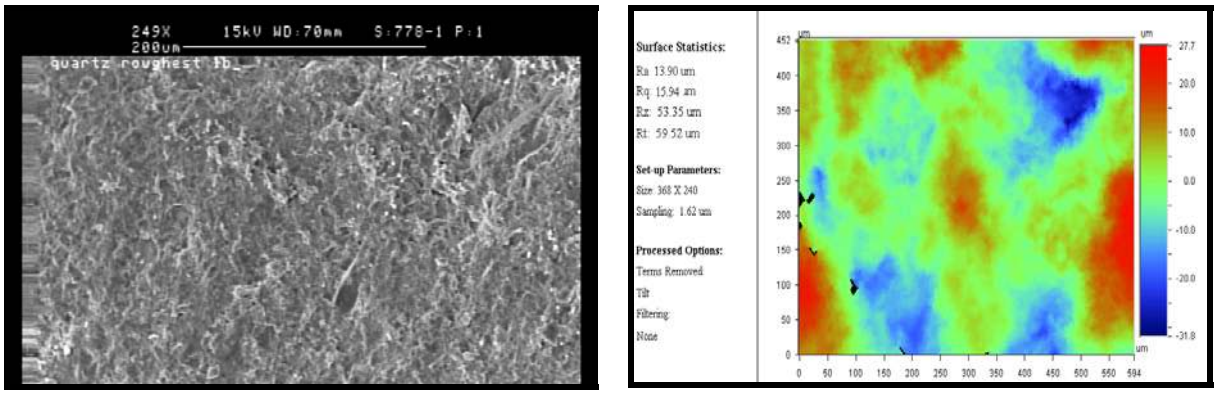

a b

Figure 26: Surface Characterization image for Quartz C (R_a = 13.9 μm) using (a) Scanning Electron Micrograph, (b) Optical Profilometer

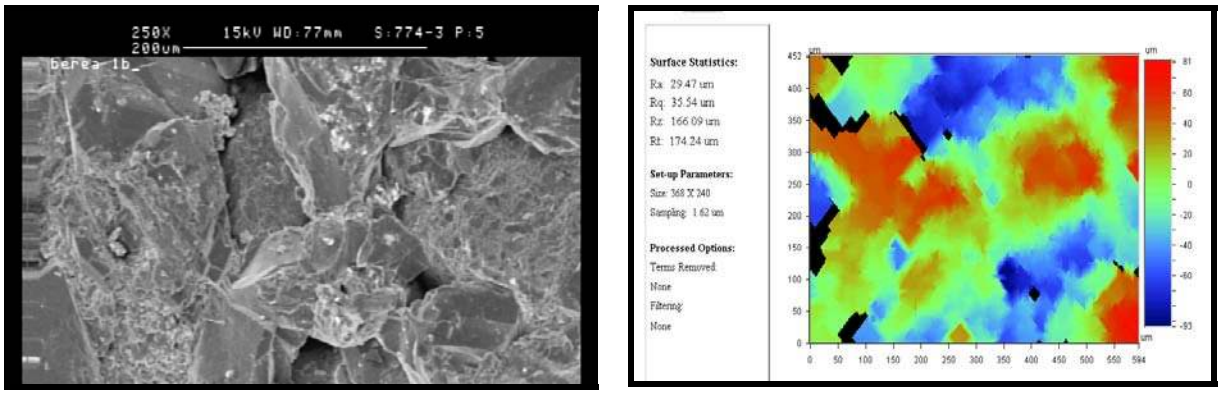

a a

Figure 27: Surface Characterization image for Berea (R_a = 30.23 μm) using (a) Scanning Electron Micrograph, (b) Optical Profilometer

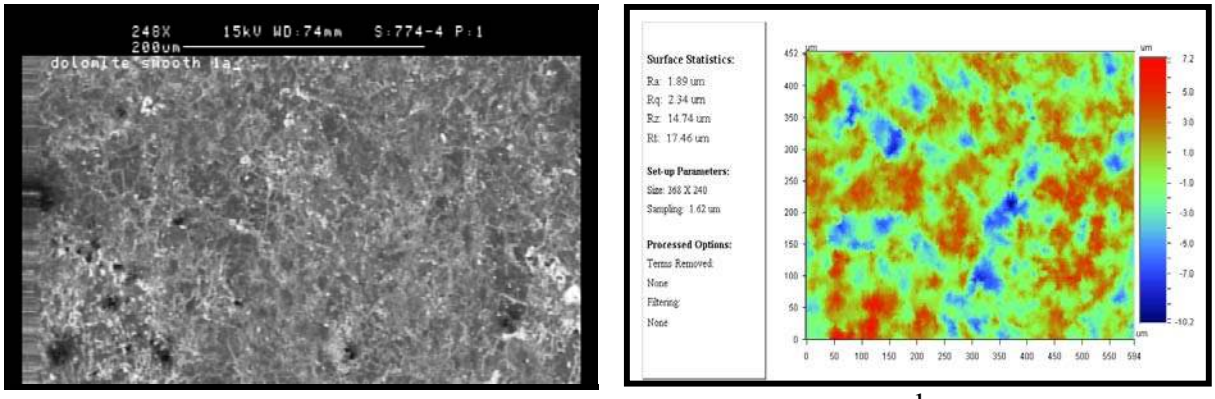

a b

Figure 28: Surface Characterization image for Dolomite A (R_a = 1.95 μm) using (a) Scanning Electron Micrograph, (b) Optical Profilometer

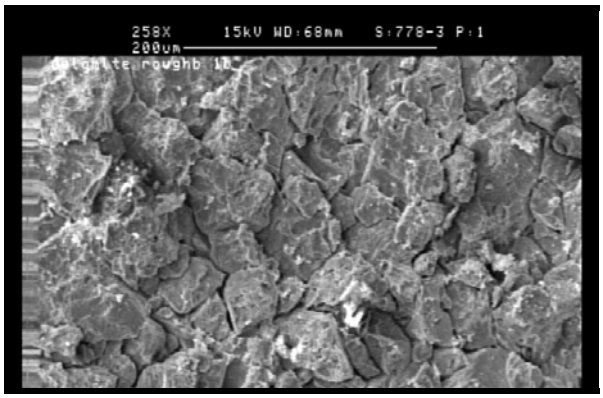

a

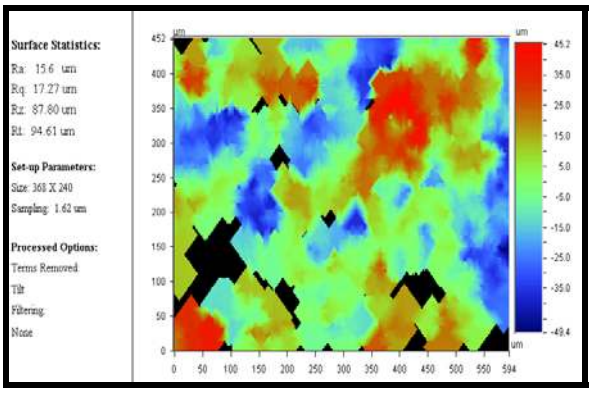

b

Figure 29: Surface Characterization image for Dolomite B (R_a = 15.6 µm) using (a) Scanning Electron Micrograph, (b) Optical Profilometer

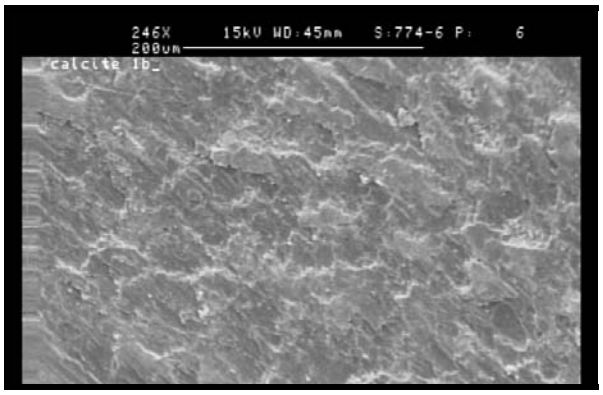

a

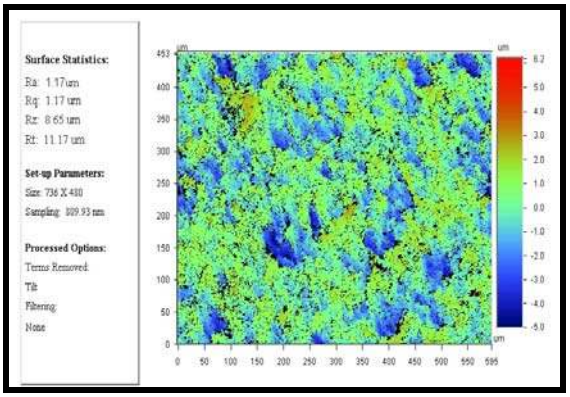

b

Figure 30: Surface Characterization image for Calcite A (R_a = 1.17 µm) using (a) Scanning Electron Micrograph, (b) Optical Profilometer

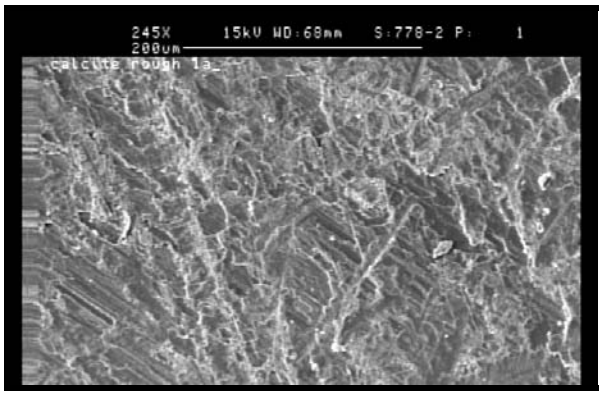

a

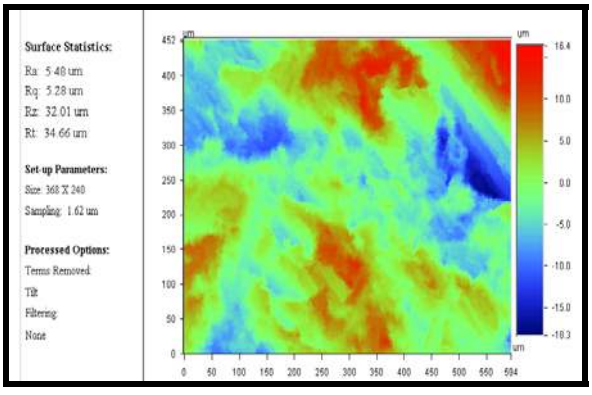

b

Figure 31: Surface Characterization image for Calcite B (R_a = 5.46 µm) using (a) Scanning Electron Micrograph, (b) Optical Profilometer

The SEM images taken at similar magnifications indicate the topographical differences between the various substrates used. Figure 32 summarizes the roughness characteristics averaged over several measurements on each substrate, and it can be noticed that glass is the smoothest with an average roughness of 0.17 μm and Berea rock being the roughest with 30.23 μm among the silica-based surfaces. The roughness variation of dolomite was about one order of magnitude, the smoothest being 1.95 μm and the roughest at 15.6 μm. Calcite surface roughness varied from 1.17 μm to 5.46 μm.

In all the experiments involving Wilhelmy and DDDC tests, brine and crude oil from the Yates field in West Texas have been used. Figure 33 shows a graph between the apparent dynamic contact angles measured on glass surface using Yates reservoir fluid pair with DDDC and Wilhelmy plate techniques at various aging times. Several observations that can be noticed; (1) very little change in the advancing/receding angles measured using the DDDC technique was observed after 4 hours of aging, (2) the striking difference in advancing/receding angles measured using the DDDC technique and the Wilhelmy plate technique, (3) the DDDC test indicated an oil-wet contact angle of 160^{o} while the Wilhelmy plate showed it to be intermediate-wet with advancing angle of 90^{o} irrespective of the aging time.

Figure 34 is a similar plot for Quartz A (R_a = 1.81 μm). Here also the advancing and receding angles measured from the DDDC and Wilhelmy techniques are compared at various aging times. It can be noticed that the advancing/receding angles measured with the DDDC are the same for 4 hours and 24 hours of aging, thereby once again proving that 4 hours of aging is sufficient. However, as noted earlier aging period of 24 hours was allowed in all the tests to be certain of the equilibrium.

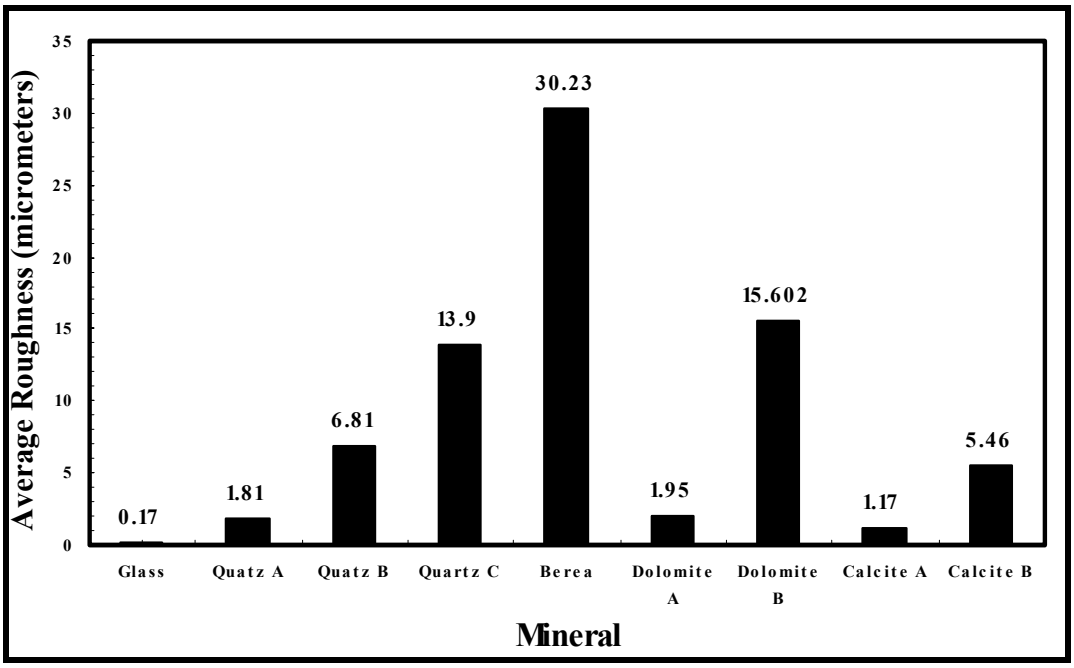

Figure 32: Roughness of Various Surfaces used in Experiments (Averaged over several separate Measurements)

The Wilhelmy test yielded 90^{o} in both the advancing and receding modes in this case also. Similar graphs were plotted for all the silica-based surfaces namely quartz B, quartz C and Berea in Figures 35-37 respectively.

Figure 38 shows the plot of dynamic contact angles against aging time for dolomite A (R_a = 1.95 μm). The advancing angles can be seen to be high (≥ 146^{o}), even at small aging times, indicating dolomite to be strongly oil-wet in nature. Here a one-week aging time experiment has been conducted to verify if advancing/receding angles change if given more time for aging. The advancing angle measured after a weeklong of aging is 166^{o} compared to 163 ^{o} for 24 hours of aging, thereby implying that 24 hours of aging is enough for the system to attain equilibrium. Another observation that is the advancing and receding angles measured by the Wilhelmy plate were both 90^{o}, and did not depend on the mineralogy of the sample.

Figure 39 is a graph for dolomite B (R_a =15.6 μm) which is almost 8 times rougher than dolomite A. Even this eight-fold change in the roughness did not seem to affect the advancing and receding angles as it can be noticed that the angles measured for 24 hours of aging were similar to those measured on smooth dolomite surface. However, at the aging time of 2 and 4 hours, there are slight differences 10 and 20^o respectively, between the two surfaces. These data points indicate that the rougher dolomite surface was closer to equilibrium advancing angle at 2 and 4 hours than the smoother dolomite surface. In general, these results indicate that roughness has little effect on equilibrium values of advancing and receding angles on dolomite surface.

Figure 40 compares the dynamic contact angles for calcite A (R_a =1.17 μm) obtained using the DDDC and Wilhelmy plate techniques. The advancing angle measured at 2 hours of aging was 160^o, showing calcite to be a strongly oil-wet surface. When a particular solid surface displays such large contact angles even at small aging times, there is practically very little room for it to increase any further even if given longer aging times. This can be seen in Figure 40, which shows a contact angle of 161^o and 162^o for 4 hours and 24 hours of aging. The DDDC receding angles also do not seem to be affected much by aging time. The Wilhelmy technique continues to remain insensitive as before.

Figure 41 is for calcite B (R_a =5.46 μm) whose roughness is about 5 times that of calcite A. Here also the advancing angle initially was 154^o and as the aging time increased the advancing angle decreased slightly (~ 2^o), but there was a very little change in the receding angle. As before the Wilhelmy technique consistently yielded 90^o, which is further discussed below

A striking feature is the 90^{o} angles consistently indicated by the Wilhelmy tests in all of the plots in Figures 33-41 indicating the insensitivity of the Wilhelmy technique to mineralogy, surface roughness and the mode of the movement of the three-phase-contact-line (whether advancing or receding). Several tests were run to verify the proper functioning of the Wilhelmy apparatus by checking with strongly water-wet and oil-wet solid-fluids systems. The apparatus yielded excellent match with the past results, as can be seen in Table 9, indicating its ability to function properly.

Table 9: Verification of proper functioning of Wilhelmy Plate Apparatus

Test Type	Fluid Pair	Solid Substrate	Advancing Angle (Degrees)	Receding Angle (Degrees)
Old	n-Hexane-DIW	Glass	51	32
New	n-Hexane-DIW	Glass	52	33
Old	Benzene-DIW	Glass	35	0*
New	Benzene-DIW	Glass	36	0*

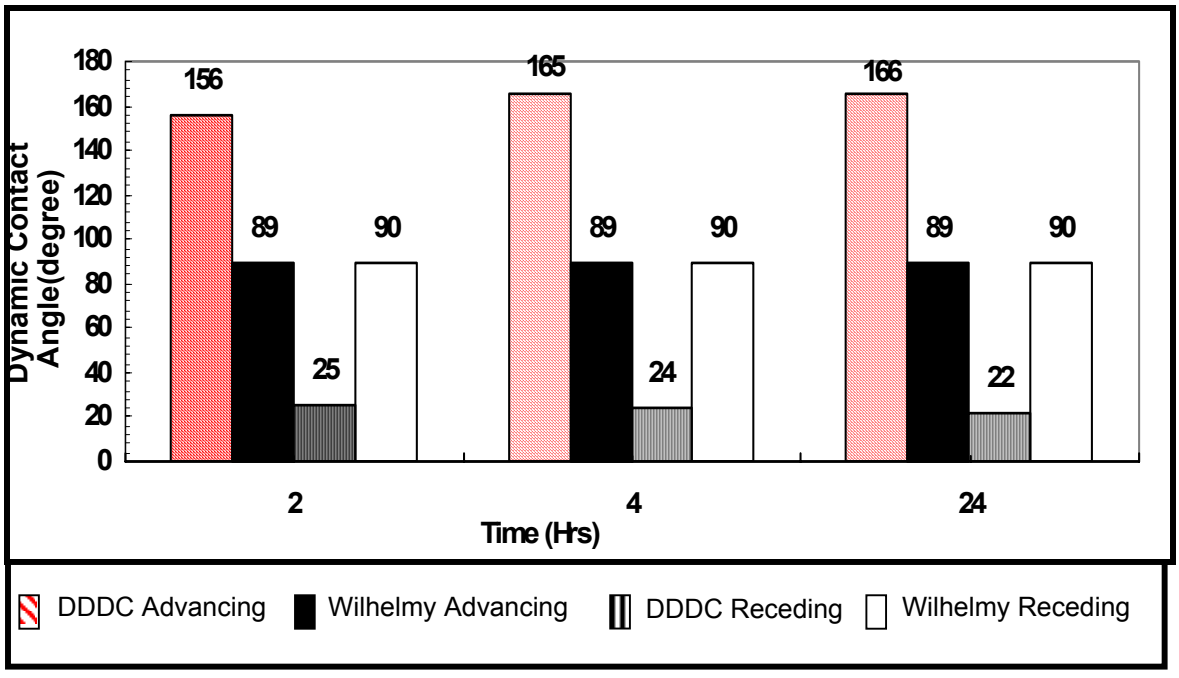

Figure 33: Comparison of Dynamic Contact Angles for Yates Crude Oil – Brine – Glass (R_a = 0.17 μm) using DDDC and Wilhelmy Techniques

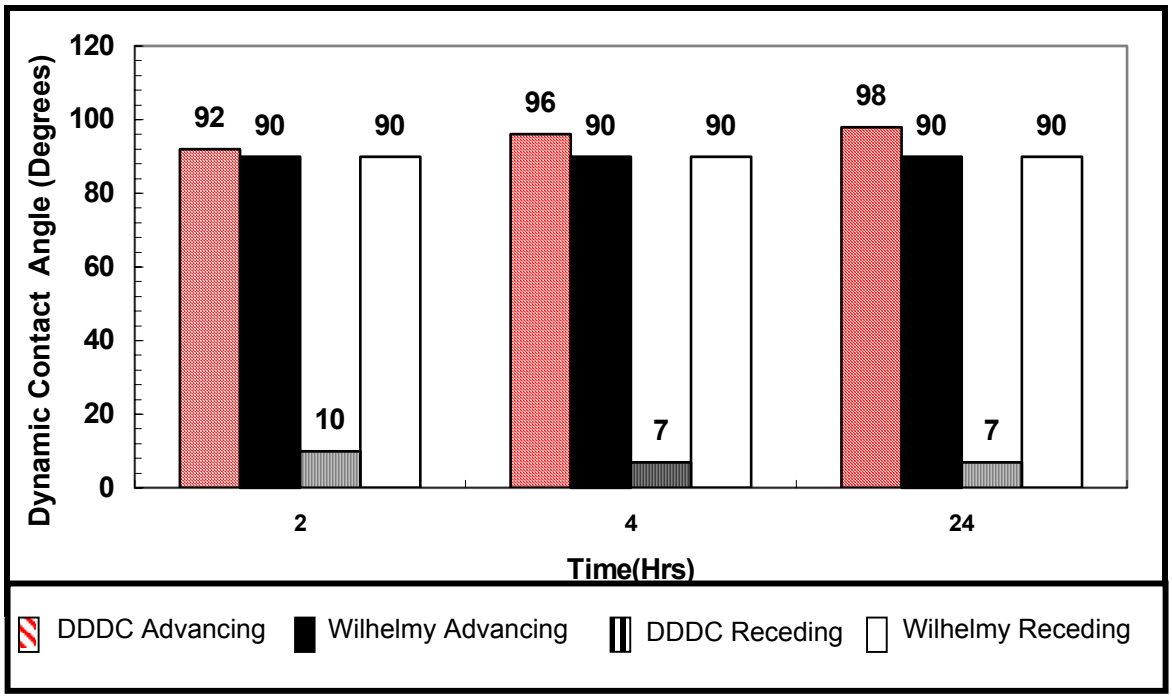

Figure 34: Comparison of Dynamic Contact Angles for Yates Crude Oil - Brine - Quartz A (R_a = 1.81 μm) using DDDC and Wilhelmy Techniques.

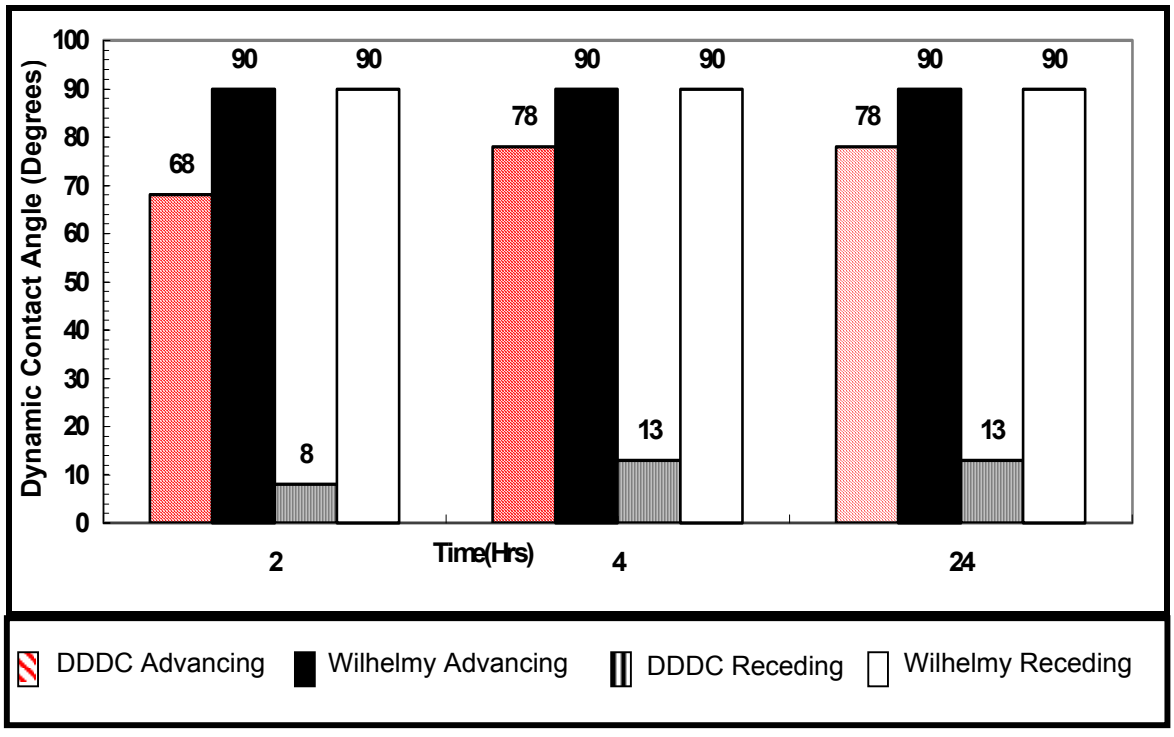

Figure 35: Comparison of Dynamic Contact Angles for Yates Crude Oil - Brine - Quartz B (R_a = 6.81 μm) using DDDC and Wilhelmy Techniques.

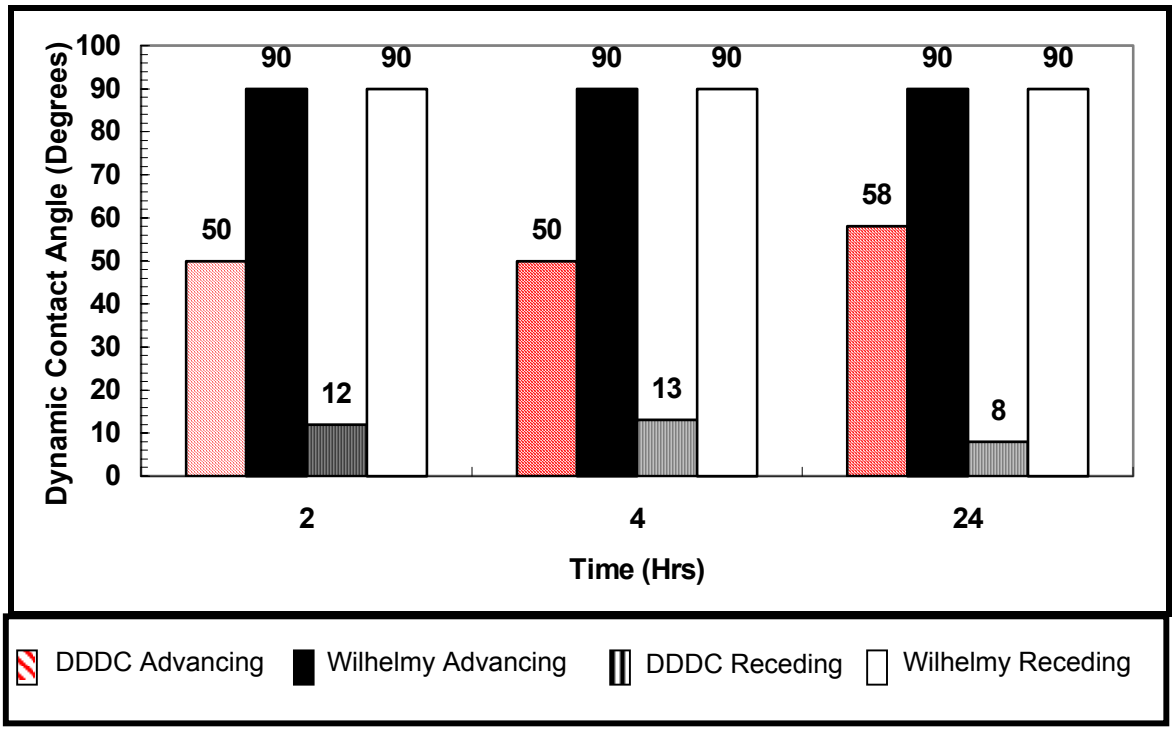

Figure 36: Comparison of Dynamic Contact Angles for Yates Crude Oil - Brine - Quartz C (R_a = 13.9 μm) using DDDC and Wilhelmy Techniques.

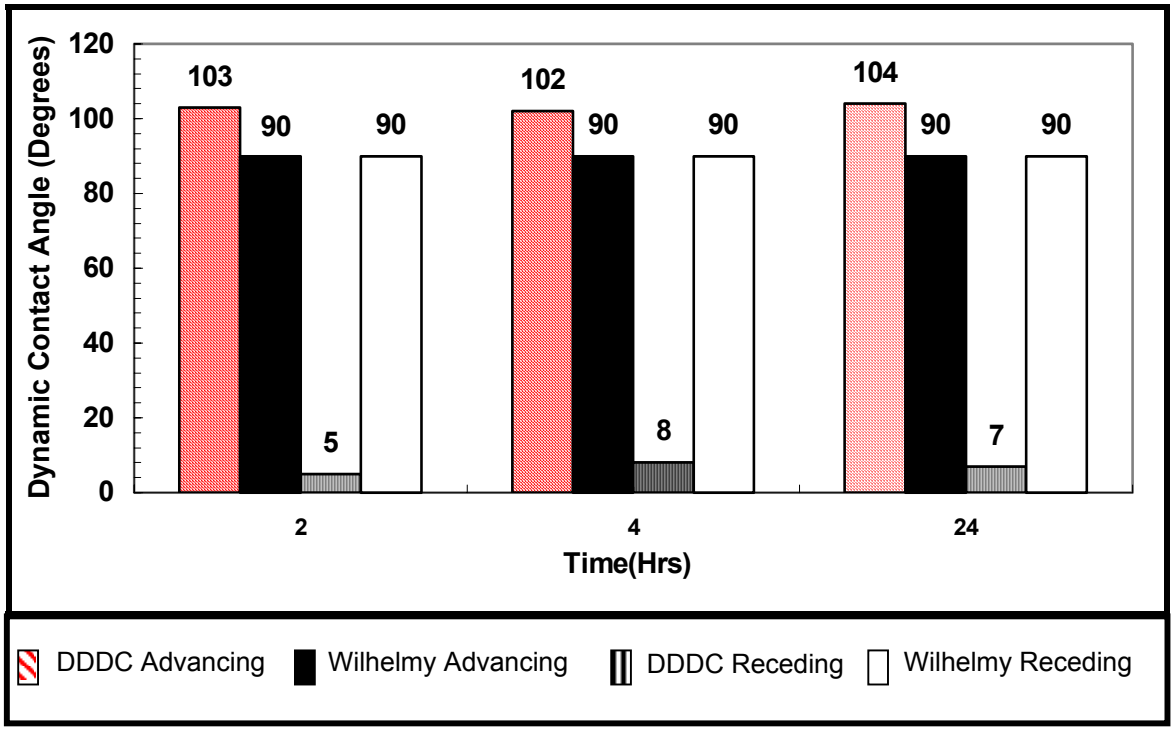

Figure 37: Comparison of Dynamic Contact Angles for Yates Crude Oil - Brine - Berea (R_a = 30.23 μm) using DDDC and Wilhelmy Techniques.

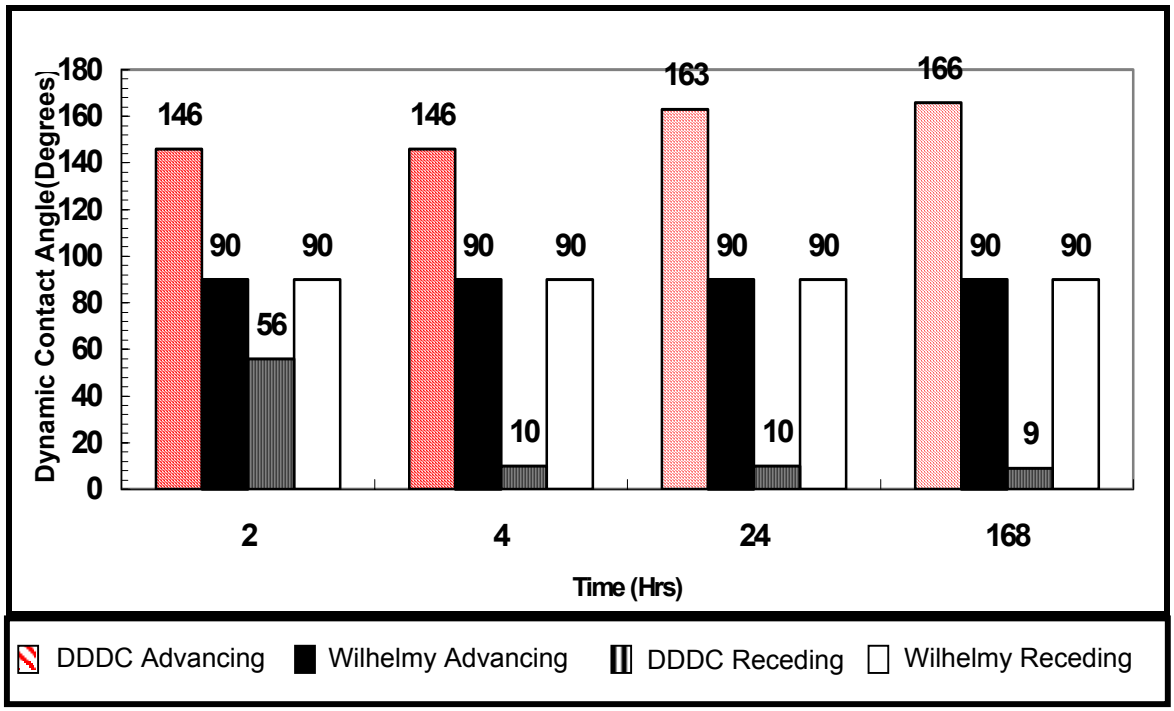

Figure 38: Comparison of Dynamic Contact Angles for Yates Crude Oil - Brine – Dolomite A (R_a = 1.95 μm) using DDDC and Wilhelmy Techniques.

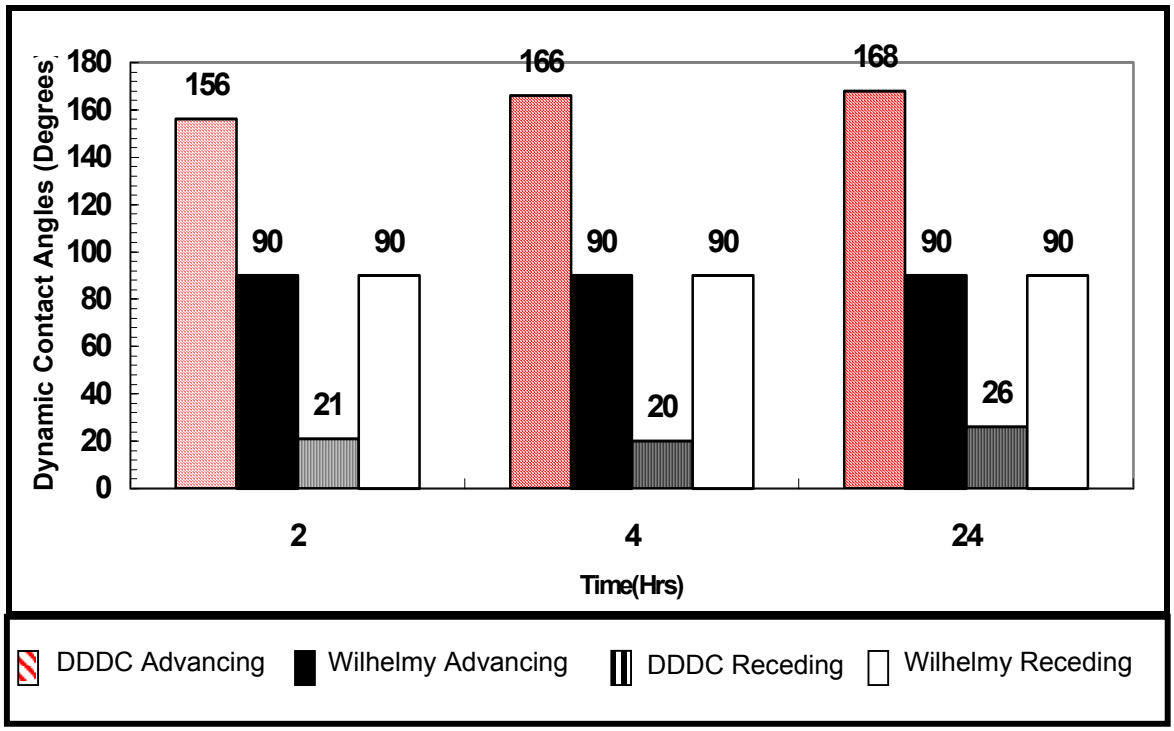

Figure 39: Comparison of Dynamic Contact Angles for Yates Crude Oil - Brine – Dolomite B (R_a = 15.6 μm) using DDDC and Wilhelmy Techniques.

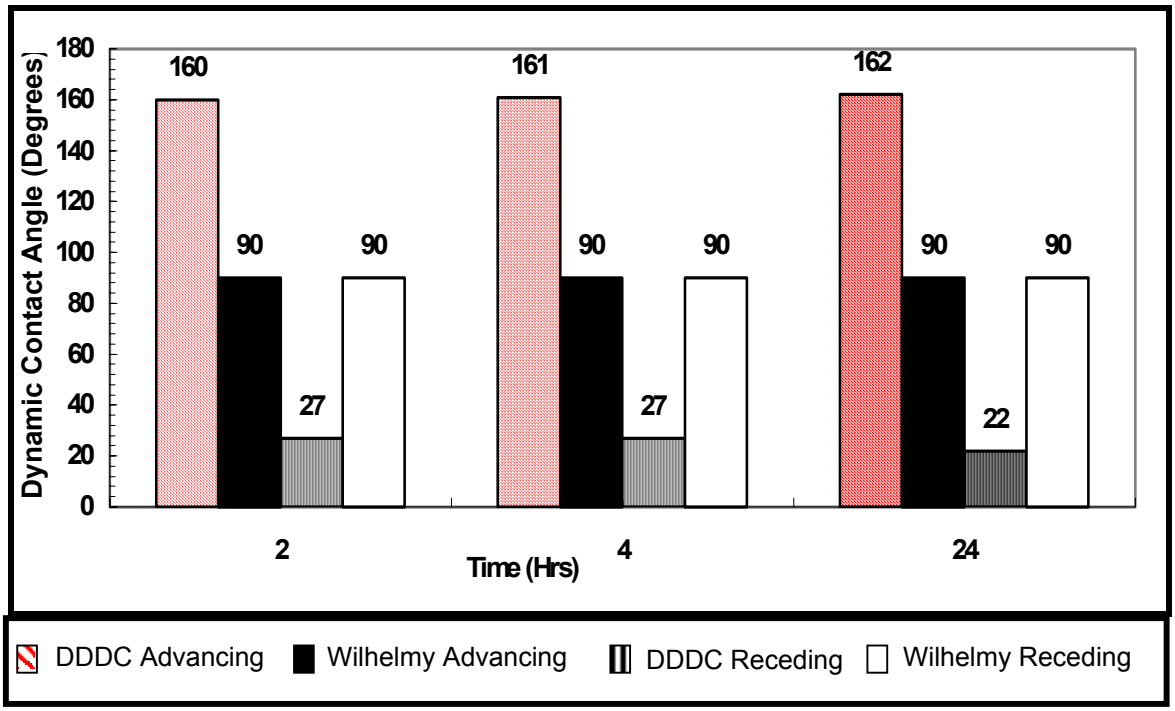

Figure 40: Comparison of Dynamic Contact Angles for Yates Crude Oil - Brine – Calcite A (R_a = 1.17 μm) using DDDC and Wilhelmy Techniques.

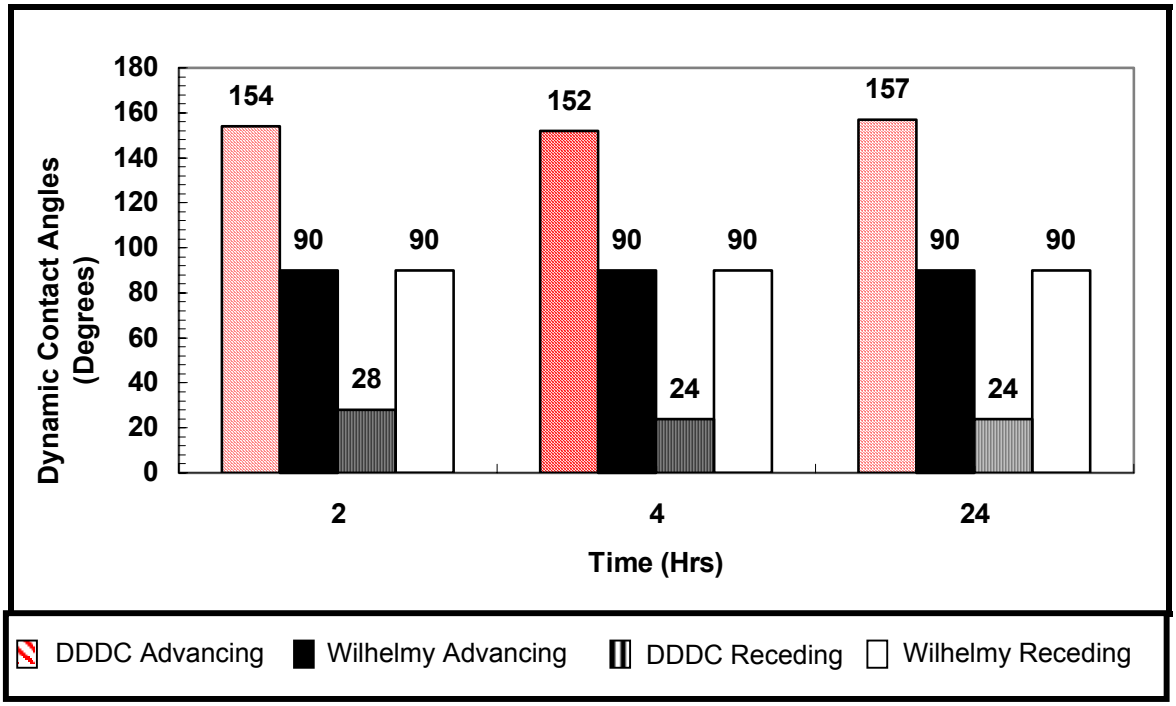

Figure 41: Comparison of Dynamic Contact Angles for Yates Crude Oil - Brine – Calcite B (R_a = 5.46 μm) using DDDC and Wilhelmy Techniques.

To examine if the weight of the glass slide was the cause for the insensitivity of Wilhelmy results, several tests were run with thinner solid substrates (shown in Table 10) to enable the microbalance to be more sensitive to the oil-water interface as it traversed across the solid substrate. Table 10 shows the values of advancing and receding angles measured with the same fluid pair but with two solid samples of different weights. Run 1 (Figure 42) was with quartz and Run 2 (Figure 43) was with lightweight quartz sample. The advancing and receding angles were measured to be 90^{o}, irrespective of the weight of the sample. In order to check dependence on mineralogy, Run 3 (Figure 44) and Run 4 (Figure 45) were conducted. These tests also resulted in 90^{o} angles confirming the relative insensitivity of the Wilhelmy technique in such contact angle measurements. This ruled out one of the initial objectives of our study to compare the dynamic angles measured using the DDDC technique with those from the well-established Wilhelmy apparatus.

Table 10: Verification for the proper functioning of the Wilhelmy Plate Apparatus with lightweight substrates

Test Type	Fluid Pair	Solid Substrate	Advancing Angle (Degrees)	Receding Angle (Degrees)
Old	Yates crude oil-Yates Reservoir brine	Quartz (2.3 mg)	90	90
New	Yates crude oil-Yates Reservoir brine	Quartz (1.3 mg)	90	90
Old	Yates crude oil-Yates Reservoir brine	Dolomite (2.6 mg)	90	90
New	Yates crude oil-Yates Reservoir brine	Dolomite (1.2 mg)	90	90

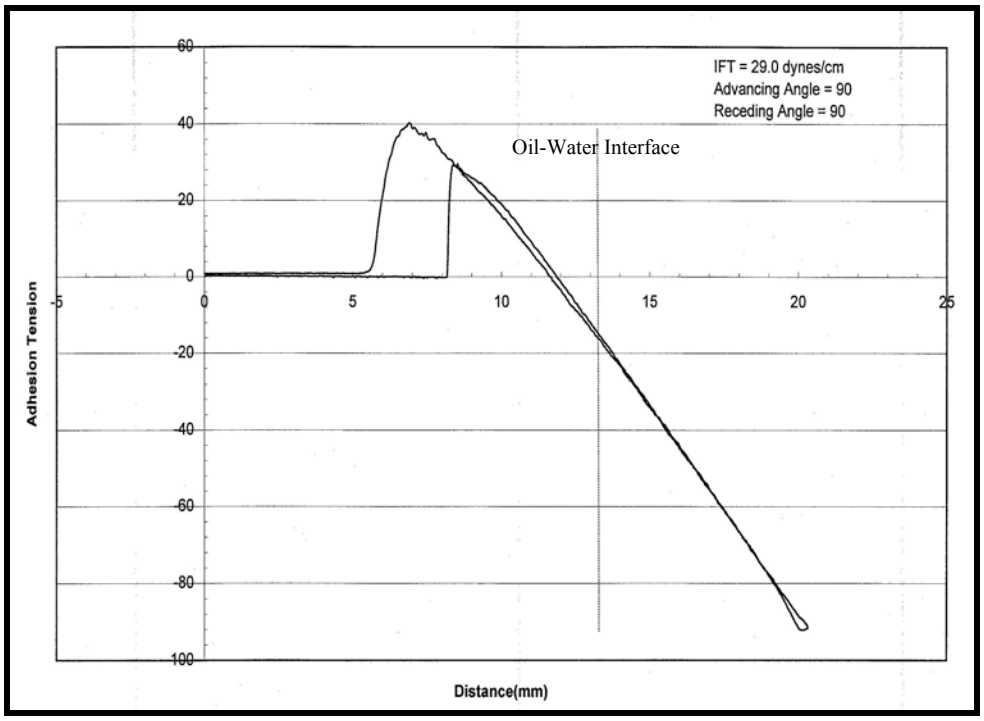

Figure 42: Advancing and Receding angles measured using Yates crude oil-Yates brine-quartz (2.3 mg) for an aging time of 24 hours

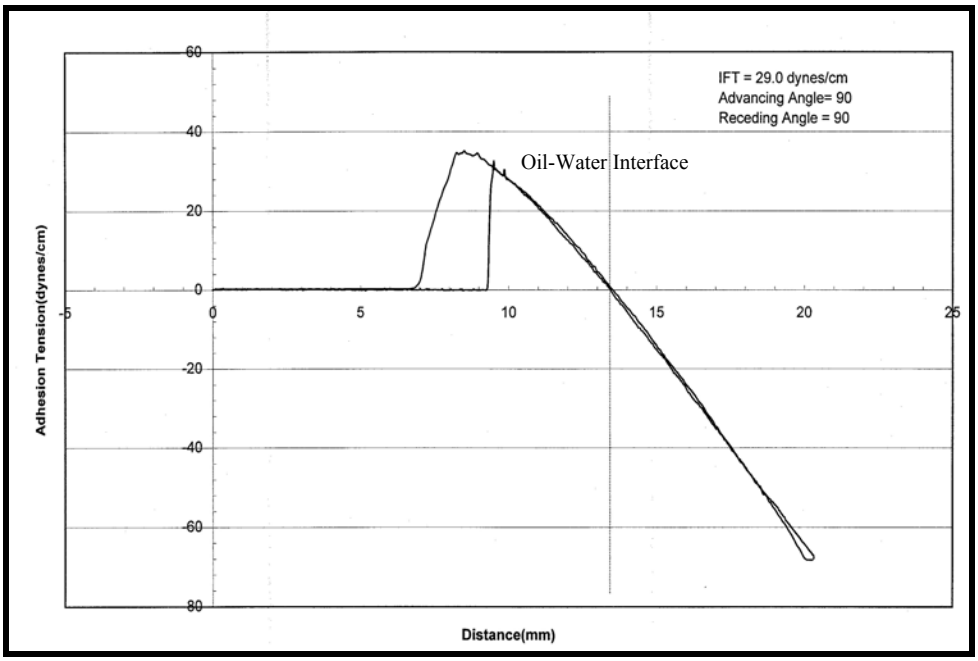

Figure 43: Advancing and Receding angles measured using Yates crude oil-Yates brine-quartz (1.3 mg) for an aging time of 24 hours

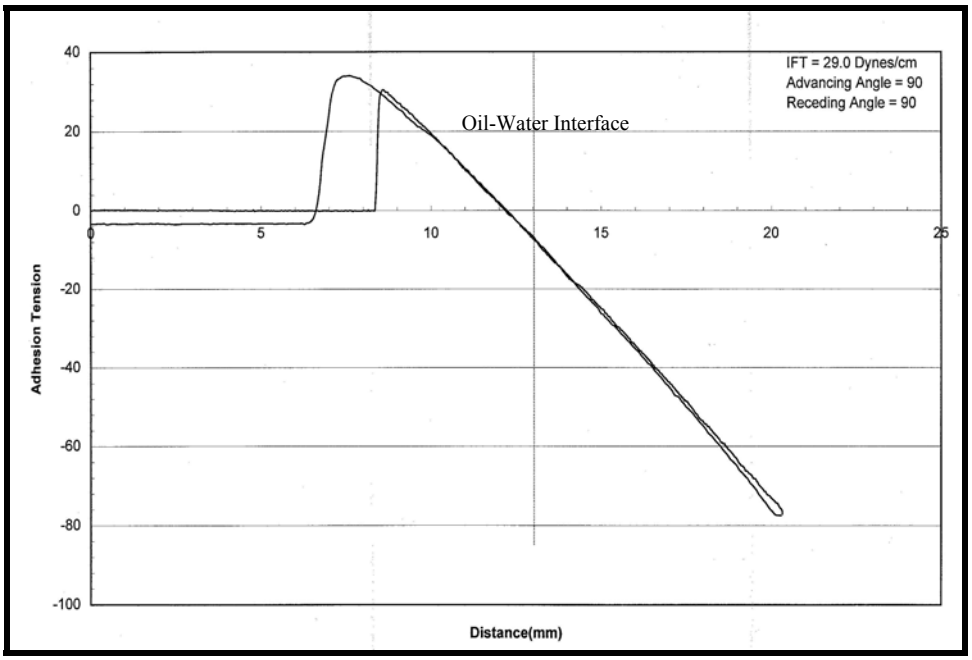

Figure 44: Advancing and Receding angles measured using Yates crude oil-Yates brine-dolomite (2.6 mg) for an aging time of 24 hours

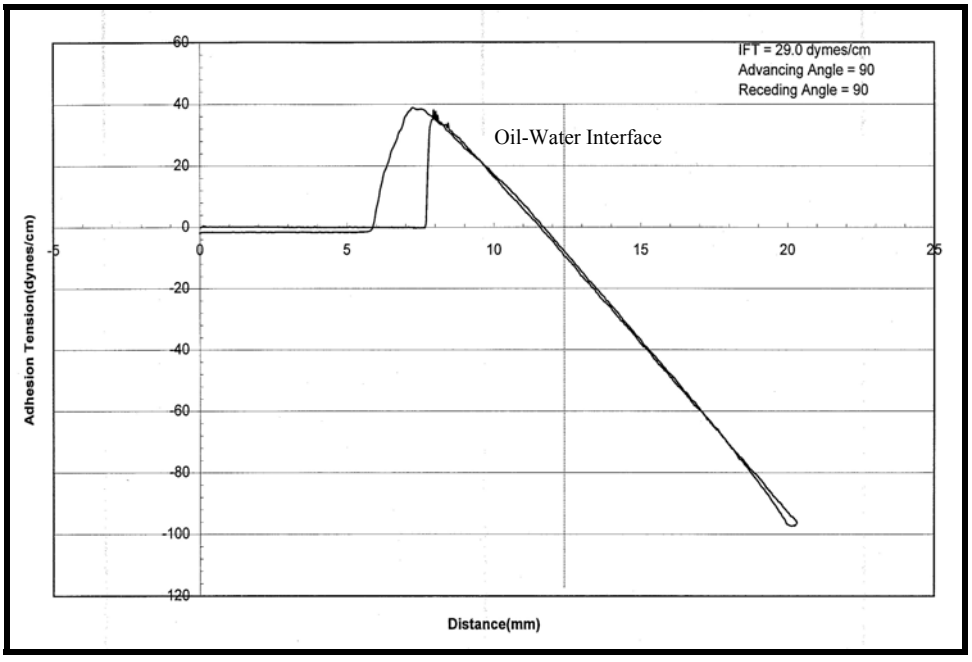

Figure 45: Advancing and Receding angles measured using Yates crude oil-Yates brine-dolomite (1.2 mg) for an aging time of 24 hours

In contrast to Wilhelmy tests, the DDDC tests yielded dynamic contact angle results that showed marked influence of mineralogy, surface roughness and the mode of contact-line movement. The DDDC tests results are shown for each of the substrates in Figures 33 to 41 have been already discussed. Summary of the DDDC data is shown in Figure 46 for silica-based surfaces and Figure 47 for dolomite and calcite surfaces.

As shown in Figure 46, the advancing angle on silica-based surfaces continuously decreased (from 166^{o} on smooth glass to 58^{o} on rough quartz C) with increasing surface roughness. Berea, although being a silica-based rock, did not fall on this decreasing trend of Figure 46. This may be related to mineralogical composition of Berea - being somewhat different from pure silica. Since the receding angles remained quite low in the range of 7^{o} - 26^{o} with increasing roughness, the overall effect of roughness on hysteresis (which is the difference between advancing and receding contact angles) decreases with roughness on silica surfaces. Decreasing trends in hysteresis with roughness were also observed, as shown in Figure 47, for dolomite and calcite surfaces, although the severity of the effect was much less than on silica-based surfaces. Dolomite and calcite were very oil-wet to start with regardless of the roughness of the surface. Roughness does not seem to affect the advancing and receding contact angles in the case of dolomite as they stayed the same even for a ten-fold change in roughness of the dolomite sample. Calcite also followed a similar trend, trend-there was a slight decrease in the angle, thereby directly opposing the Wenzel's relation.

These results appear to refute the general notion (originating from studies concerned with solid-liquid-air systems as discussed earlier in section 2.4) that hysteresis increases with roughness. Also, the Wenzel equation does not appear to hold good in such solid-liquid-liquid

systems where the expectation from Wenzel's equation that initially oil-wet angles would increase with roughness appears to be refuted by the data of these experiments.

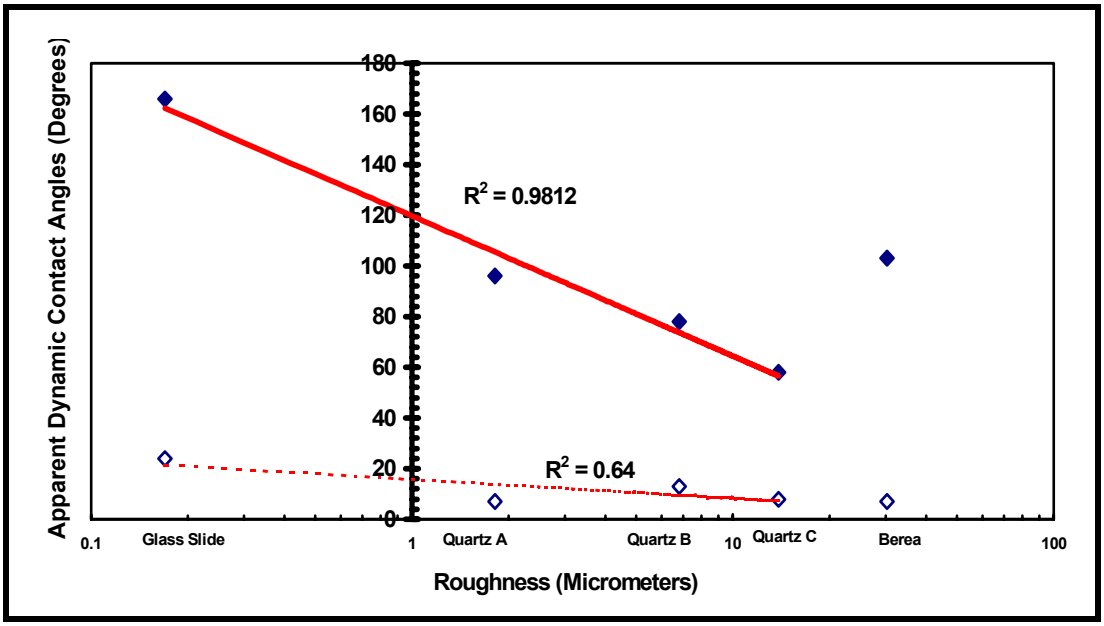

Figure 46: Effect of Surface Roughness on Dynamic Contact Angles on Silica-Based Surfaces

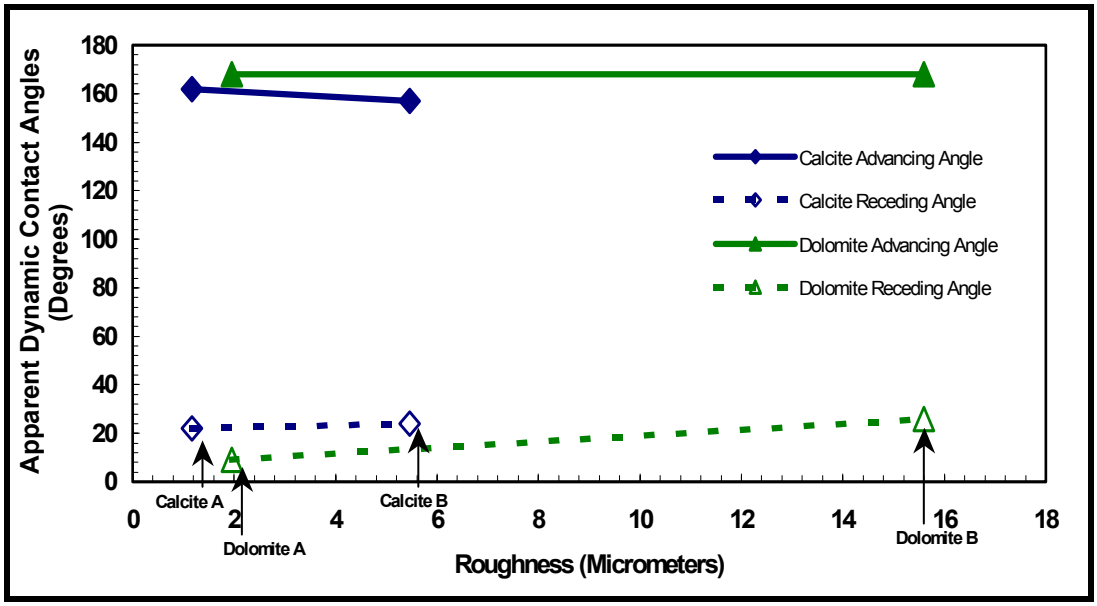

Figure 47: Effect of Surface Roughness on Dynamic Contact Angles on Dolomite and Calcite Surfaces

4.5 Effect of Rock Mineralogy on Reservoir Wettability

The composition of reservoir rocks is another important aspect in determining wettability as the rock interacts with both the reservoir brine and the hydrocarbon phase. Experiments were conducted to study the effect of rock mineralogy on reservoir wettability. DDDC tests were performed with different solid surfaces (Quartz, Dolomite and Calcite) having similar roughness using Yates Crude oil and Yates reservoir brine. Table 11 gives the summary of results. As can be observed, Quartz, displayed an advancing angle of 97° showing intermediate-wet behavior while the dolomite and calcite surfaces indicated strongly oil-wet nature with advancing angles of 160 and 162°, respectively. All these results clearly confirm Anderson's data[14] that there appear to be more non-water-wet reservoirs than water-wet ones, contrary to the general notion.

Table 11: Effect of Mineralogy on Reservoir Wettability

Mineral	Roughness (Micrometers)	Advancing Angle (Degrees)	Receding Angle (Degrees)
Quartz	1.81	97 (Intermediate-Wet)	7
Dolomite	1.95	160 (Oil-Wet)	10
Calcite	1.17	162 (Oil-Wet)	22

4.6 Effect of Ethoxy Alcohol Surfactant Concentration on Oil-Water Interfacial Tension and Contact Angles

Ethoxy alcohol surfactant is being used by Marathon Oil Company for enhanced oil recovery in the Yates field in West Texas. This surfactant is an ethoxylate C9-C11 linear primary alcohol with complete solubility in water. This surfactant was supplied by Marathon Oil Company along with Yates brine and crude oil to study the effect of surfactant concentration on wettability and interfacial tension.

A series of DDDC tests were conducted to determine the effect of concentration of ethoxy alcohol surfactant in Yates reservoir brine on dynamic contact angles in the Yates fluids-dolomite system. The results are given in Tables 11 and 12 and plotted in Figures 48 and 49. As can be seen in Table 11 and Figure 48, the interfacial tension decreases rapidly with increasing surfactant concentration in Yates brine, up to a level of 1000 ppm and remains reasonably constant thereafter.

Table 12: Summary of Interfacial Tension Measurements of Yates Crude oil-Yates Brine and Ethoxy Alcohol Surfactant at various concentrations using du Nuoy Ring Technique and the Drop Shape Analysis Technique

Interfacial Tension (dynes/cm)		
Fluid Pair	**du Nuoy Ring Method**	**DSA**
Yates Crude Oil – Yates Brine	28.0	29.00
Yates Crude Oil – Yates Brine – 50 ppm Ethoxy Alcohol Surfactant	17.85	15.84
Yates Crude Oil – Yates Brine – 100 ppm Ethoxy Alcohol Surfactant	13.40	9.42
Yates Crude Oil – Yates Brine – 350 ppm Ethoxy Alcohol Surfactant	6.90	4.19
Yates Crude Oil – Yates Brine – 1000 ppm Ethoxy Alcohol Surfactant	1.20	0.69
Yates Crude Oil – Yates Brine – 3500 ppm Ethoxy Alcohol Surfactant	0.48	0.19

The effect of surfactant concentration can be shown from Figure 48, which shows the initial oil-wet nature (158^o at 0 ppm of surfactant) of Yates fluid pair on dolomite surface. On addition of surfactant, the interfacial tension of the Yates crude oil-Yates brine mixture went on decreasing to reach a very low value and remained constant thereafter. The advancing angle, which also represents wettability, reduced from 158^o (0 ppm of surfactant) to 36^o for 3500 ppm

(the same being used in Yates field application) of surfactant, rendering the system water-wet. This preliminary investigation indicates the effect of ethoxy alcohol surfactant in altering strongly oil-wet Yates rock-fluids system to one of water-wet nature.

When surfactants like ethoxy alcohol can help reduce the interfacial tension between the fluids pairs, the flow of crude oil will be easier as the capillary number increases, thereby improving oil recovery. If these surfactants also result in the wettability alterations, especially of an initial oil-wet surface to a water-wet one, further enhancement in oil recovery beyond that due to interfacial reduction can be expected.

Table 13: Dynamic Contact Angles using DDDC Technique for the Yates Crude Oil – Yates Reservoir Brine – Dolomite system for various Concentrations of Ethoxy Alcohol Surfactant at Ambient Conditions for an initial aging time of 24 hours

Surfactant Concentration (ppm)	**Advancing Angle (Degrees)**				**Receding Angle (Degrees)**			
	Trial 1	**Trial 2**	**Trial 3**	**Average**	**Trial 1**	**Trial 2**	**Trial 3**	**Average**
0	158	156	158	158	8	6	7	7
50	141	142	141	141	nv*	nv	nv	nv
100	124	125	124	124	nv*	nv	nv	nv
1000	81	82	79	81	30	31	31	31
3500	39	39	40	39	26	25	26	26

nv* : not visible clearly to enable

4.7 Effect of Brine Dilution on Reservoir Wettability

There have been reports in the literature, as discussed in Section 2.5, that brine composition affects wettability. In order to study the effects of brine composition on wettability using the DDDC technique, reservoir brine was mixed with deionized water (DIW) at various proportions.

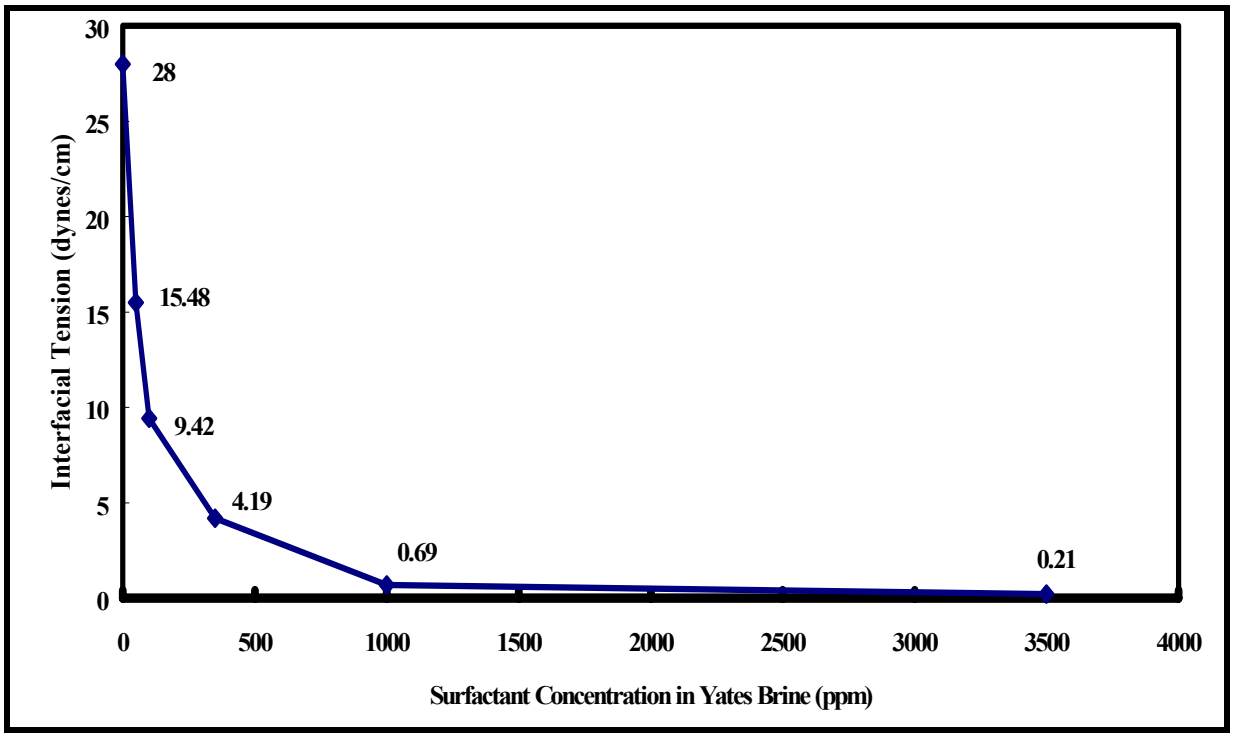

Figure 48: Effect of Ethoxy Alcohol Surfactant Concentration on Interfacial Tension of Yates Reservoir Crude Oil and Brine at Ambient Conditions

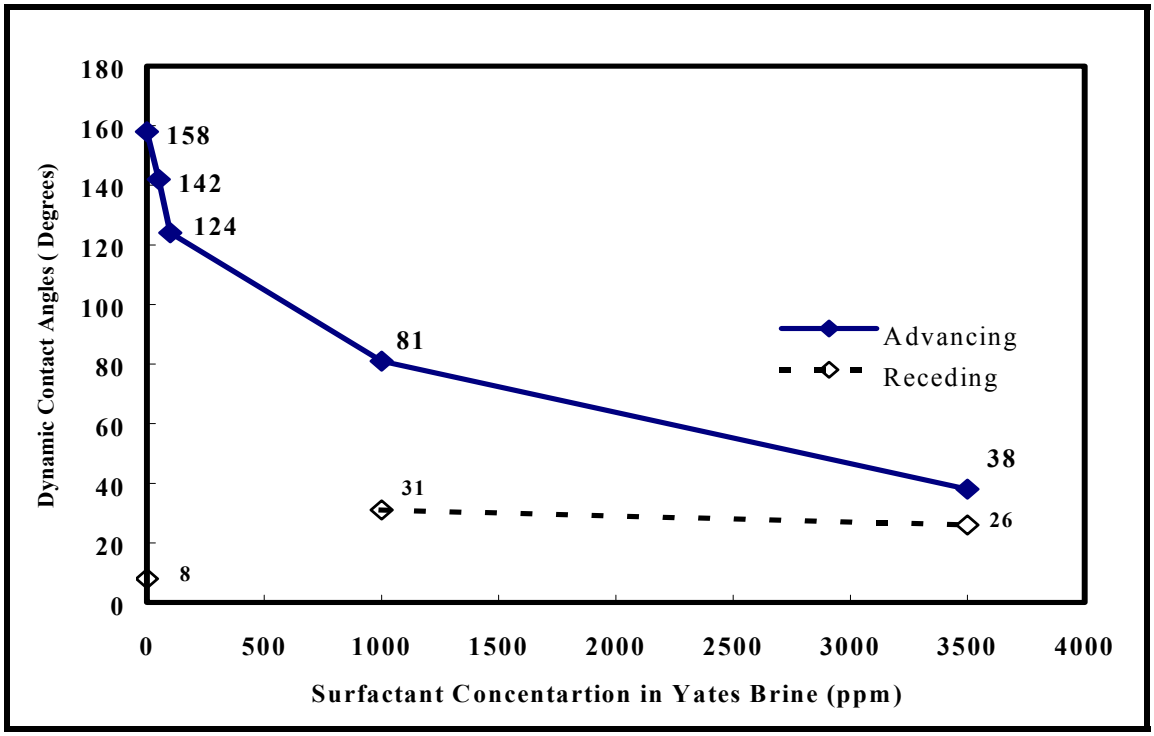

Figure 49: Dynamic Contact Angles using DDDC Technique for Yates Crude Oil – Yates Brine – Dolomite at Ambient Conditions for various concentrations of Ethoxy Alcohol Surfactant

These diluted brine samples were then used to measure the oil-water interfacial tension using the Drop Shape Analysis Technique and dynamic contact angles (using the DDDC technique).

Figure 50 shows the trend of interfacial tension with brine composition. As the volume % of reservoir brine in the mixture increased, the interfacial tension decreased from 25.3 dynes/cm for 100% deionized water (DIW) to 10.2 dynes/cm for the 50-50 mixture and then increased on further increasing the volume percent of reservoir to a maximum of 27.9 dynes/cm for 100% brine.

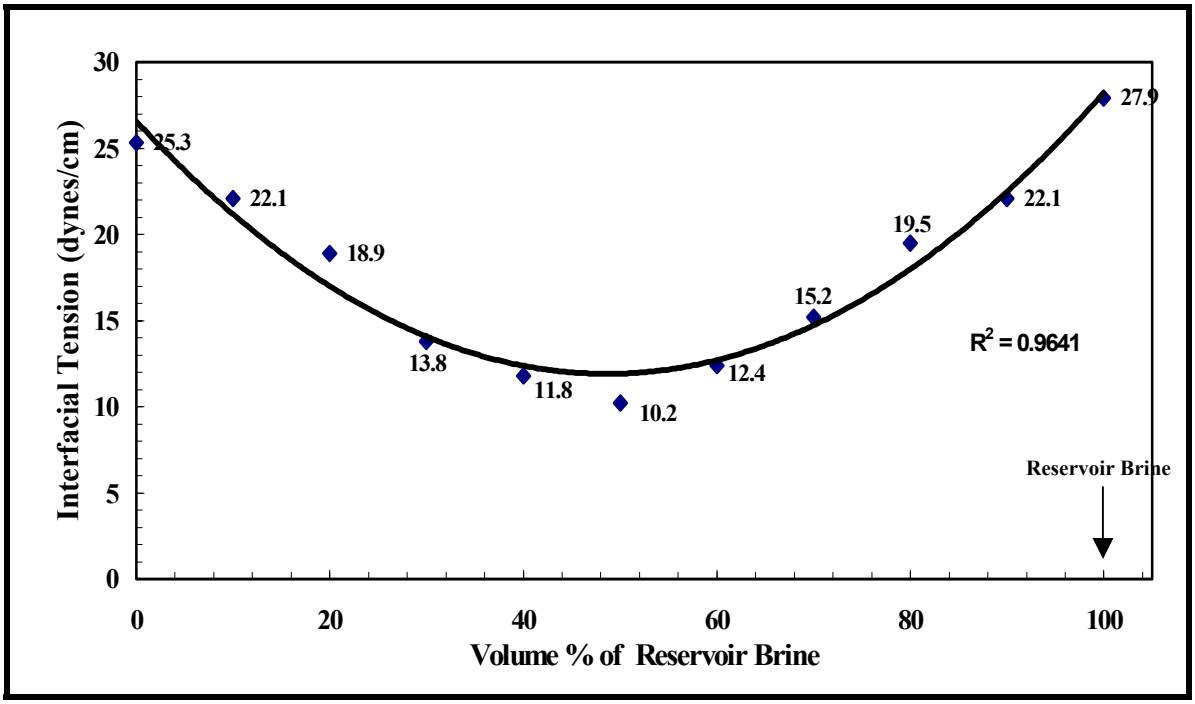

Figure 50: Effect of brine dilution on Interfacial Tension between Yates Reservoir brine and Yates Crude oil

Experiments were conducted with several mixtures to study the effect of brine dilution on dynamic contact angles using the DDDC technique. Initial values of advancing (156^{o}) and receding (10^{o}) contact angles with 100% reservoir brine were already measured in experiments. Hence a 90% brine-10% deionized water mixture with an oil-water interfacial tension of 22.1 dynes/cm as measured by the drop shape analysis was chosen for the next DDDC test. There was a slight change in the advancing angle (152^{o}) and not so noticeable a change in the receding

angle (8^o). Next a mixture of 10% brine and 90% deionized water, which had a similar interfacial tension (22.1 dynes/cm), and the advancing angle was measured to be 146^o with the receding angle at 17^o.

Then a mixture with the lowest interfacial tension (50-50 mixture with an oil-water interfacial tension of 10.2 dynes/cm) was tested. As soon as the oil drop was placed on the crystal surface, it started to spread, and after a two hours of aging, the drop spread like a pancake attaining large receding angles that reached equilibrium value of 140^o as shown in Figure 51. In order to further investigate the spreading phenomenon, a mixture of 60% reservoir brine and 40% deionized water, which had an oil-water interfacial of 12.4 dynes/cm, was studied for the advancing and receding angles. Surprisingly, the drop did not spread and, the advancing angle was measured to be 150^o and a relatively small receding angle was measured (19^o).

To explain this strange behavior it was decided to check for the advancing and receding angles of a mixture whose interfacial tension was in-between 10.2 and 12.4 dynes/cm. A 45% brine and 55% deionized water was prepared and measured for its interfacial tension and the advancing and receding angles. The interfacial tension was 10.9 dynes/cm. The drop started spreading as soon as it was placed on the rock surface, but the spreading stopped when the receding angle reached a value of 90^o. The advancing angle was measured to be 146^o and the receding angle was 90^o as can be seen in Table 14.

Table 14: Interfacial tension and dynamic contact angles for various mixtures of Yates reservoir brine with deionized water

Volume % of Yates Reservoir brine	Interfacial Tension dynes/cm	Receding Angle θ_r	Advancing Angle θ_a
100	27.9	10	156
90	22.1	8	152
60	12.4	19	150
50	9.8	140	146
45	10.9	90	146
10	22.1	17	152

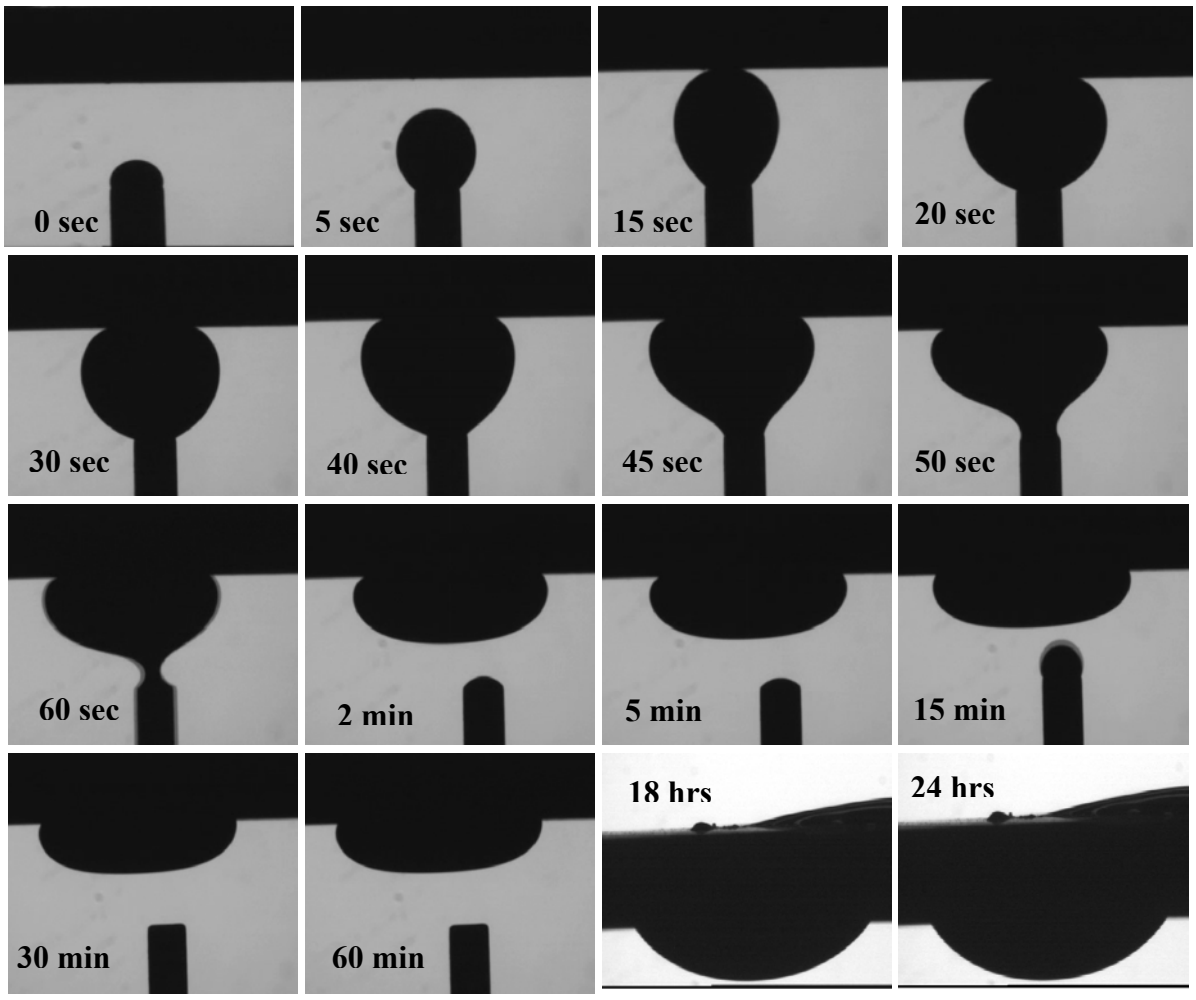

Figure 51: Spreading of Yates crude oil drop against brine (containing 50% reservoir brine and 50% deionized water) on smooth dolomite surface

This peculiar spreading behavior in crude oil-brine-rock systems was earlier reported by Rao [24] while studying the effects of temperature on spreading and wettability in heavy oil reservoirs. This spreading was attributed to the receding angle. Hence an attempt was made here to correlate this spreading behavior observed as an effect of changing brine composition against oil-brine interfacial tension. A graph as shown in Figure 52 between interfacial tension and receding contact angle is plotted. Such a plot is generally referred to as the Zisman plot [36], after Zisman [36] who originated it a few decades ago for spreading behavior observed in solid-liquid-vapor systems as explained below.

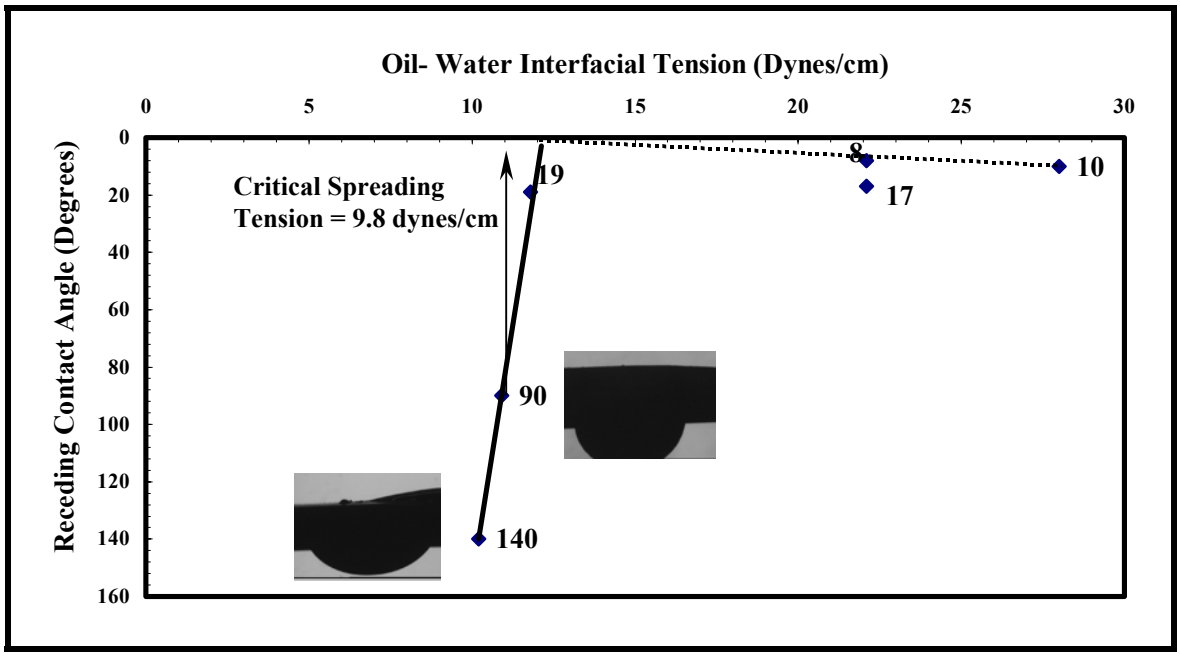

Figure 52: Zisman-type Spreading correlation for the Yates Brine -Yates Crude Oil-Dolomite Rock System

Zisman [36] developed a linear relationship based on contact angle θ, and the surface tension. He defined the critical spreading tension γ_c, as that value of surface tension, where the extrapolated straight line between Cos θ and surface tension cuts the contact angle line at Cos θ = 1, θ =90^o. Figure 53 is a reproduction of a relationship between contact angle and surface tension for n-alkanes on PTFE. In this the value of surface tension where the line intersects Cos θ = 1 axis is about 19 dynes/cm and is termed as the critical surface tension for that particular solid surface. Zisman noted that any liquid having a surface tension less than this critical value, would immediately spread on the surface. Figure 54 shows another Zisman plot from the literature.

Rao [24] plotted a graph, similar to Zisman's, for Solid-Liquid-Liquid systems and termed the value of interfacial tension at which the receding angle reached 90^o as the Critical Spreading Tension for that particular solid-liquid-liquid system. Accordingly, the interfacial tension of

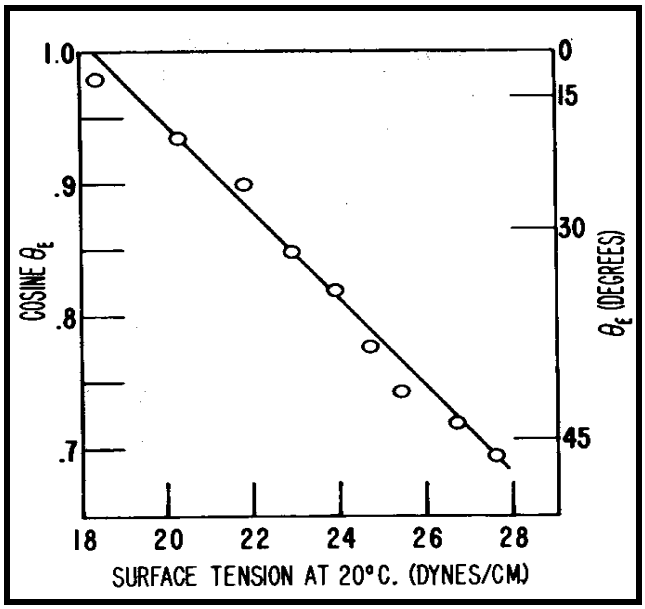

Figure 53: Wettability of Polytetraflouroethylene by n-alkanes (Reference #36)

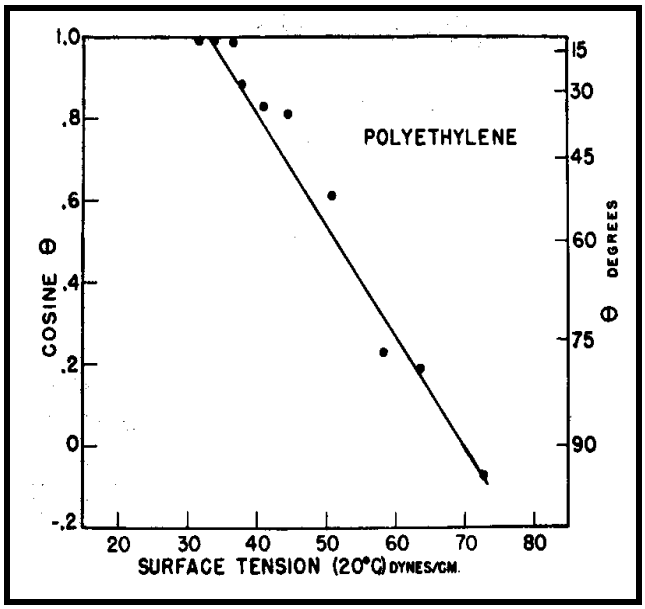

Figure 54: Wettability of Polyethylene (Reference #36)

10.9 dynes/cm in Figure 52 is the Critical Spreading tension for the Yates crude oil-Yates brine-Dolomite system. The plot of Figure 52 also proves the hypothesis put forward by Rao [24] that

for any interfacial tension below the critical, the drop phase spreads on the solid surface with large receding angles.

A study was conducted with synthetic brine to see if it behaved the same way as with reservoir brine. Synthetic brine was prepared basing on the composition of reservoir brine as shown in Table 14. This brine was filtered through Whatman filter paper # 1 and then through 0.2 μ filter paper under vacuum. Various mixtures of synthetic brine with deionized water were prepared and interfacial tension of these mixtures against crude oil was measured.

A similar trend in the interfacial tension was observed as for the reservoir brine. First an initial decrease up to a minimum of 9.8 dynes/cm for 50-50 mixture as shown in Figure 55 and then a gradual increase was observed. Then DDDC experiments were conducted with various mixtures of synthetic brine with deionized water (DIW) for measuring advancing and receding angles. Table 15 and Figure 56 show the results. The critical spreading tension at which the receding angle reaches 90^{o} for this particular system is 13.2 dynes/cm. If the best-fit line is extrapolated, it would intersect the receding angle axis at an oil-water interfacial tension of 22.6 dynes/cm. At any interfacial tension values higher than 22.6 dynes/cm, it appears that the receding contact angle would be close to zero. A previous experiment on brine dilution using 75% synthetic brine and 25% deionized water saw the drop phase spreading instantly on the rock surface (shown in Figure 57) yielding large receding angles. This phenomenon was not quite repeatable at the same concentration of synthetic brine the second time. This might be due to a slight difference in the surface texture of the rock surface, but the spreading of the crude oil on the rock surface was seen at a different concentration yielding large receding angles.

Table15: Composition of Yates Reservoir Brine

Test	Concentration Units
PH	7.39 pH Units
Total Dissolved Solids	9200 mg/l
Calcium, Total	425 mg/l
Magnesium, Total	224 mg/l
Potassium, Total	50.5 mg/l
Sodium, Total	1540 mg/l
Hardness as $CaCO_3$	1500 mg/l
Hardness as Carbonate	810 mg/l
Hardness as Non-Carbonate	730 mg/l
Alkalinity as Bicarbonate	800 mg/l
Alkalinity as $CaCO_3$	810 mg/l
Sulfate	660 mg/l
Chloride	3700 mg/l

Table 16: Interfacial tension and dynamic contact angles for various mixtures of Yates synthetic brine with deionized water

Volume % of Yates Synthetic brine	Interfacial Tension dynes/cm	Receding Angle θ_r	Advancing Angle θ_a
100	18.5	36	155
75	14.4	90	153
50	9.9	12	142
40	12.1	90	152

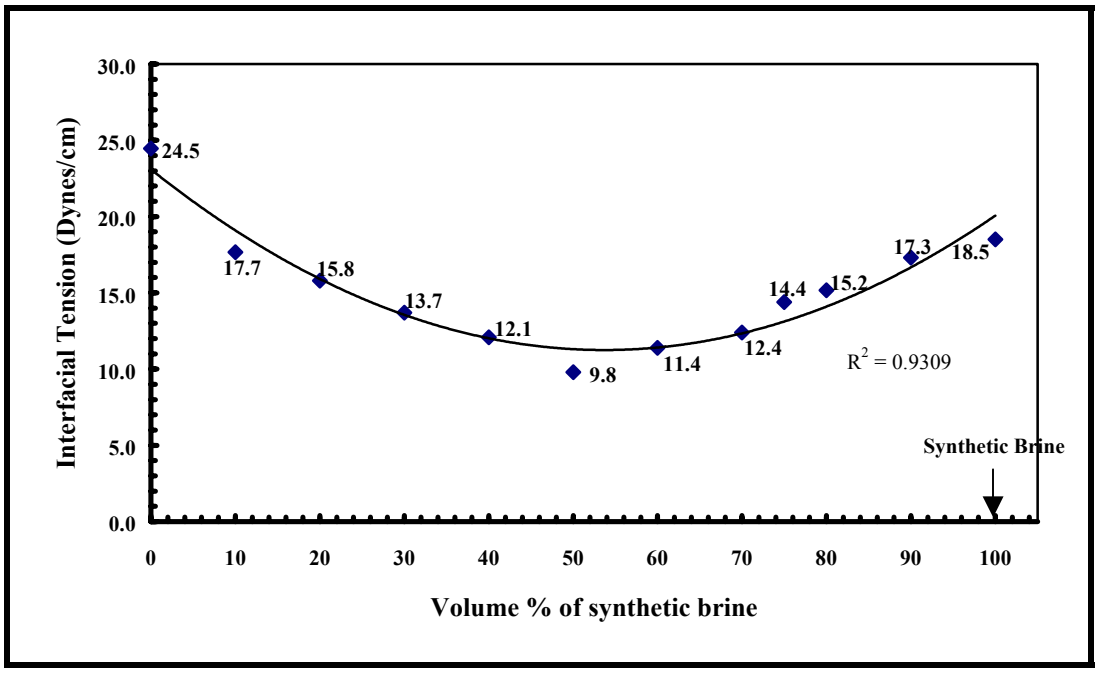

Figure 55: Effect of brine dilution on Interfacial Tension between Yates Synthetic brine and Yates Crude oil

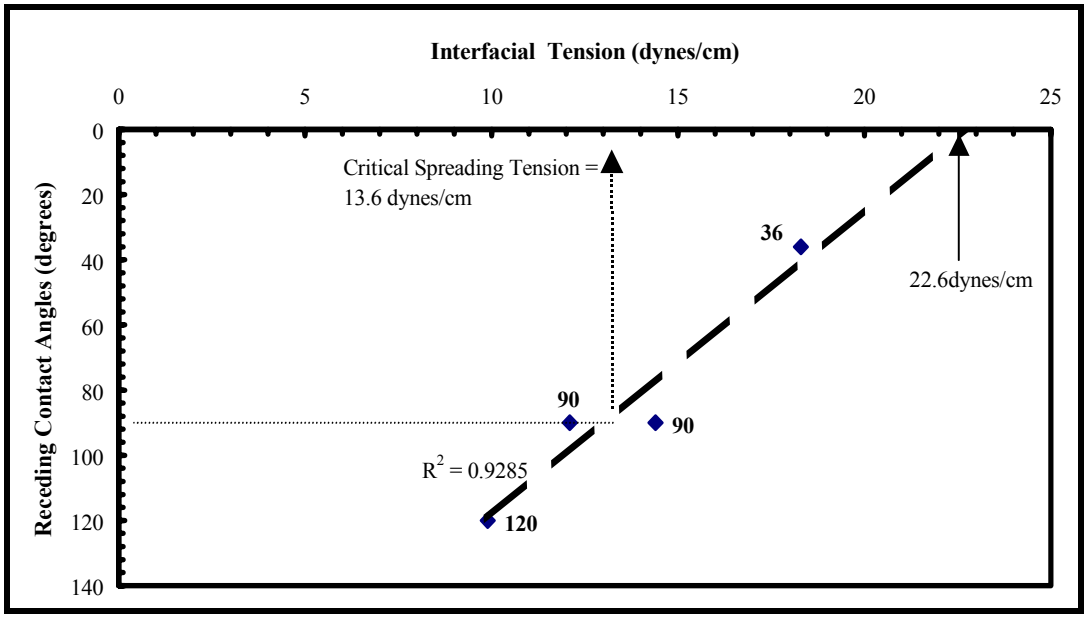

Figure 56: Zisman type-spreading correlation for the Synthetic brine-deionized water mixture-Yates crude oil on dolomite rock system

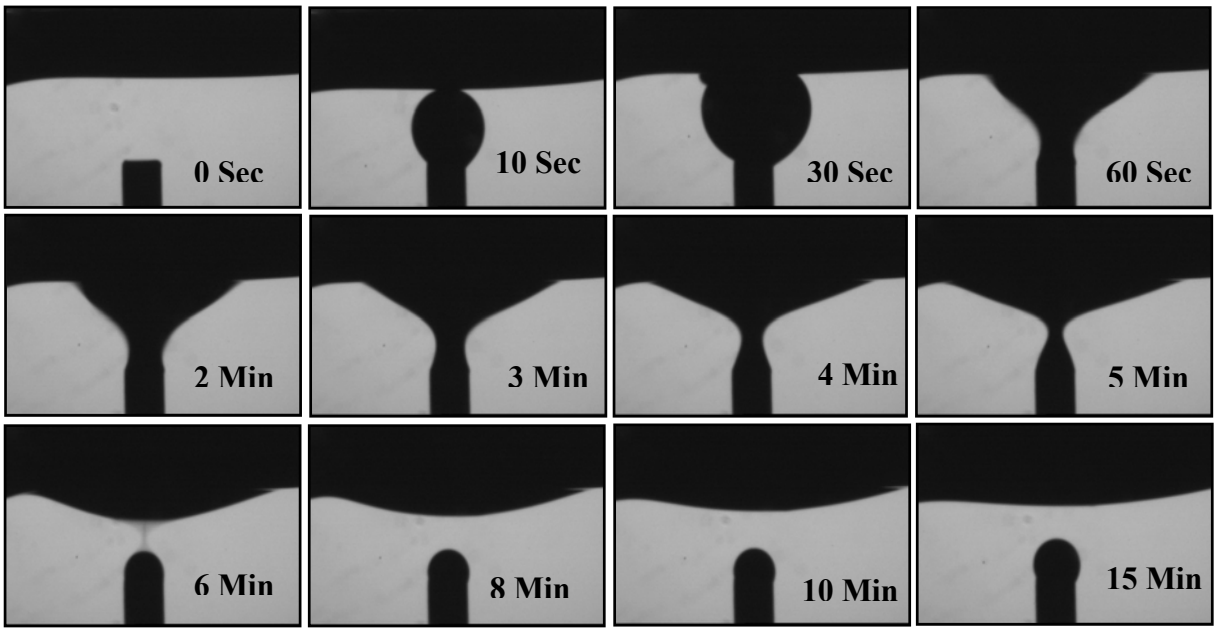

Figure 57: Spreading of Yates Crude Oil Drop against Brine (containing 75% synthetic brine and 25% DIW) on Smooth Dolomite Surface

Spreading can be an advantage when the crude oil tends to form a thin layer of film on the entire rock surface yielding a path for the oil to drain. It makes a nice passage for the remaining oil trapped in the pores of the rock to migrate towards well bore, thus enhancing the recovery. This spreading may not always be favorable as in the case with initially non-water wet rock fluid systems.

CHAPTER 5

CONCLUSIONS AND RECOMMENDATIONS

5.1 Summary and Conclusions

A computerized Wilhelmy Plate apparatus and the Dual-Drop-Dual-Crystal apparatus have been used in this study to characterize the effects of rock and fluid characteristics on reservoir wettability. Although unable to simulate reservoir conditions of pressure and temperature, the ambient DDDC cell is easy to use and yields highly reproducible dynamic (advancing and receding) contact angles. It has been used to evaluate the effects of rock mineralogy, rock surface roughness, brine dilution and the addition of non ionic surfactant on advancing and receding contact angles, wettability and spreading behavior. The Wilhelmy apparatus has been used in several cases to enable comparison to DDDC results.

The main findings of this experimental study are:

1. The Wilhelmy apparatus displayed insensitivity when used to infer dynamic contact angles and their variations with solid surface characteristics. It consistently indicated 90^o angles irrespective of the surface type, roughness and whether the oil-water interface was advancing or receding.
2. The DDDC technique, on the other hand, indicated significant effects of rock mineralogy, surface roughness and mode of measurement (advancing or receding) on dynamic contact angles. The weeklong ambient condition DDDC tests of this study indicate an aging time of 24 hours to be sufficient for attaining solid-fluids equilibrium.
3. All three mineral surfaces quartz, dolomite and calcite showed strong oil-wet tendencies ($155 < \theta_a > 166$) with Yates reservoir fluids.

4. The water-advancing contact angles on silica-based surfaces showed a sharp decline with increasing surface roughness indicating a shift from oil-wet nature on smooth surface to either intermediate-wet or weakly water-wet on rougher surfaces. Measurements on actual Berea rock samples, though not falling on the same trend as the other silica surfaces, also indicated intermediate-wettability. The dolomite and calcite surfaces, though displaying a slight decline in advancing angle with roughness, retained strongly oil-wet nature within the range of roughness examined. The receding angles on all surfaces remained low (7-22^{o}) indicating their insensitivity to surface type and roughness. These results appear to refute the general notion of increasing hysteresis with roughness.
5. Addition of a nonionic ethoxy alcohol surfactant decreased the interfacial tension between Yates Crude oil and Yates brine from 29 to 0.19 dynes/cm at 3500 ppm of surfactant concentration. This is accompanied with the decrease in water advancing angle of 156^{o} (strongly oil-wet) on smooth dolomite surface for zero concentration of the surfactant to 39^{o} (water-wet) for a concentration of 3500 ppm of the surfactant. This reduction in contact angle signifies a change in wettability from a strongly oil-wet to a water-wet condition induced by the nonionic ethoxy alcohol surfactant.
6. The effect of brine composition was found in this study to be quite surprising and significant. Changing Yates reservoir brine composition by mixing it with deionized water yielded an unexpected effecting that the drop phase (crude oil) was found to spread on the solid surface below a particular value of interfacial tension. Similar results were found with synthetic brine. The value of interfacial tension at which the receding angle reaches 90^{o} is termed as the critical spreading tension. When the oil-water interfacial tension drops below this critical value, oil spreads on the solid surface. This finding has

serious implications in fields where water flooding is employed for secondary recovery. If a particular composition of the brine-water mixture yielded interfacial tension below the critical, the crude oil would spread on the rock surface and influence the recovery.

5.2 Recommendations for Future Work

The Dual-Drop-Dual-Crystal Technique is used to study the effects of surface roughness, surfactant concentration and brine compositions on reservoir wettability at ambient conditions of temperature and pressure. To gain a better understanding of the wettability phenomenon in the reservoir, there is a need to measure the water advancing and receding contact angles on rough surfaces and reservoir rocks at actual reservoir conditions of temperatures and pressure.

The effect of various kinds of nonionic, anionic, cationic or amphoteric surfactants on various mineral surfaces at both ambient and reservoir conditions need to be studied in order to fully understand and apply this knowledge to reservoirs.

The effect of multivalent cations such as Ca^{2+} and Mg^{2+} in brines and the effect of brine dilution using synthetic brine with deionized water at both ambient and reservoir conditions with various minerals need to be studied as they are known to have a significant effect on influencing wettability alteration.

Studies should be conducted by deasphalting and deresining the crude oil to study the effects of oil composition on wettability at both ambient and reservoir conditions.

REFERENCES

1. First Ten Angstroms: "What are contact angles?", Application notes 2001.

2. Rao, D.N., "Fluid-Fluid and Solid- Solid Interactions in Petroleum Reservoirs," Petroleum Science and Technology, 19(1 & 2), 157-188, 2001.

3. Anderson.W.G., "Wettability Literature Survey- Part 2: Wettability Measurement.", JCPT, Nov.1986.

4. Rao, D. N., and Girard, M.G., "A New Technique For Reservoir Wettability Characterization", JCPT, Jan1996, Vol35, No.1.

5. Adamson, A.W., "Physical Chemistry of Surfaces; 4th Edition, John Wiley and Sons Inc., New York City (1982) 332-68.

6. Johnson, R.E., and Dettre, R.H., "Wettability and Contact Angles," Surface and Colloid Science, E.Matijevic (ed.), Wiley Interscience, New York City (1969) 2,85-153.

7. Extrand, C.W., and Kumagai, Y., "An Experimental Study of Contact Angle Hysteresis", Journal of Colloid and Interfacial science 191, 378-383 (1997).

8. Marmur, A.V., "Contact Angle Hysteresis on Heterogeneous Smooth Surfaces", Journal of Colloid and Interfacial science, 168, 40-46 (1994).

9. R.N. Wenzel, "Surface Roughness and Contact Angle" , J. Phys. Colloid Chem., 53, 1466 (1936).

10. A.D.B. Cassie and S. Baxter, "Absorption of Water by Wool", Trans. Faraday Soc., 40,456 (1944).

11. J. F. Oliver, C. Huh and S. G. Mason, " Resistance to Spreading of Colloids by Sharp Edges", J. Colloid Interface Sci., 59, 568 (1977).

12. S.G. Mason, in "Wetting Spreading and Adhesion" (J.F. Padday Ed.), pp.321-326, Academic Press, New York and London (1978).

13. N.R. Morrow, "The Effects of Surface Roughness on Contact Angle Petroleum Technol., 14, 42 (1975).

14. Anderson, W.G.: "Wettability Literature Survey—Part 3: The Effects of Wettability on the Electrical Properties of Porous Media," JPT (Dec. 1986) 38, No. 13, 1371-1378.

15. M. Robin, A. Paterson, L. Cuiec and C. Yang, "Effects of Chemical Heterogeneity and Roughness on Contact Angle Hysteresis: Experimental Study and Modeling," Paper No.37291, Proc. SPE International Symposium On Oilfield Chemistry, Houston, (1997).

16. S.Y. Yang, G.J. Hirasaki, S. Basu, and R. Vaidya, "Mechanisms for contact angle hysteresis and advancing contact angles," Petroleum Sci. & Eng., 24 (1999) 63-73.

17. Jones, F.O.: "Influence of Chemical Composition of Water on Clay Blocking of Permeability", Journal of Petroleum Technology (April 1964), 441-446.

18. Mungan, N.: "Permeability Reduction Through Changes in pH and Salinity", Journal of Petroleum Technology (December 1965), 1449-1453.

19. Kwan, M.Y., Cullen, M.P., Jamieson, P.R. and Fortier, R.A.: "A Laboratory Study of Permeability Damage to Cold Lake Tar Sands Cores", Journal of Canadian Petroleum Technology, 28 (1), (January-February 1989), 56-62.

20. Souto, E. and Bazin, B.: "Ion Exchange Between Hydrogen and Homoionic Brines Related to Permeability Reduction", SPE Paper 25203, presented at the SPE International Symposium on Oil Field Chemistry, New Orleans, LA, (March 2-5, 1983), 491-500.

21. Yildiz, H.O. and Morrow, N.R.: "Effect of Brine Composition on Recovery of Moutray Crude Oil by Waterflooding", Journal of Petroleum Science and Engineering, Vol. 14, 1996, 159-168.

22. Tang, G. and Morrow, N.R.: "Salinity, Temperature, Oil Composition and Oil Recovery by Waterflooding", SPE Reservoir Engineering, 1997, 269-276.

23. Yildiz, H.O., Valat, M. and Morrow, N.R.: "Effect of Brine Composition on Recovery of an Alaskan Crude Oil by Waterflooding", Journal of Canadian Petroleum Technology, 1999, Vol. 38, 26-31.

24. Rao, D.N., "Wettability Effects in Thermal Recovery Operations", SPE Reservoir Evaluation and Engineering, 2 (5), October 1999, pp. 420-430.

25. Opawale, F.O., and Burgess, D.J., "Influence of Interfacial properties of Lipophilic Surfactants on Water-in-Oil Emulsion Stability," Journal of Colloid and Interface Science (1998), Vol.42, pp.142-150.

26. Sophany,T., Trogus,F.J., Schechter,R.S., and Wade, W.H., "Static and Dynamic Adsorption of Anionic and Nonionic Surfactants," SPE Journal (Oct.1977),pp. 337-344.

27. Lawson,J.B., "The adsorption of Non-Ionic and Ionic Surfactants on Sandstone and Carbonate," SPE 7052 presented at the 1978 5th SPE symposium on Improved Methods for Oil Recovery, Tulsa,Apr.16-19.

28. Bock,J., Valiant,Jr., P. Varadaraj,R., Zushma,S., and Brons,N., "Fundamental Interfacial Properties of Alkyl-Branched Sulfate and Ethoxy Sulfate Surfactants Derived from Guebert Alcohols," Journal of Colloid and Interface Science (1991), Vol. 95, pp.1679-1681.

29. Teeters, D., Wilson, J.F., Andersen, M.A., and Thomas, D.C., "A Dynamic Wilhelmy Plate Technique Used for Wettability Evaluation of Crude Oils," Journal of Colloid and Interface Science (1988) Vol. 126, pp. 641-644.

30. Andersen, M.A., Thomas, D.C., and Teeters, D.C., "A New Formation Wettability Test: The Dynamic Wilhelmy Plate Wettability Technique," paper SPE/DOE 17368 presented at the 1998 SPE/DOE Enhanced Oil Recovery Symposium, Tulsa, Apr.17-20.

31. Rotenberg, Y., Boruvka, L., and Neumann, A., "Determination of Surface Tension and Contact Angle from the shapes of Axisymmetric Fluid Interfaces", J. Colloid Interface Sci.93**,** 169 (1983).

32. Adamson, A.W., and Gast, A.P., Physical Chemistry of Surfaces, 6th ed. John Wiley & Sons, Inc., New York, NY, (1997), pp. 22.

33. Green, D.W., and Willhite, G.P., Enhanced Oil Recovery, SPE Textbook Series Vol.6, (1998), SPE, Richardson, TX. pp.15.

34. Muhammad.Z., "Compositional Dependence of Reservoir Wettability" , Masters Thesis, The Craft and Hawkins Department of Petroleum Engineering, Louisiana State University, Baton Rouge, LA, May 2001.

35. Kruss, USA., "DSA-10: Drop Shape Analysis Users Manual".

36. Zisman,W.A., " in Contact Angle, Wettability and Adhesion", Advances in Chemistry Series 43, ACS, Washington, D.C., 1964.

37. Handbook of Chemistry and Physics, 49th edition, The Chemical Rubber Company, Cleveland, OH.

VITA

Chandra S Vijapurapu, son of Kothanda Rao Vijapurapu and Kalyani, was born in Visakhapatnam, India, on October 1,1978. He obtained a bachelor's degree with distinction in chemical engineering in 2000 from Andhra University, India. He then enrolled at Louisiana State University in Fall 2000 to work towards a degree of Master of Science in Petroleum Engineering.